Design and Synthesis of a Multi-tag Exchangeable Nosyl-type Diazirine in Photoaffinity Labeling

（マルチタグ交換可能な新規ジアジリン光アフィニティープロブの創製）

A Thesis Submitted for the Degree of
Doctor of Life Science

Aimi Suhaily Saaidin

Laboratory of Chemical Biology
Transdisciplinary Life Science Course
Graduate School of Life Science
Hokkaido University, Japan

March 2020

Table of Contents

Abbreviations

ACT: 2-Aryl-5-tetracarboxy tetrazole

Boc: tert-butyloxycarbonyl

BODIPY: Boron-dipyrromethene

BSA: Bovine serum albumin

$CHCl_3$: Chloroform

DBU: 1,8-Diazabicyclo[5.4.0]undec-7-ene

DCC: *N,N'*-Dicyclohexylcarbodiimide

DCDMH: 1,3-dichloro-5',5-dimethylhydantoin

DHFR: Dihydrofolate reductase

DIPEA: *N*,*N*-Diisopropylethylamine

DMAP: 4-Dimethylaminopyridine

DMF: *N*,*N*-dimethylformamide

DMSO: Dimethyl sulfoxide

EDC: 1-Ethyl-3-(3-dimethylaminopropyl) carbodiimide

ESI-MS: Electrospray ionization mass spectrometry

Et_3N: Triethylamine

EtOAc: Ethylacetate

Fmoc: Fluorenylmethoxycarbonyl

HATU: 1-[Bis(dimethylamino)methylene]-1H-1,2,3-triazolo[4,5-b]pyridinium-3-oxide hexafluorophosphate

HBTU: 3-[Bis(dimethylamino)methyliumyl]-3H-benzotriazol-1-oxide hexafluorophosphate

HPLC: High performance liquid chromatography

HRMS: High resolution mass spectrometry

HRP: Hydrogen peroxidase

IBX: 2-Iodoxybezoic acid

MeOH: Methanol

Ms: Mesyl

MTX: Methotrexate

NBD: 4-Chloro-7-nitro-1,2,3-benzoxadiazole

NCS: *N*-Chlorosuccimide

NMR: Nuclear magnetic resonance

Ns: Nosyl

PEG: Polyethylene glycol

Pd/C: Palladium on carbon

PTSA: *p*-Toluenesulfonic acid

PVDF: Polyvinylidene fluoride

r.t: room temperature

TBAF: Tetra-*N*-butyl ammonium fluoride

TFA: Trifluoroacetic acid

TLC: Thin layer chromatography

Ts: Tosyl

SDS-PAGE: Sodium dodecyl sulfate polyacrylamide gel electrophoresis

Thesis abstract

In early stage of drug discovery, identifying the molecular interactions between the bioactive compound and its target protein is one of the crucial steps. Over the years, it has been known that identifying target protein at the molecular level is cumbersome for certain diseases. For this purpose, photoaffinity labeling (PAL) has been developed as a quintessential strategy to identify the targets of active biomolecules, owing to its capability to form a covalent bond with its target. Diazirines are one of the important photolabile moieties used in photoaffinity labeling due to their superior photo labeling characteristics. Conventional photoaffinity label consists of three main components; a photophore (ie diazirine), a ligand and detection/purification tags. Although this method has been widely used, target identification is still a challenging task. Herein, we reported on the design and synthesis of nosyl bearing diazirines which consist of photophore and bioactive ligand.

In chapter one, general introduction on the concept of photoaffinity labelling was discussed. Types of photolabel and their advantages and disadvantages were also discussed in detail. A brief explanation on some of the successful study of protein identification utilizing photoaffinity labelling approach, followed by literature review on the most recent application of photolabeling concept.

The second chapter is consists of preliminary studies on the development of nosyl diazirines in terms of synthesis and identification of the optimum condition for photolabeling. The exchangeable reaction of tag was also discussed in detail using a different fluorophore as the identification tag. Confirmation of the feasibility of this approach was demonstrated using biotin nosyl diazirine as model compound and BSA as model protein. Upon conducting the photolabeling experiment, we successfully proved that the photolabeling efficiency is increased and the insertion of the identification tag was achieved in high yield.

This photoaffinity label was further explored using methotrexate (MTX), a widely known inhibitor of dihydrofolate reductase (DHFR) was used as a bioactive ligand. We successfully synthesized the probe via 4 steps. The protein identification experiment was also discussed in detail.

Chapter 1

General Introduction

Chapter 1 General Introduction

1.1 Photoaffinity labeling

Comprehending the molecular interaction between ligands and proteins is an important step in numerous fields including chemical biology, drug design and discovery. Through out the years, X-ray crystallography and NMR spectroscopy have been a valuable technique to identify the protein-ligand interaction. Although these techniques offer valuable information, they require having the protein at a reasonable purity. In comparison to NMR-based studies, for X-ray crystallography, it is essential that the protein-ligand complex able to be crystalized and the protein-ligand complex in solution usually difficult to be inferred. As an alternative, photoaffinity labeling is a powerful tool used for the study of protein-ligand interactions, where it can identify unknown targets of ligands, assist in the elucidation of protein structures, functions and conformational changes as well as identify novel or alternative binding sites in proteins. This concept was first introduced by Frank Westheimer and co-workers in 1960's, using acylation to incorporate an aliphatic diazo group into the enzyme chymotrypsin, which formed an intramolecular crosslink on photolysis [1] (Fig.1). Although it has been nearly five decades since it was first reported, this concept has gradually emerged as a useful tool for the identifications of protein-ligand interaction especially in some cases of low abundance proteins and low affinity interactions that fail to survive disruptive washing steps [2].

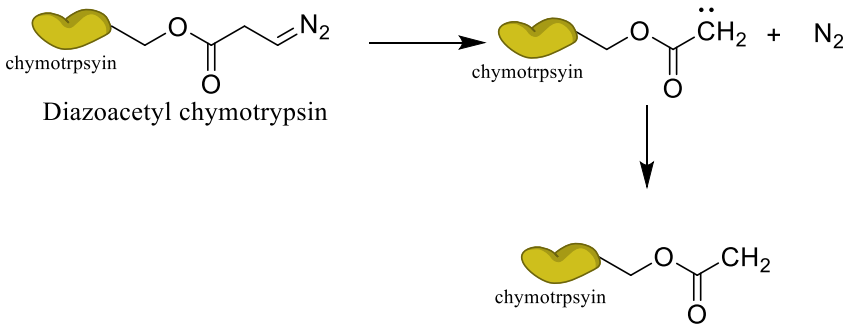

Fig. 1 First concept on photoaffinity labeling by Westheimer

Photoaffinity labels is generally consists of three main components: (i) a bioactive ligand, a unit that target the specific protein (ii) Photoreactive moiety, which would form a cross-link with the target protein upon photoactivation (iii) Purification or identification tag that could be used after post-labelling to labelled the target protein [3]. The photoaffinity label binds with the target protein due to the affinity of the ligand and upon photoactivation, the

photoreactive moiety from the photolabel generates a reactive species that covalently cross-link with proximate biomolecules. Labeled and tagged proteins are separated with other proteome by affinity purification or subjected to mass spectroscopic analysis to identify the protein and binding region of the protein, which means it is not necessary to have the protein of interest pre-purified (Fig.2).

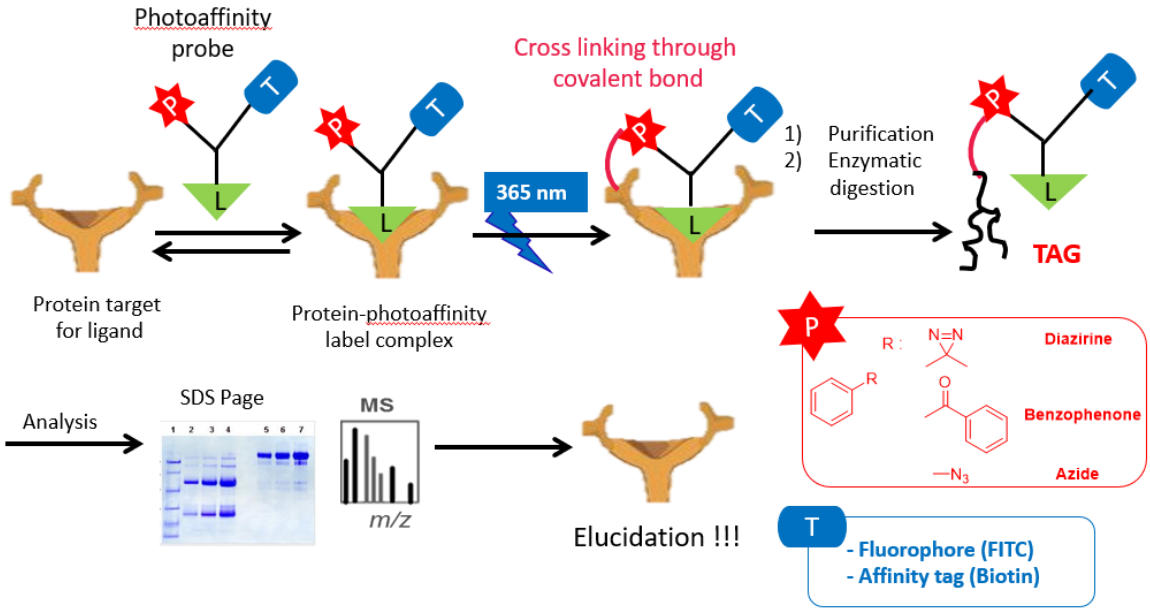

Fig 2. Pictorial representation of photo affinity labeling

1.2 Types of photoaffinity probe

Designing a photoaffinity label could be a cumbersome process. The ideal characteristics of a probe are stable in the dark at a range of pHs, maintain original binding affinity and little steric hindrance. Plus, it also requires activation wavelength that have minimal damage to the proteins, but still have highly reactive intermediates, and capable of forming a stable new bond. The new formed bond must still be intact through out the isolation and detection process. For these purposes, choosing the best photophore is one of the crucial tasks. Currently, diazirine/phenyl diazirine, phenyl azide, benzophenone and tetrazole were among the common photoreactive, where the reactive intermediates were formed on irradiation with specific wavelengths of light to give carbene, nitrene, diradical and nitrile imine (Fig. 3)[4].

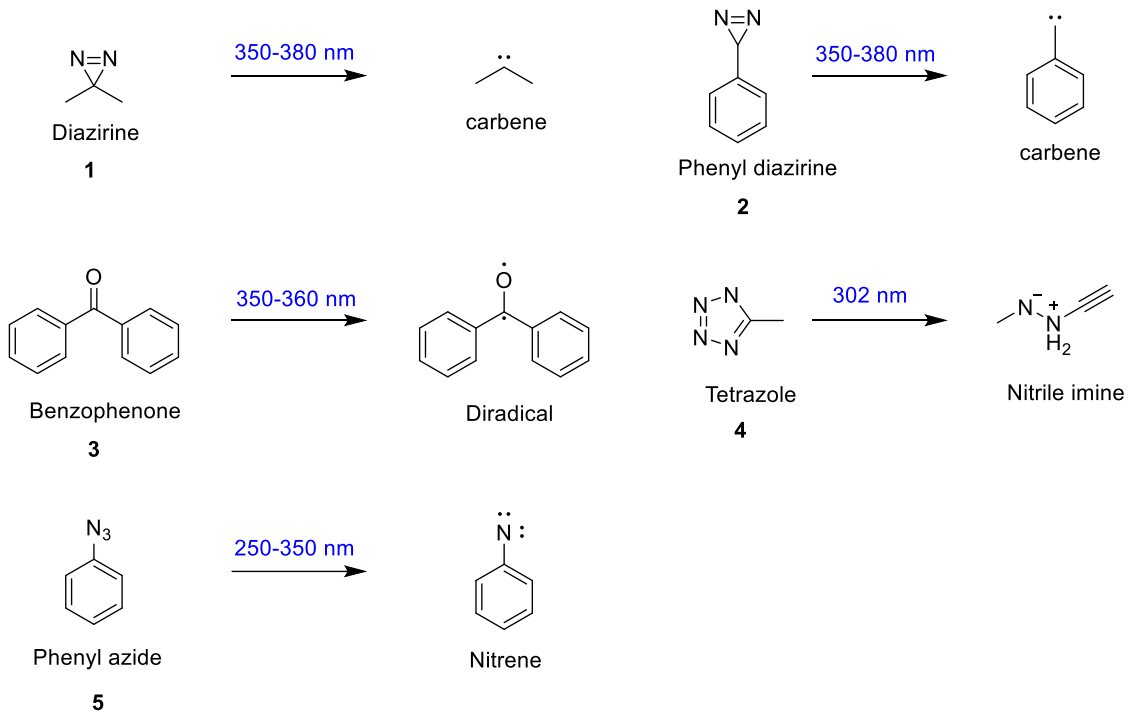

Fig 3. The major photoaffinity functional groups and their reactive intermediates

Although phenylazides are most commonly used photoaffinity label, it requires shorter wavelength for excitation, which will cause damage to other biological molecules. Plus, upon photoirradiation, nitrene intermediates formed and decreases photoaffinity yields compare with carbenes. Besides, nitrene can also rearrange to form benzazirines and ketenimines as undesired product[5].

As for benzophenones, they generate reactive triplet radical and are photoactivated under longer wavelength which lower the possibility of damaging the biomolecules but increase the unspecific labelling[6]. In addition, their bulky structure effect the interaction between the affinity pharmacophore and target protein, this steric hindrance may also lead to unspecific labelling[7]. Despite this, benzophenones are still attractive as they are easy to be prepared and able to penetrate membrane cell due to their hydrophobic characteristic.

Among these photolabels, diazirines, particularly trifluoromethylphenyl diazirines are favored due to its excellent stability toward number of factors such as temperature, nucleophiles, and both acidic and basic condition. Besides, they also require having a shorter irradiation time and longer wavelength which can reduces the risk of damaging other biomolecules. The carbene intermediates formed during photoactivation is extremely reactive

and has a short life, which rapidly forms covalent cross-links with other biomolecules and easily quenched with water molecules. However, this feature is an advantage as it can minimizes unspecific labelling.

1.3 Identification tags for photoaffinity labeling

In photoaffinity labelling, other factors that need to be considered is the reporter tag. Reporter tags are incorporated directly or indirectly in the probe upon photoactivation to facilitate separation of the photolabeled protein. There are two major methods used to isolate the target protein. First, is the utilization of click chemistry, a reaction that allows the introduction at the later stage. In this approach, the two components of photolabeling probe where the photoreactive and bioactive ligand are in a separate molecule to the reporter tag, while the two components of alkyne and azide on the two halves allows formation of triazole via 1,3-cycloaddition reaction (Fig. 4).

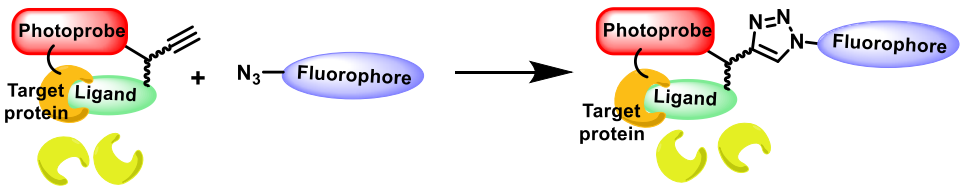

Fig. 4 Photoaffinity labeling technique utilizes click reaction

Fluorophore are frequently used for activity-based proteomics and has a wide range of variety. Most commonly used fluorophores are fluorescein, BODIPY, Rhodamine and NBD (nitrobenz-2-oxa-1,3-diazole) (Fig. 5). Each class has their own advantage and disadvantages. Generally, these tags are bulky, hydrophobic and can penetrate the cell membranes easily. Fluorescein and rhodamine are inexpensive compared to with the other tags: however they suffer from photo bleaching which is a major drawbacks. In comparison, BODIPY exhibit high absorption coefficients, narrow absorption peaks providing clearer detection and identification.

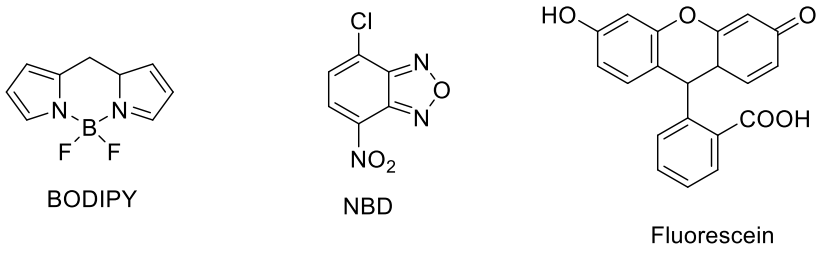

Fig. 5 Examples of fluorophore

Another method is the application of affinity probe. The most commonly used affinity tag is the avidin-biotin system, which utilizes the strong affinity between biotin and avidin. The avidin-biotin complex can be detected by chemiluminescence detection that have the same sensitivity as achieved by radioisotope analysis. This type of probe is called biotin probe. This affinity tags allow easier enrichment of avidin-containing proteins, isolation of the labeled proteins and are detected by relevant antibodies. However, these tags are usually bulky and non-cell permeable, and they may cause steric hindrance between the bioactive ligand and the target proteins.

Besides these methods, radioactive isotopes such as ^{125}I and ^{3}H are also frequently used as tag reporter for photoaffinity labeling. However, the main disadvantage of this method is that it does not provide a direct means to isolate labeled proteins from the rest of proteome. Other disadvantage is fast degradation of the radiolabel due to its short half-lives.

1.4 Application of photoaffinity labeling

Next is the examples of photoaffinity labels using biotin tag, fluorescent dye and tritium (radiolabel) as reporter tag, respectively. Pladienolides are natural products that exhibit antitumor activity in a variety of in vivo and in vitro systems but until recently, uncertainty remained about their protein target(s). Kotake *et al*.[8] prepared three types of pladienolide-derived probes; a 3H-labeled analog, a fluorescence-tagged (BODIPY-FL) compound and a photoaffinity probe (Fig. 6). These molecules were constructed based on the results of previous SAR. HeLa cells were treated with the tritiated probe, and the subcellular distribution of the radioactive signal was evaluated. This revealed that the nuclear fraction exhibited the highest radioactivity, strongly suggesting that pladienolides have a high affinity toward a nuclear protein. In order to limit the number of possible targets, immunoprecipitation experiments were performed using specific antibodies for a range of nuclear proteins on the nuclear fraction from the tritiated probe-treated HeLa cells. The radioactivity was detected in six of the co-precipitates, five of which were formed using antibodies known to recognize components of the ribonuclear protein U2 snRNP, which has a key splicing apparatus function at the 3′ site of mRNA. The main target of these natural products was identified by treating fractionated HeLa cells with the photoaffinity probe. An immunoprecipitate of the nuclear fraction was formed using an anti-SAP155 antibody, and the photoaffinity probe was activated by UV creating a covalent bond between the probe and its target. Western blotting with streptavidin horseradish peroxidase revealed a significant band of around 140 kDa. This was identified using LC–

MS/MS peptide sequencing. Overall, the results showed that pladienolides have affinity to SAP130 of the SF3b complex and can therefore inhibit mRNA splicing. This work demonstrated that mRNA splicing machinery may be a viable antitumor drug target.

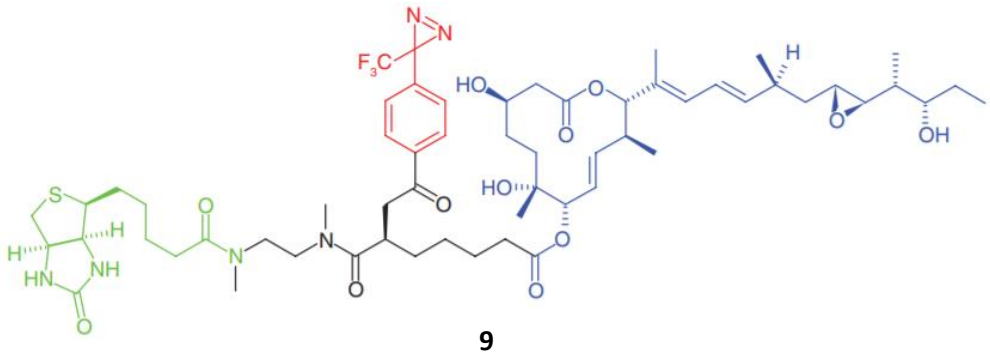

9

Fig 6. Pladienolides **9** derived photoaffinity probe containing phenyl diazirine and biotin

The transcription factor HIF promotes angiogenesis and metastasis and is a potential target for cancer therapy. The small molecule LW6 inhibits HIF1α accumulation and consequential HIF transcriptional activity; however the molecular targets responsible were unknown. Lee et al. [9] designed and synthesize photoaffinity probes of LW6 based on prior SAR studies (Fig. 6), which were placed in HCT116 cells, irradiated and click conjugated with a fluorescent reporter tag. The proteins were separated by SDS- PAGE and visualized by in-gel fluorescence scanning, giving a prominent band around 37 kDa. Following trypsin digest and sequencing of the peptides by MS, this protein was identified as MDH2, a mitochondrial enzyme involved in the tricarboxylic acid cycle. Further studies showed LW6 interacted with and inhibited MDH2. It also known that inhibitor of MDH2 potently inhibited HIF transcriptional activity.

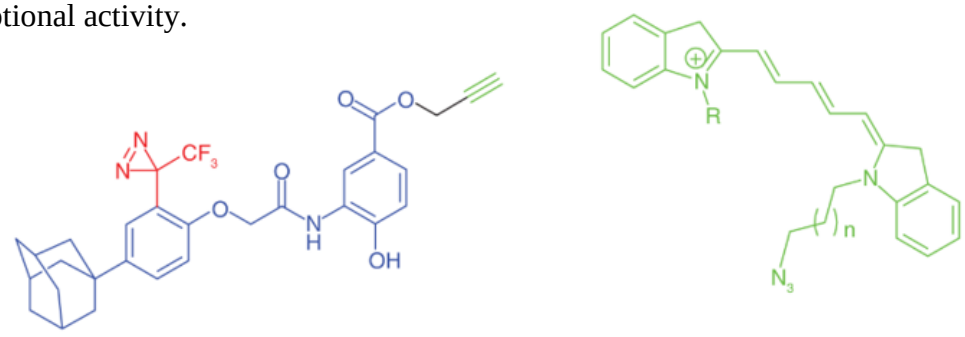

Fig 6. LW6 derived phenyl diazirine photoaffinity label utilized click chemistry

Tamoxifen is a selective ER modulator (SERM) used to treat ER-positive breast cancer in pre- and post-menopausal women. There are proteins and protein complexes which possess antiestrogen binding sites (AEBS) that have high affinities for triphenylethylenic com- pounds like tamoxifen. These proteins were thought to be responsible for some of the other biological effects of tamoxifen, such as changes in serum lipid composition. To identify AEBS-containing proteins that directly interacted with tamoxifen, Mésange et al. [10] developed a tritiated photaffinity probe, 4-(2-morpholinoethoxy) benzophenone ([3H]MBoPE) (Fig. 7) which did not bind to ER but retained activity against hmEH, a known AEBS-containing protein identified from a previous PAL experiment [10]. Labeling of this protein by [3H]MBoPE was clearly competed by increasing concentrations of tamoxifen. [3H]MBoPE was incubated in solubilized microsomal proteins, and following irradiation, subsequent separation, isolation and MS sequencing; three proteins were identified. These were the previously known target, hmEH and two novel targets; ES10 and L-FABP. Both proteins are involved in lipid metabolism and their discovery as molecular targets of tamoxifen suggested they may account for the mode of action by which tamoxifen affects serum lipids

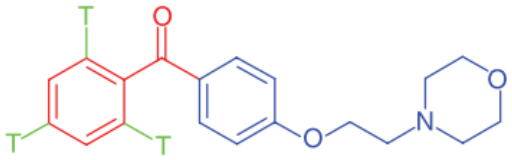

Fig 7. Tamoxifen derived photoaffinity labelling containing tritiated benzophenone

1.5 Examples of previous works

As a result of rapid development on mass spectrometry and bioinformatics in chemical biology, increasing number of biological targets have been identified. In addition, the approach on photoaffinity labels also have been rapidly developed. Some of the recently reported works on new approaches utilizing photoaffinity labeling are discussed as follows.

Hatanaka and co-workers have developed a photo-switchable fluorescent flagging approach to identify photoaffinity-labeled peptides in target protein[11]. In this approach, they incorporate o-hydroxycinnamate diazirine functionality. This photolabel (Fig.8) is photoirradiated twice, which the first irradiation is to generate a carbene for photocross-linking and the second irradiation is to form *E-Z* photo isomerization of the cinnamate group. The photo isomerization of the cinnamate group induces intramolecular lactonization *via* nucleophilic substitution by a hydroxy group at the *ortho* position (Fig. 9). The authors applied

this concept in identifying the substrate-domain of the vacuolar sorting receptor (VSR) of soybean. Photolabel was treated with recombinant luminal soybean VSR with 360 nm light. Western blotting using horseradish peroxidase (HRP) revealed a band around 55 kD and the yield of cross-linking was about 5%. This was determined by comparison with the emission intensity of biotinylated BSA. Then upon second photoirradiation, fluorescence intensity increased with the irradiation time in response to the formation of coumarin. On the other hand, the emission intensity of ligand-cross-linked decreased along with time as the biotin was released upon formation of coumarin. After purification and digestion of the labeled GmVSR, the resulting peptides were separated using HPLC and were easily detected with high intensity using emission at 420 nm because of the coumarin. This tag switching strategy may allows a rapid identification of the labeled protein but the yield for *E-Z* photoisomerization was quite low and may decrease the photolabeling efficiency.

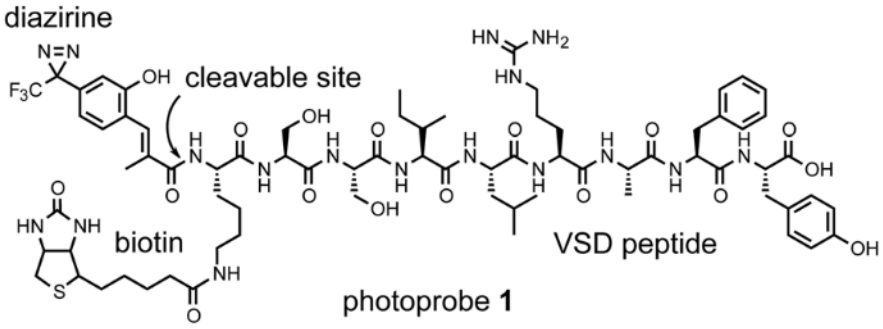

Fig 8. Structure of photoreactive VSD probe

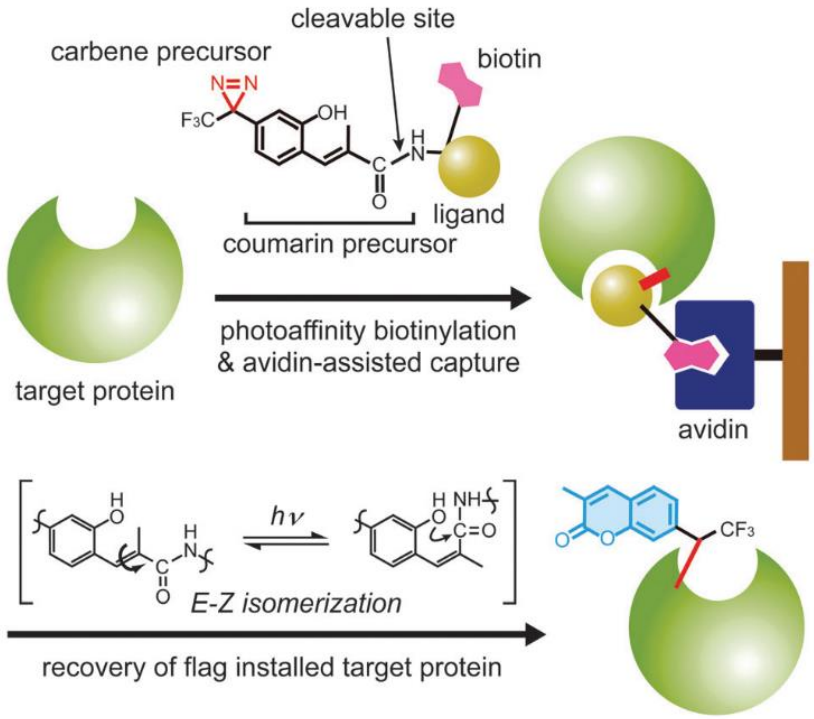

Fig 9. Tag-switching strategy for the identification of target proteins by sequential photoirradiation

Other examples of photoaffinity labeling approach was reported by Qing Lin et al, which designed new photoaffinity label, 2-aryl-5-tetracarboxytetrazole (ACT)[12]. In this concept, ACT interacts with the target protein via reaction between the photogenerated carboxynitrile imine and the proximal nucleophile near the target active site. In order to prove their concept, photolabel (Fig. 10) that composed of ACT and dasatinib as bioactive ligand are treated in recombinant BTK and BRD4 proteins. The photo-cross-linked adducts were detected using in-gel fluorescence analysis after copper-catalyzed click chemistry with rhodamide azide. Next, the cross-linked sites on the target protein was digested and subjected to LC-MS/MS. Based on the results obtained, they proposed that the photoadduct is formed via nucleophilic addition of glutamate carboxylate to the carboxy-nitrile imine intermediate followed by a 1,4-acyl shift (Fig. 11). Although, this new photoaffinity label, 2-aryl-5-carboxytetrazole (ACT) able to form an in-situ target capture and subsequent identification, it requires a nucleophile in the proximal area of the active site.

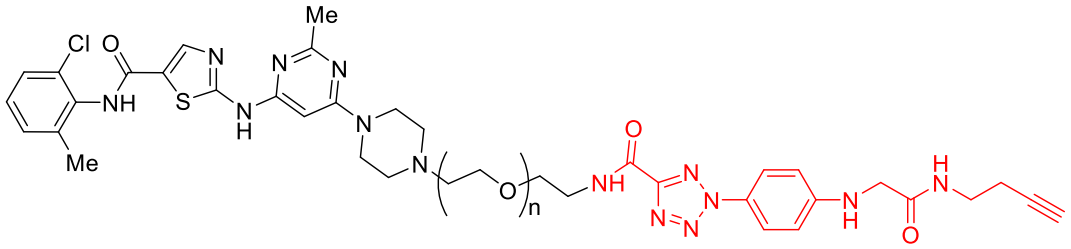

Fig 10. Proposed mechanism of the ligand-dependent nucleophilic addition to the carboxy-nitrile imine followed by the O → N acyl shift to generate the specific photoadduc

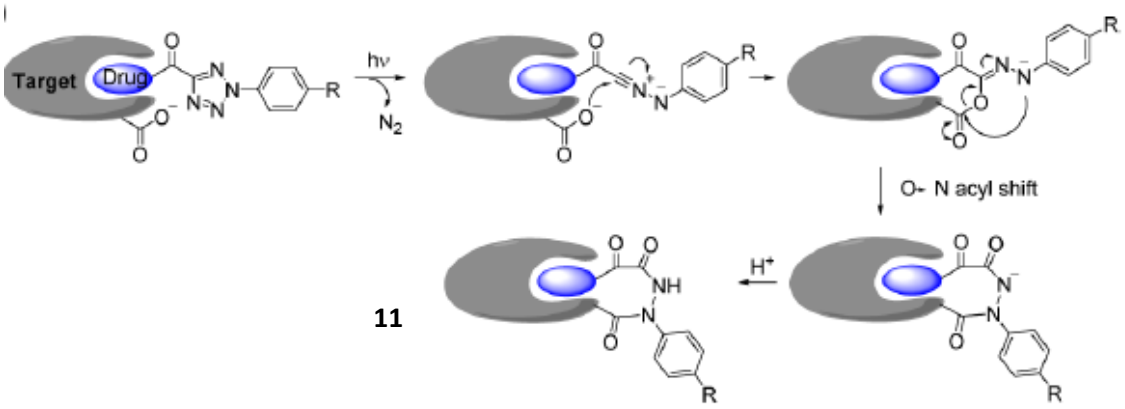

Fig 11. Dasatinib derived photoaffinity probes containing 2-aryl-5-carboxy tetrazole (ACT)

1.6 Meisenheimer complex, nosyl protection and its application

Nucleophilic aromatic reaction is an important reaction in organic synthesis, where a nucleophile is introduced into an aromatic ring containing electron deficient group. Generally, it proceeds through an addition-elimination mechanism[13]. In the first step the nucleophile would preferably attack the position ipso to the electron withdrawing group of the electron deficient aromatic ring to yield an anionic sigma adduct intermediate. Typically, this intermediate with a tetrahedral (sp^3) carbon is unstable, and the reaction could either proceed forward by rearomatization to generate the substituted product or simply revert back to the reactants. When the aromatic ring is substituted with various electron withdrawing groups (EWG) such as $-NO_2$, -CN, $-CF_3$ or $-SO_2CF_3$, the anionic sigma complex is stabilized due to the added delocalization of the negative charge by the EWG in conjugation with the aromatic ring (Scheme 1). These intermediates are also called σ- or Jackson-Meisenheimer-complexes, named after the scientists who proposed a possible quinoid-like structure of the compound

formed after adding an equimolar amount of sodium methoxide to an acetone solution of 2,4,6-trinitroanisole [2,3]

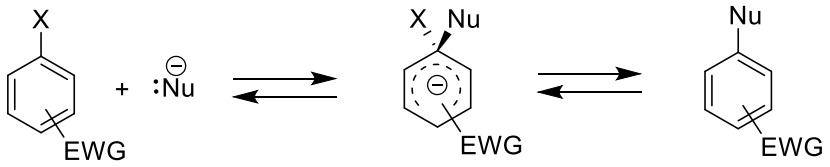

Scheme 1. Formation of Meisenheimer complex

Fukuyama et al. introduced 2- and 4-nitrobenzenesulfoamides which could be use as a secondary amine protection group. It is easily prepared from primary amines and undergo smooth alkylation by Mitsunobu reaction or by conventional methods to give N-alkylated sulfonamides. These sulfonamides could be deprotected readily via Meisenheimer complexes upon treatment with thiolates giving secondary amines [14]. Intrigued by this mechanism, a few works have been reported on the application of nosyl functionality in chemical biology.

Reactive oxygen species (ROS) regulates various biological processes by modifying reactive cysteine in the proteins participating in the relevant signaling pathways. Lee et al. designed and synthesized a specific reagent containing nitrobenzesulfoamide that could identify reactive oxygen species (ROS)-sensitive cysteine sulfhydryls[15]. They validated its specificity by allowing it to react with recombinant proteins followed by peptide sequencing. In addition, mutant studies were also conducted to identify the cellular proteins containing redox-sensitive cysteine residues (Fig. 12)

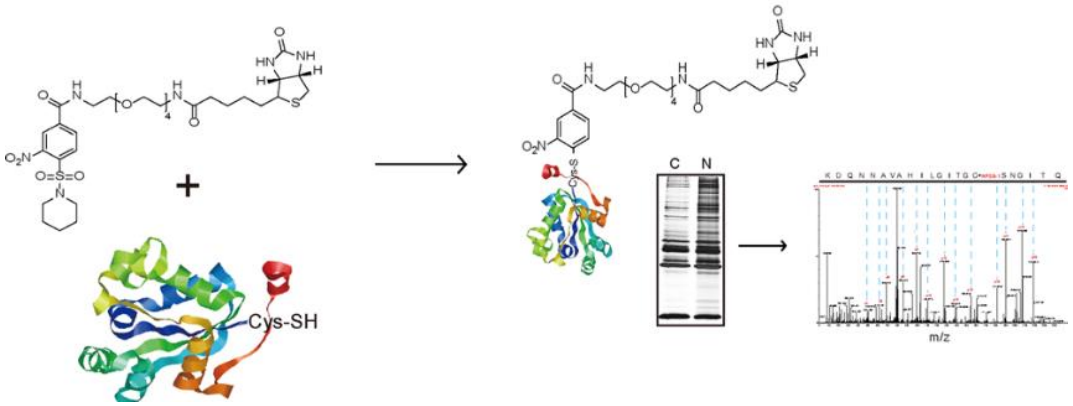

Fig. 12 Reaction of nitrobenzene sulfonamide containing NPSB-1 with sulfyhydryl cysteine in model compounds

Based on this, it attracts our attention to utilize 2,4-dinitrobenzenesulfonamide (Nosyl) into our photoaffinity labelling approach. The following scheme describes the mechanism whereby the nitro group stabilizes the anion intermediate to produce the corresponding amines[16] (Scheme 1). Stabilization of the anionic intermediates by electron-withdrawing groups facilitates the reaction. Details on the concept and experiments of this approach are discussed in the next chapter

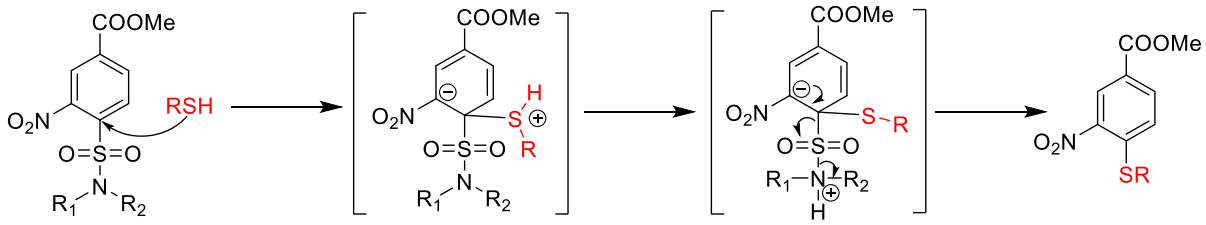

Scheme 2. Mechanism on the deprotection of Nosyl group

1.7 References

1. Singh, A., Thorton E. R., Westheimer, F. H., The photolysis of diazoacetylchymotrypsin. *J. Biol. Chem.*, **237**, (1960).

2. Smith, E. & Collins, I. Photoaffinity labeling in target-and binding-site identification Europe PMC Funders Group. *Futur. Med Chem* **7**, 159–183 (2015).

3. Gris, D. Public Access NIH Public Access. **185**, 974–981 (2013).

4. Wang, J., Chen, Q., Shan, Y., Pan, X. & Zhang, J. Activity-based proteomic profiling: The application of photoaffinity probes in the target identification of bioactive molecules. *TrAC - Trends in Analytical Chemistry* (2019). doi:10.1016/j.trac.2019.03.028

5. Geurink, P. P., Prely, L. M., Van Der Marel, G. A., Bischoff, R. & Overkleeft, H. S. Photoaffinity labeling in activity-based protein profiling. *Topics in Current Chemistry* **324**, 85–113 (2012).

6. Terstappen, G. C., Schlüpen, C., Raggiaschi, R. & Gaviraghi, G. Target deconvolution strategies in drug discovery. *Nat. Rev. Drug Discov.* **6**, 891–903 (2007).

7. Adakane, Y. S. & Atanaka, Y. H. Sadakane Y, Hatanaka Y. Photochemical fishing approaches for identifying target proteins and elucidating the structure of a ligand-

binding region using carbene-generated photoreactive probes. Anal. Sci. 2006; 22:209–218. [PubMed: 16512410]. **22**, 209–218 (2006).

8. Kotake, Y. *et al.* Splicing factor SF3b as a target of the antitumor natural product pladienolide. *Nat. Chem. Biol.* **3**, 570 (2007).

9. Lee, K. *et al.* Identification of malate dehydrogenase 2 as a target protein of the HIF-1 inhibitor LW6 using chemical probes. *Angew. Chemie - Int. Ed.* **52**, 10286–10289 (2013).

10. Mésange, F. *et al.* Identification of two tamoxifen target proteins by photolabeling with 4-(2-morpholinoethoxy)benzophenone. *Bioconjug. Chem.* **13**, 766–772 (2002).

11. Online, V. A. Photoaffinity casting of a coumarin flag for rapid identification of ligand-binding sites within protein †. (2013). doi:10.1039/c3cc38594a

12. Herner, A. *et al.* 2-Aryl-5-carboxytetrazole as a New Photoaffinity Label for Drug Target Identification. *J. Am. Chem. Soc.* **138**, 14609–14615 (2016).

13. Al-Kaysi, R. O., Gallardo, I. & Guirado, G. Stable spirocyclic Meisenheimer complexes. *Molecules* **13**, 1282–1302 (2008).

14. Fukuyama, T., Jow, C. K. & Cheung, M. 2- and 4-Nitrobenzenesulfonamides: Exceptionally versatile means for preparation of secondary amines and protection of amines. *Tetrahedron Lett.* **36**, 6373–6374 (1995).

15. Lee, J. J. *et al.* Sulfhydryl-specific probe for monitoring protein redox sensitivity. *ACS Chem. Biol.* **9**, 2883–2894 (2014).

16. Schwan, A. L., Verdu, M. J., Singh, S. P., O'Donnell, J. S. & Ahmadi, A. N. Diastereoselective alkylations of a protected cysteinesulfenate. *J. Org. Chem.* **74**, 6851–6854 (2009).

Chapter 2
Designed, synthesis and evaluation of the nosyl diazirine

Abstract

Photoaffinity labelling is a powerful tool for identifying molecular interactions between bioactive molecules (ligand) and targeted biomolecules. Traditional photoaffinity label consists of three main components; a photophore (ie diazirine), a ligand and detection/purification tags. Although this method has been widely used, target identification is still a challenging task. The bulkiness of the photolabel sometimes interferes in capturing the target biomolecules, which will decrease the affinity of the original active ligand. Herein, designed and synthesized of nosyl diazirine which incorporated two functional groups (photophore and ligand) was reported. In this approach, the formation of Meisenheimer complex was utilized to install various tags for identification purposes.

Chapter 2 Design of an "exchangeable tag" photoaffinity label

2.1 Introduction

Identification of target protein holds a vital role in early stage of drug discovery[1]. It has been known that biotechnology at the genetic level still has some limitations in identifying molecular target for certain diseases. For these purposes, several approaches have been rapidly developed such as X-ray crystallography and solution state NMR. X-ray crystallography is a very valuable technique in understanding the nature or ligand-protein interaction. While, 3D structural determination could be achieved *via* NMR spectroscopy and homology modelling, it requires large quantities of expressed proteins. Although these conventional methods provide a valuable information in elucidating the target protein, it requires a relatively pure protein. Nowadays, photoaffinity labelling (PAL) has been developed as an important technique used for the study of protein-ligand interaction, where it can identify unknown targets of ligands, assist in elucidation of protein structures, functions and conformational changes as well as identify novel or alternative binding sites in proteins[2].

Concept of photoaffinity labelling was first introduced by Frank Westheimer in 1960s, using acylation to incorporate an aliphatic diazo group into the enzyme chrymotrypsin, which formed an intramolecular crosslink on photolysis. Conventional photoaffinity label is consist of three main components, which are photoreactive moiety, bioactive ligand and reporter/identification tag. Although this approach has been widely used due to the ability to cross-link with its target protein, it also has some disadvantages. First, steric hindrances caused by the incorporation of three bulky functional group often reduces the affinity between the bioactive ligand and its target protein. Second, difficulties in purification process by inevitable contamination that is due to non-specific labelling and significant lost of the sample. Third, design and synthesis of the photolable composing of photoreactive, ligand and reporter tag are quite cumbersome. In order to overcome these problems, we have designed and synthesized a nosyl diazirine by photoaffinity probe.

Fukuyama and co-workers reported that nitrobenzenesulfonyl chloride can be used as amine protecting group with that their deprotection could be specifically achieved by treatment with thiol groups via formation of meisenheimer complex[3]. Intrigued by the selective deprotection of nosyl group by thiol group, we designed and synthesized a substituted phenyl sulfoamide with nitro group at the meta position and trifluromethyl diazirine at the para

position. The function of nitro group at the meta position of benzyl sulfoamide is i) to facilitate the formation of meisenheimer complex during S_NAr reaction and ii) to enhance the generation of carbene during photoactivation (Fig. 1). Our approach highlighted the introduction of modified thiol tags via Meisenheimer complex into the photoaffinity labelled complex which was irradiated under UV lamp in the presence of proteins.

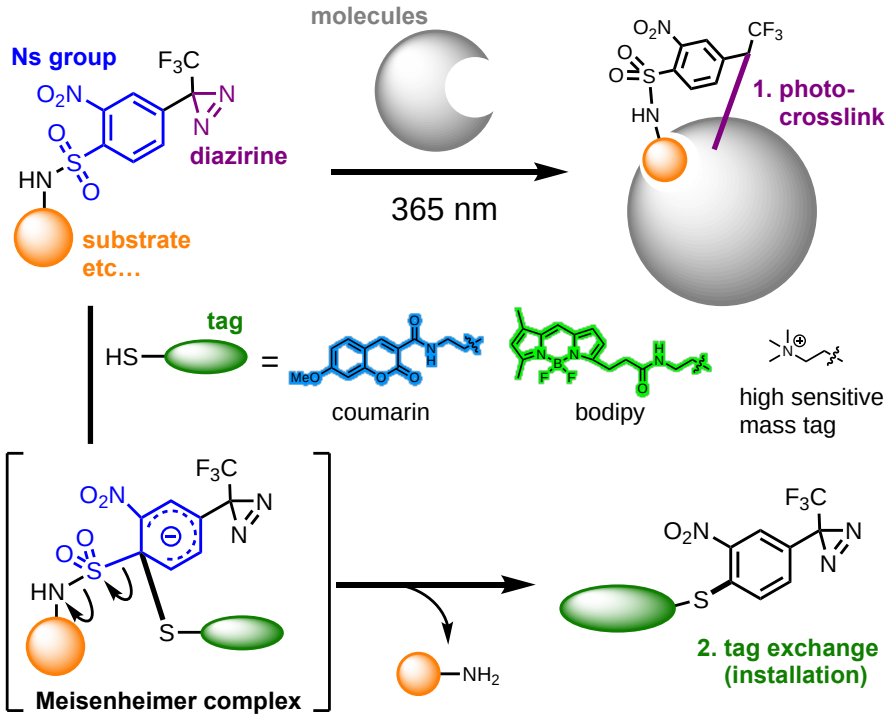

Fig. 1. Structure of the Ns-based photo-crosslinker and its functional

2.2 Synthesis of novel nosyl diazirine

The synthesis of the proposed novel nosyl diazirine began with the introduction of nitro functionality *via* substitution aromatic nucleophilic reaction in the presence of potassium nitrate and sulphuric acid which gave us 86% yield of nitro benzaldehyde, **13**. The desired compound **13** was then treated with trimethylsilyl and followed by the deprotection of TMS in acidic condition. Next, we performed the oxidation reaction using oxone as described by Konno *et al.* which gave us with ketone, **15** in moderate yield of 68%[4]. Based on the nmr spectra, a mixture of our desired ketone was obtained together with diol as side products. In order to optimize this step, oxidation using synthesized IBX in DMSO/H_2O was attempted and it gave us with a high yield of 83% [5]. The corresponding ethenone oxime, **17** was obtained via the

treatment of **15** with oxime hydrochloride in pyridine. The oxime group in **17** can be activated to form a good leaving group by using p-tosyl chloride (TsCl) to give a tosyl oxime, **18** before converting to diaziridine **19** in liquefied NH_3 [2]. Next **19** was oxidized to diazirine using manganate oxide in diethylether. Finally, benzyl mercaptan was directly introduced into the diazirinyl benzene, **20** in the presence of diisopropylethyl amine as base with yield of 90% [6].

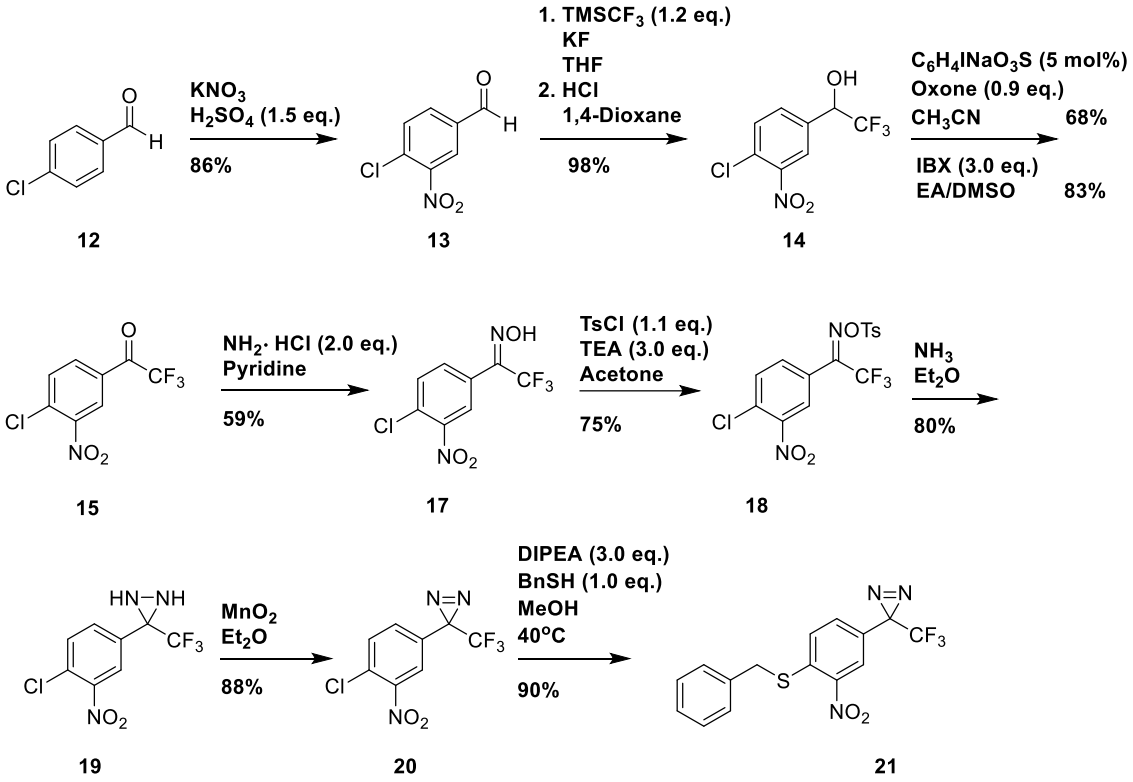

Scheme 1. Synthesis of diazirinyl benzene mercaptan

Having successfully synthesized the diazirinyl benzene mercaptan, **21**, we then proceed on with the oxidative chlorination reaction which is the key step in this synthetic strategy. Diazirine mercaptan, **21** was treated with N-chlorosuccimide (NCS) in the presence of acetic acid and sodium chloride[6].

Based on the result obtained, NCS was effective in converting our nosyl diazirine mercaptan to the corresponding sulfoxide, but ineffective in breaking the C-S bond required for the formation of sulfonyl chloride. Thus, as an alternative, the oxidative chlorinating reagents was changed to an effective and easy to use 2,4-Dichloro-5,5-dimethyl hydantoin (DCDMH)[7]. Remarkably, when our compound **21** was subjected to the reaction conditions with 3 equivalents of DCDMH in combination of acetonitrile, acetic acid and water, the starting

material was completely consumed. However, the desired compound sulfonyl chloride, **22** was found out to be unstable as it was immediately hydrolysed to sulphuric acid compound **23**.

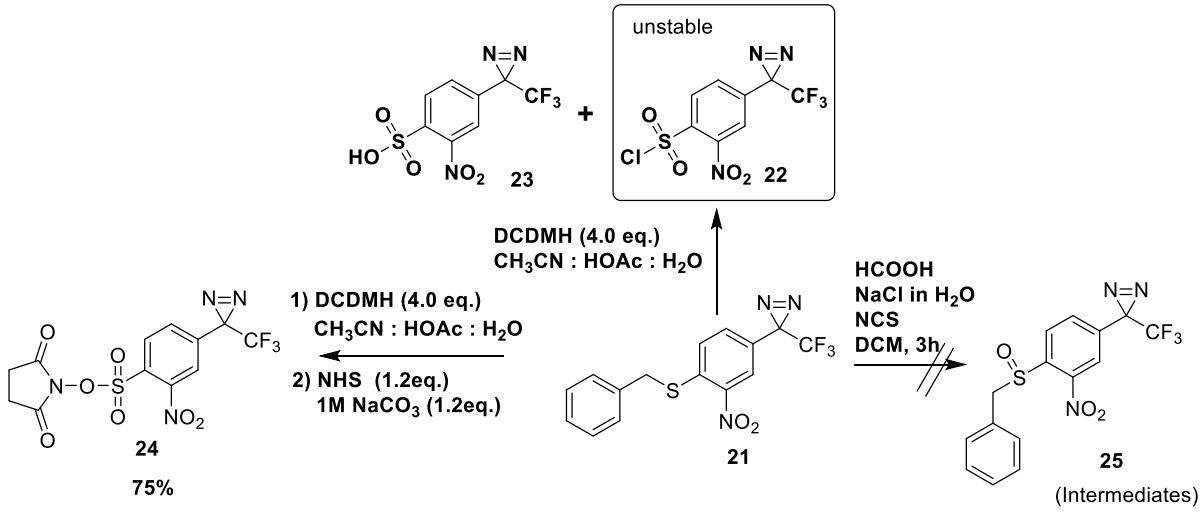

Scheme 2. Optimization of oxidative chlorination reaction

Thus, we changed our approach by incorporating a more stable N-hydroxysuccinimide which we foresee that it will act like a protecting group. Upon the conversion to sulfonyl chloride, the synthesized sulfonyl chloride was treated with NHS and sodium carbonate. This reaction was successfully proceeded with high yield which afforded us with NHS protected phenyl diazirine, **24**.

Having NHS protected diazirine, **24** in hand, we then proceeded with the introduction of amine to form a sulfoamide. However, to our surprised, an unknown compound was obtained instead of the desired sulfoamide. In order to identify the cause, similar reaction using a simpler model compound was performed. As we expected, the desired compound, **28** was not observed. We proposed that it might undergo a Lossen-like rearrangement[8], which is induced by the nucleophilic secondary amine functionality of piperidine and gave us with diamide, **31**.

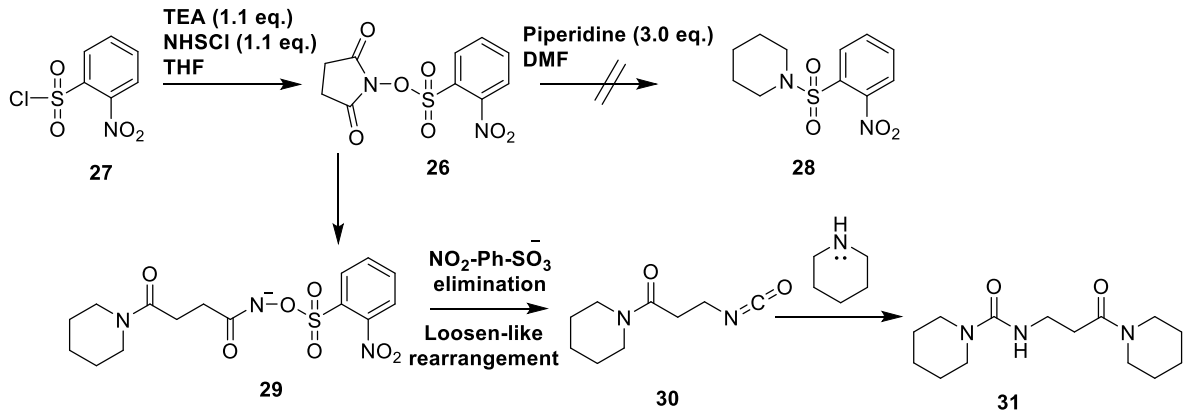

Scheme 3. Proposed mechanism for the formation of side product 21

With the regards of the above information, next we decided to directly introduce an amine upon the conversion to sulfonyl chloride *via* 2 steps. Diazirinyl benzene mercaptan, **21** was treated with DCDMH in combination of acetonitrile, acetic acid and water followed by the introduction of aminoethanol in solution of Na_2CO_3 which gave us with sulfoamide, **32** in yield of 64%. Compound **32** was then used as a model compound for the evaluation of carbene generation.

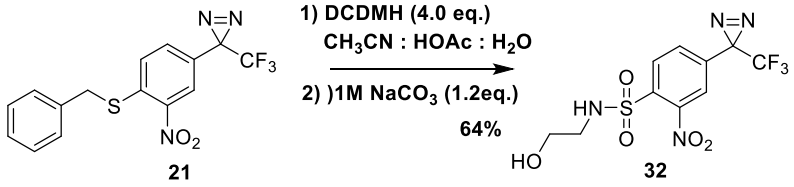

Scheme 4. Synthesis of our model photolabel compound

2.3 Photoactivation

As shown in Scheme 5, upon photoactivation the diazirine is converted into a singlet carbene, which in turn forms an insertion product with the solvent, and the linear diazo compound[9]. Due to the high reactivity of the carbene, it can rapidly react with the bound receptor before the activated photoaffinity dissociates. Although the undesired diazo compound is produced, it can be easily generated to carbene on the use of shorter wavelength[10] or with longer irradiation time[11]. Since it was reported that longer irradiation time for the generation of reactive species could cause cell death, there is a need to identify the time required for photoirradiation.

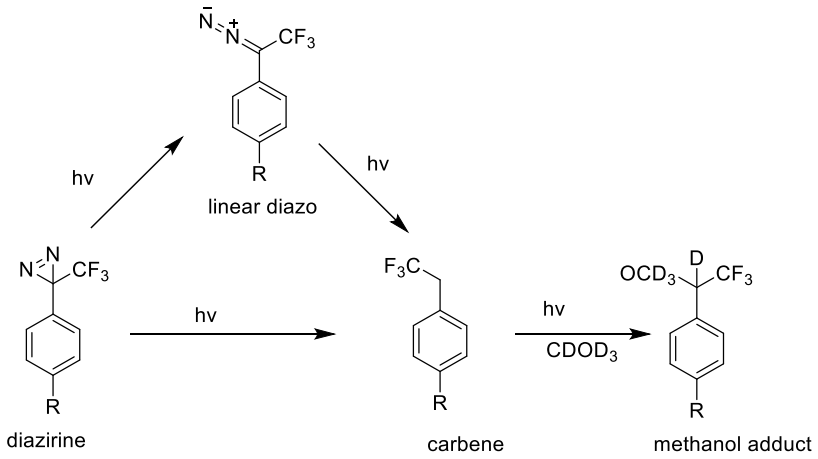

Scheme 5. Photoactivation path of diazirine photolabels

In order to evaluate its photoreactive properties and kinetic photolysis, our model compound **32** was compared to normal phenyldiazirine by irradiation of both compounds under black light (30W) in methanol. The results revealed a decrease in the absorbance of diazirine at around 355 nm as the irradiation time proceeds (Fig. 2).

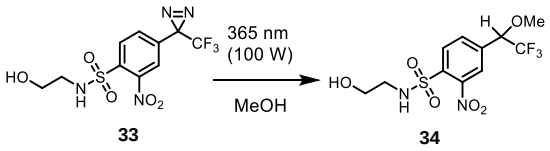

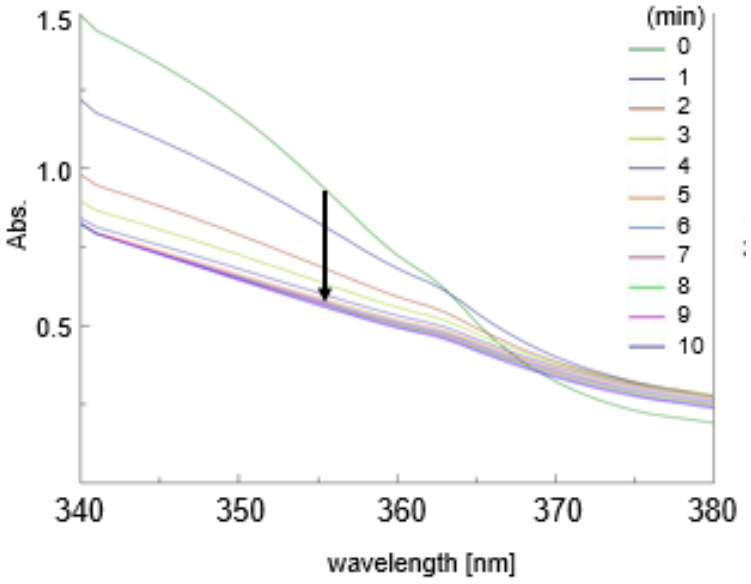

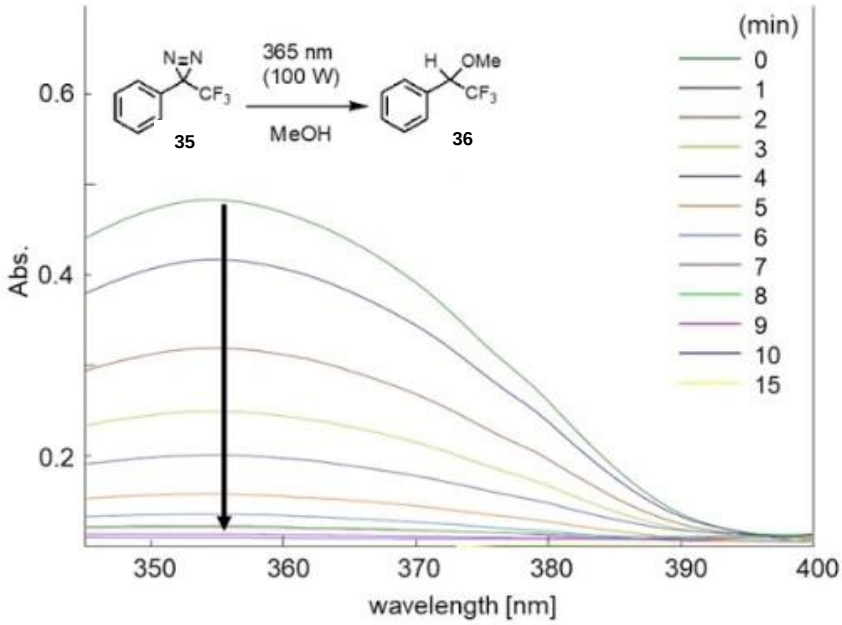

Fig. 2**.** UV-vis spectra in methanol of A) Ns diazirine **33** (2.00 ×10^{-3} M), B) trifluoromethyl phenyldiazirine **35** (2.00 ×10^{-3} M) under irradiation of 365 nm light at 0 °C in a sealed quartz cuvette

Based on these results, Ns diazirine was found to be photolyzed more rapidly in comparison with normal phenyl diazirine as the calculated half-lives ($t_{1/2}$) are 2.5 and 4.5 min, respectively. The methoxylated compound **34** was also confirmed with ESI-MS (m/z 382.2 M^+Na^+) and ^{19}F NMR after completion of photolysis (Fig.3). These results indicated that the irradiation effectively promoted decomposition of the Ns diazirinyl ring and the generation of highly reactive carbene. This strengthen the fact that Ns diazirine exhibited suitable characteristics for the photoaffinity reagent.

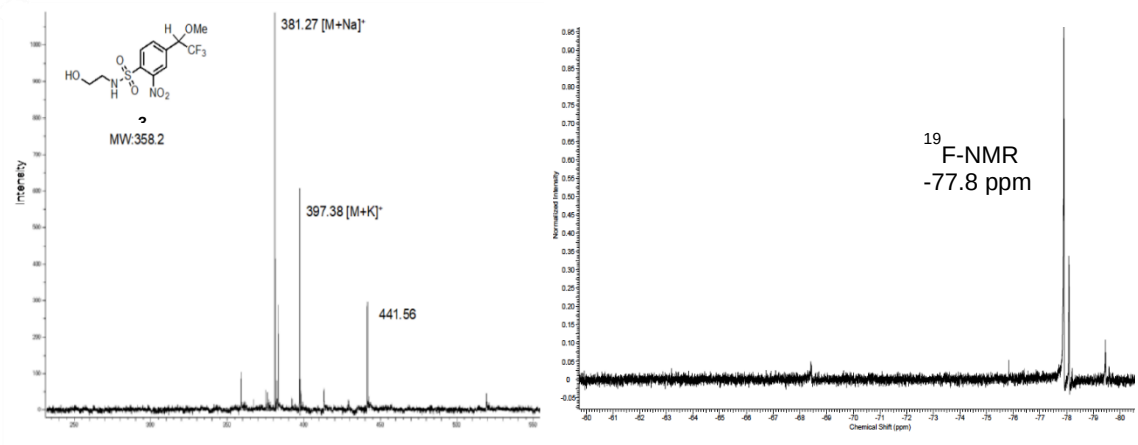

Fig. 3. ESI-MS analysis and ^{19}F NMR spectra of compound **33** after photoirradiation for 10 min.

2.4 Evaluation of "Meisenheimer complex"

4-Nitrobenzene sulfoamides (nosyl) group has been widely used as a protection of secondary amine and that their deprotection of nosyl group can be specifically obtained by treatment of thiol group via the formation of meisenheimer complex. Thus, in this section, modifications of the thiol tag and optimization of the removal of nosyl group will be further discussed.

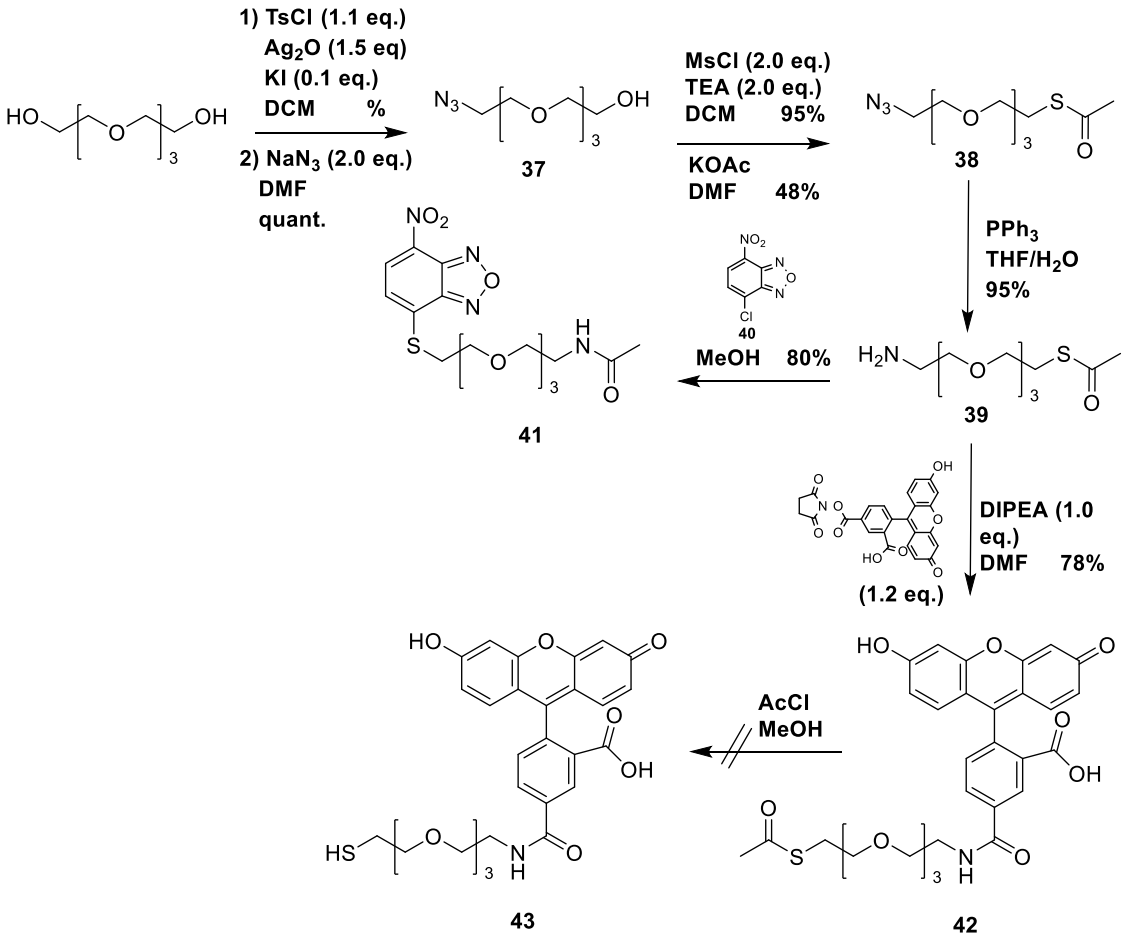

Scheme 6. Towards the synthesis of NBD- and Fluorescein linker

2.4.1 Synthesis of the modified thiol tag

In the effort to synthesize the thiol identification tag, first the thioacetate amine linker was synthesized through 5 steps as described below (Scheme 6). Our synthetic strategy of synthesizing the linker began with mono-tosylation of polyethylene glycol and followed by

azidation using sodium azide, which gave us compound **37** in quantitative yield. Next, mesylation of the remaining hydroxyl group was carried out before it was converted to thioacetate. Then reduction of azide was carried out in the presence of PPh_3 in THF/H_2O and afforded us with amine **39** with 94 % yield. Subsequently, the amine linker was coupled with NHS-Fluorescein to give fluorescein amine, **42** in yield of 80%. The final step of thioactate deprotection was carried out in acidic condition (TFA), but the desired product **43** was failed to obtain due to the instability of the fluorophore. Thus, we changed our identification tag to the commonly used 4-chloro-7-nitrobenzofuran, **33** (NBD-Cl). NBD-Cl was coupled with the amine linker in the same condition as the previous ones with 70% yield. However, to our surprised, methyl amide NBD, **41** was obtained instead of the thioacetate NBD. Hence, we hypothesized that it might have undergo a rearrangement upon the introduction of amine linker due to high nucleophilicity observed by the previously formed secondary amine.

Having to know this, NBD was once again treated with amino hydroxyl PEG, which was synthesize from compound **37** via reduction using Pd/C and H_2 to give pegylated NBD, **45** with 42% yield. Next, the hydroxyl group was protected with mesyl and followed by the introduction of thioacetate which afforded 71% of thioacetate NBD, **40**. Finally, the removal of thioacetate was performed in an acidic condition of TFA to give us with our desired thiol-NBD tag, **47** in quantitative yield.

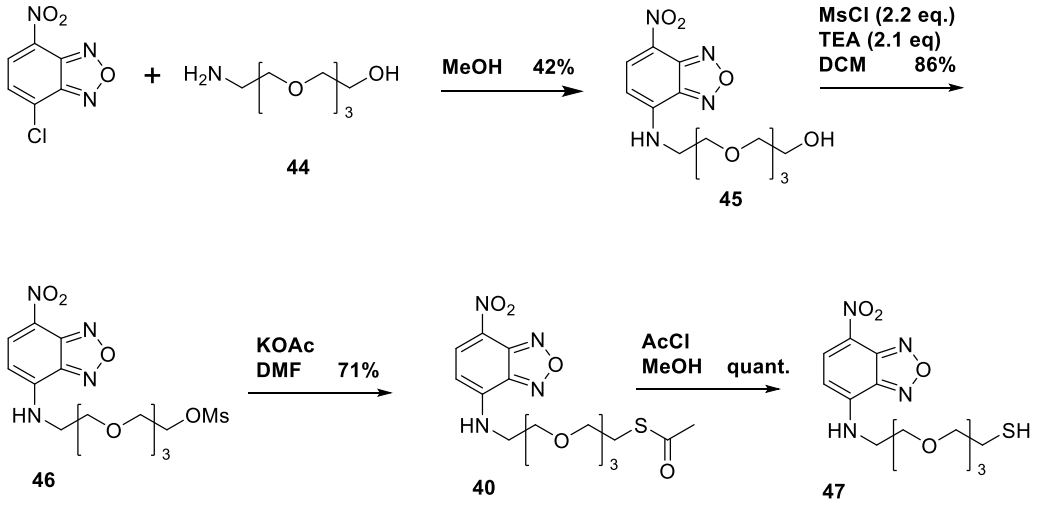

Scheme 7. Synthesis of thiol NBD

Besides NBD thiol tag, we also modified methoxy coumarin and BODIPY as an alternative tag. The synthesis of these compounds was performed via one step by coupling aminoethanthiol with N-succimidyl-7-methoxy coumarin carboxylate and BODIPY FL N-

hydroxy succinimide ester which afforded us with the desired tag with 87% and 20% yield respectively (Scheme 8).

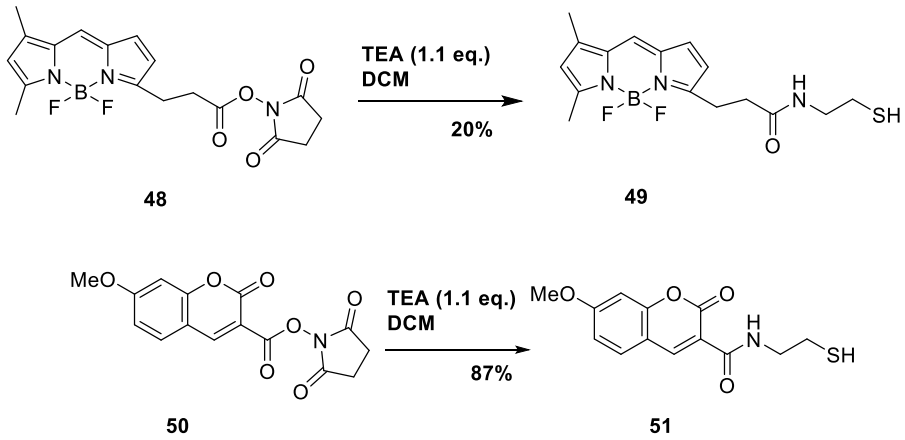

Scheme 8. Synthesis of thiol methoxy coumarin and BODIPY

2.4.2 Introduction of thiol modified tag via formation of meisenheimer complex

Having our modified thiol tags in hand, we then attempted to cleave the sulfoamide unit under physiological conditions. Amino ethanol bearing Ns diazirine, **33** was used as the model compound and treated with 1.5 equiv. of methoxy coumarin thiol derivatives **51** in different conditions. All the reactions progress was monitored by TLC and determined by isolation of compound **52**. The S_NAr proceeded smoothly in THF with the presence of Cs_2CO_3 to afford Ns diazirine coumarin, **52** in excellent yield, whereas the tag-exchanged reaction without basic condition did not proceed entirely (Table 1). In contrast, this reaction proceeded moderately in ethanol and acetonitrile with the yield of 70-80%. Moreover, the S_NAr reaction was also carried out under aqueous condition, in which photoaffinity labelling is often performed. The cleavage reaction proceeded smoothly in aqueous media in the presence of Cs_2CO_3 which gave **52** in excellent yield 92%. However, in the case of using $NaHCO_3$ and triethylamine (TEA) as weak bases, the reaction required longer than 24 h reaction time. According to these results, although longer time is required for the reaction to be consumed under aqueous media, the tag-exchanged reaction proceeded smoothly, which means it is further applicable under physiological condition.

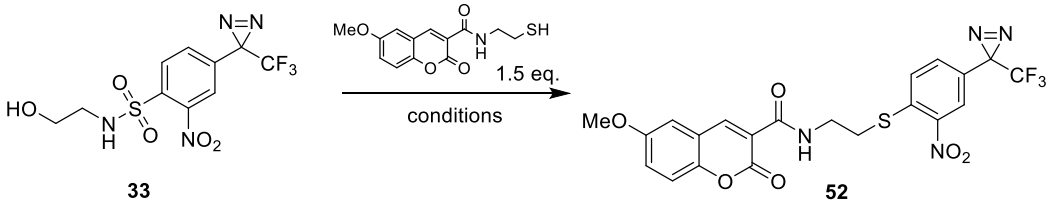

Scheme 9. Optimization of S_NAr via meisenheimer complex

Entry	Solvent	Base (3eq)	Time (h)	[a]Yield (%)
1	THF	–	24	0
2	THF	Cs_2CO_3	1	90
3	EtOH	Cs_2CO_3	2	73
4	CH_3CN	Cs_2CO_3	2	78
5	5% DMSO in H_2O	Cs_2CO_3	24	82
6	H_2O	Cs_2CO_3	24	92
7	H_2O	$NaHCO_3$	24	47
8	H_2O	TEA	24	35

Table 1. Optimization of S_NAr via meisenheimer complex formation

Besides methoxy coumarin thiol tag, we also attempted using other tags such as BODIPY and high sensitive mass tag to prove generality of tag-exchanged reaction between Ns diazirine and thiol linkages tags. These tags were subjected to Ns diazirine in the same conditions as described above. Expectedly, both **53** and **49** successfully confirmed the feasibility of tag-exchanged reaction to produce the tag inserted Ns diazirine **54** and **55**. Additionally, to confirm the advantage of high sensitive mass tag, compound **54** was subjected to measuring the ESI-MS after tag-exchanged reaction without any purification. Compound **54** exhibited strong intensity peak (m/z 349.1), which is 120 times higher than that of the reference compound, *N*,*N*,*N*-diethylamine type **56** (m/z 363.1) in the same condition (Fig. 4). Therefore,

we envisaged that photolabeled target molecules with Ns diazirine will simplify its analysis procedure with the installation of high sensitive mass tag by S_NAr.

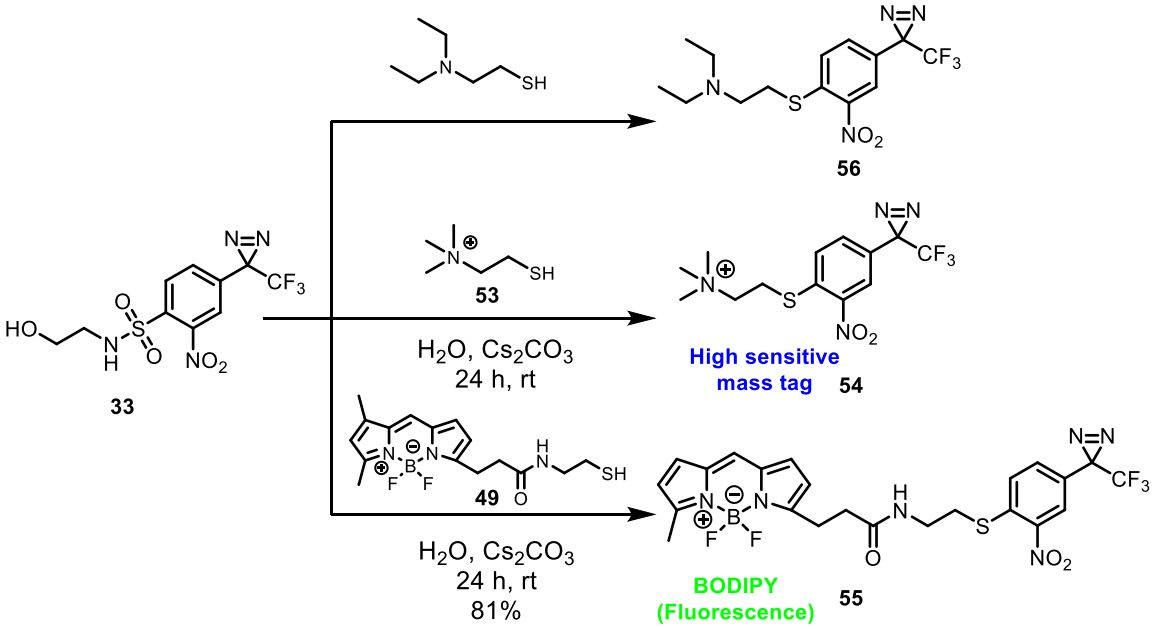

Scheme 10. The utility of the tag-exchanged reaction on Ns diazirine

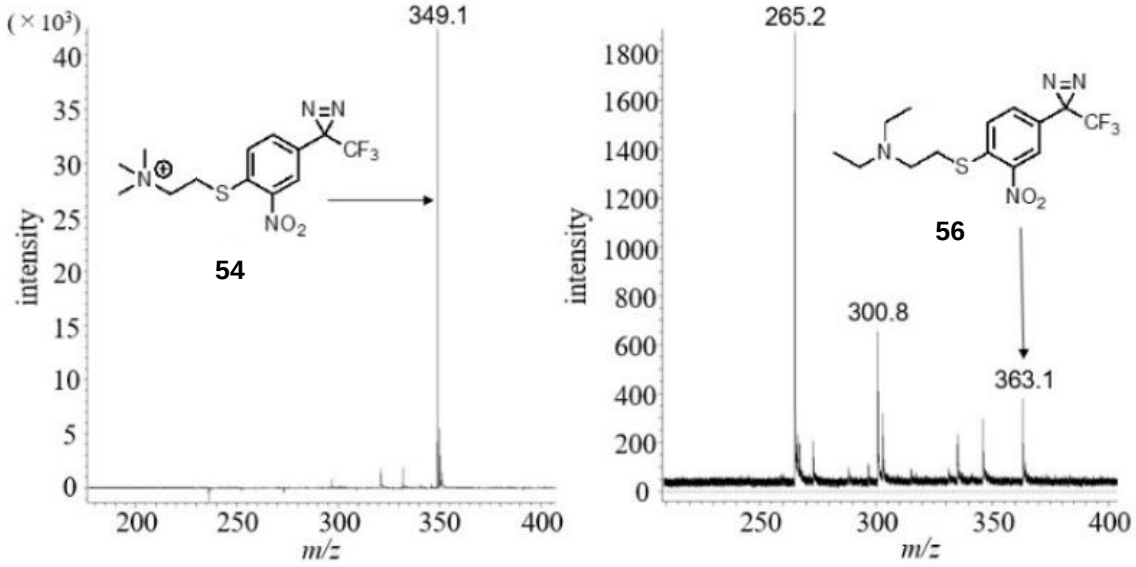

Fig. 4. ESI-MS analysis of compound 54 and 56 without purification after S_NAr reaction

2.5 Evaluation of photoaffinity labels

Next, we examined the utilities of Ns diazirine in term of cross-linked efficiency and photolabeling efficiency using bovine serum albumin as the model protein. Hence, the

biotinylated Ns diazirine probe was first synthesized as illustrated in Scheme 11. The synthesis of model photolabel, **33** began with protection polyethylene glycol with tosyl group with 96% yield. Then, both tosylate group were converted to azide by treatment with sodium azide followed by reduction using Pd/C in methanol which afforded us with the final diamine linker, **58** in quantitative yield. The synthesized linker **58** was then coupled with the NHS activated biotin, **60** before it was subjected to diazirinyl sulfonyl chloride, which undergo oxidative chlorination using DCDMDH to give our desired photolabel probe, **61** in 12%

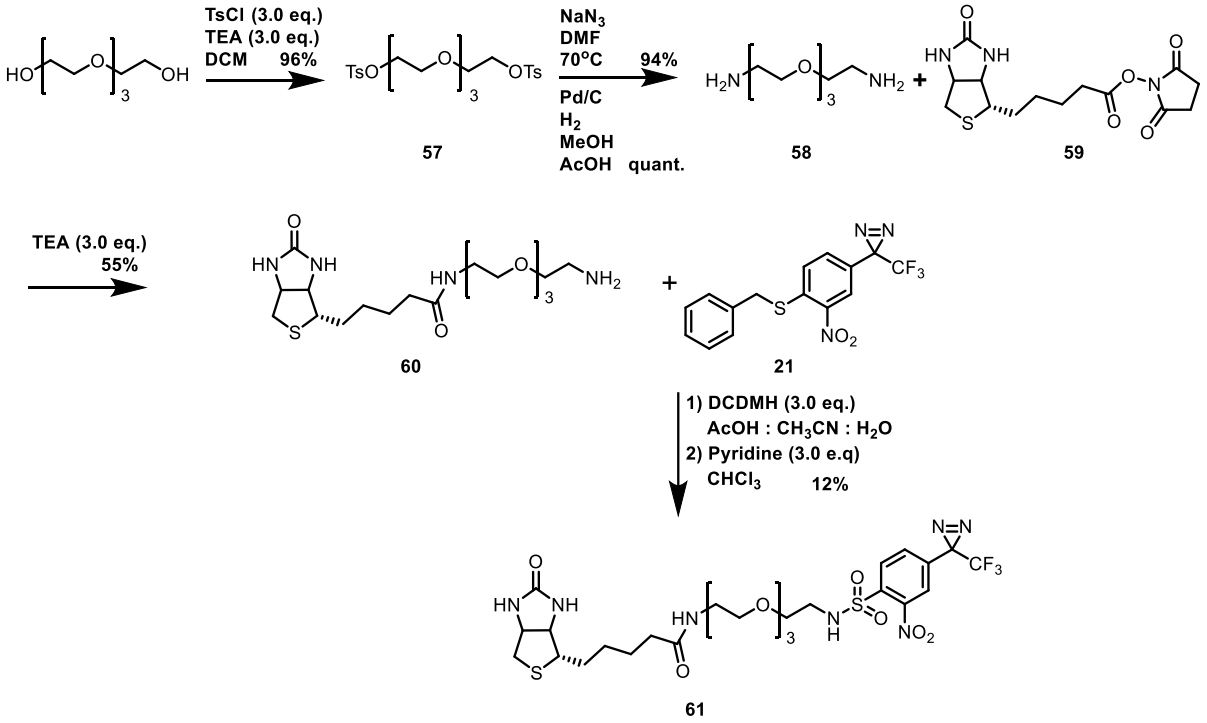

Scheme 11. Synthesis of the pegylated biotin photoaffinity label

We then performed photolabeling to evaluate the efficiency of the photolabel. The synthesized probe, **61** was subjected to BSA, which was used as a model protein. It was incubated for 10 min before irradiated under UV lamp for 2 min. The photo-labeled products were then subjected to 12% SDS Page gel and detected by chemiluminescence method by horseradish peroxidase (HRP)-conjugated avidin after blotting onto a PVDF membrane. To estimate the efficiency, BSA-biotin calibration curve was drawn by varying the protein's concentration (Fig. 5 and 6).

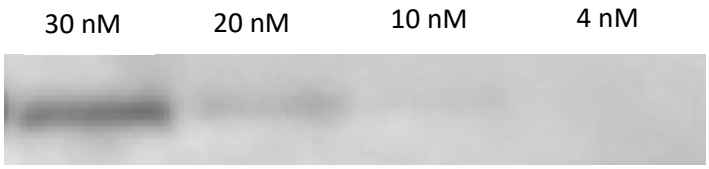

Fig. 5. Chemiluminescence detection for BSA-Biotin for labelling efficiency calibration curve

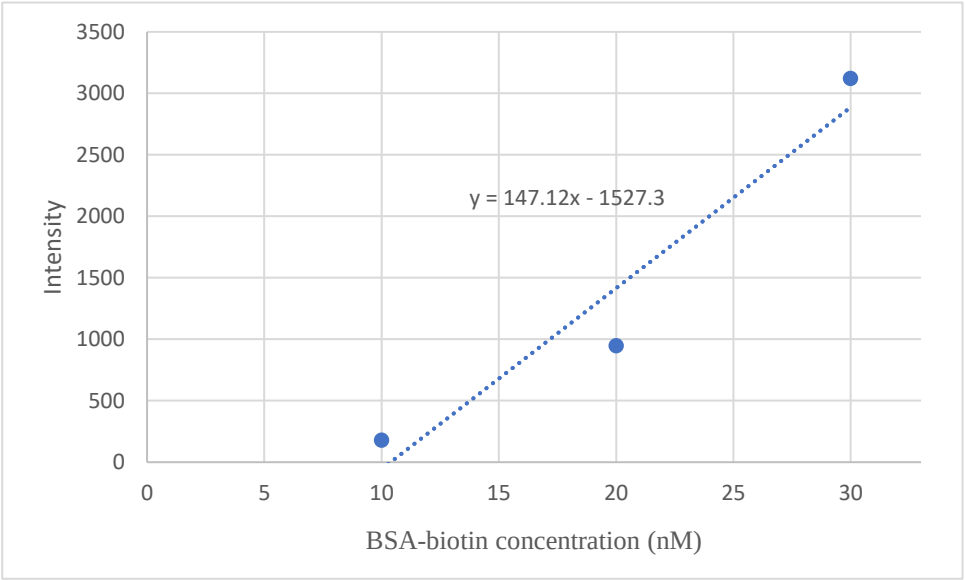

Fig. 6. Calibration curve for labelling efficiency

Based on the emission band intensity, the efficiency of the photolabeling was calculated to be 20%. Calculation of the efficiency was compared to a calibration curve of BSA biotin. In comparison with other reported photolabeling probes, our probe's efficiency could be considered as high because the efficiency of conventional photo labelling is known to be around 10%.

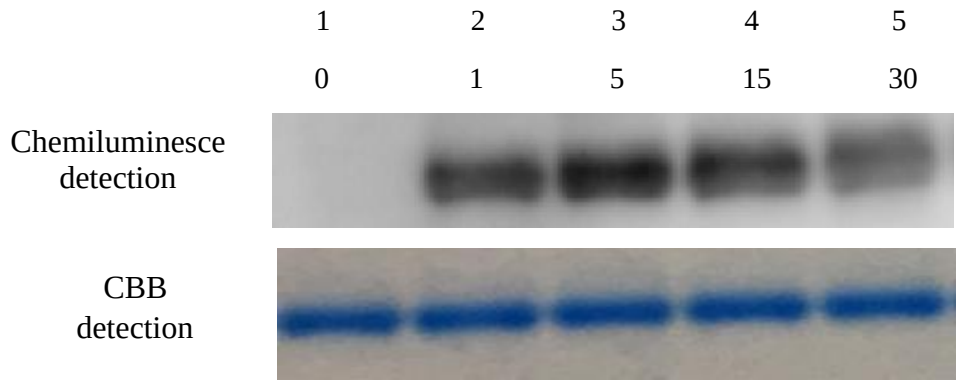

Fig. 17. Labelling conditions for labelling efficiency : 5 µM BSA, 5 µM biotin diazirine probe at room temperature under UV light

The following S_NAr was performed using SH-BODIPY as fluorophore to calculate efficiency of the exchangeable reaction. Upon photoactivation, dilution of SH-BODIPY (100 eq.) and Cs_2CO_3 (100 eq.) in H_2O was added and left reacted for the allocated time. Then, fluorescence detection of the BSA cross-linked with photoprobe was observed using Fujifilm LAS 4000. The fluorescence emission intensity of BODIPY-thioether linked BSA band at 525 nm increased accordingly with time in response to the exchange of biotin-PEG linker. In addition, the yield for the S_NAr reaction is 78%, which was calculated based on the emission band intensity observed by chemiluminescent method. Further investigation on the feasibility of our approach using Methotrexate as bioactive ligand is discuss in the next chapter.

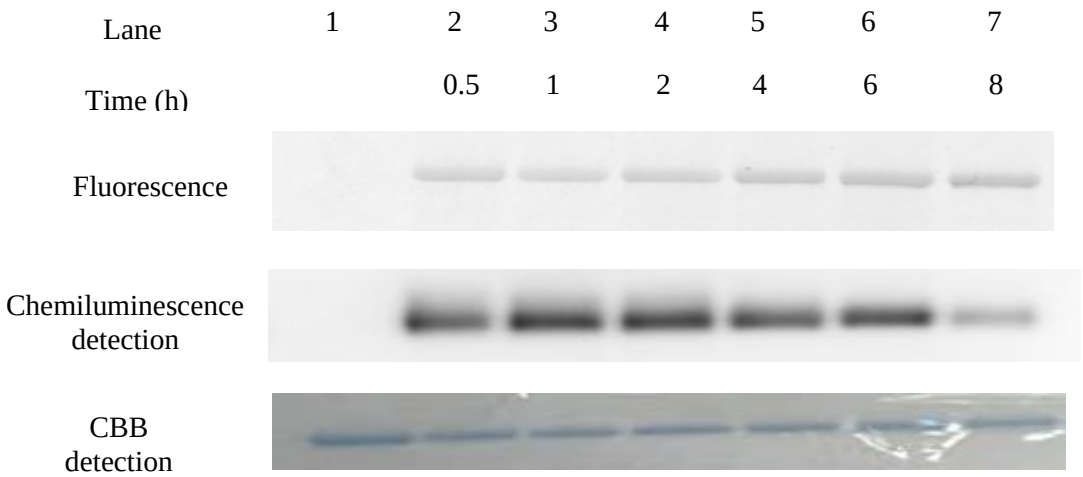

Fig. 18. Photolabelling conditions: 5 µM BSA, 5 µM biotin diazirine probe, 500 µM $CsCO_3$, 500 µM BODIPY-SH with 15 µl each at 50°C

2.6 Conclusions

We successfully synthesized the first bifunctional Ns diazirine based photoaffinity labelling probe with higher photoreactivity in comparison with the normal phenyldiazirine. Additionally, this probe also proves the feasibility of the tag-exchangeable reaction via formation of Meisenheimer complex by installing fluorescent or high sensitive mass tag in relatively high yield even in aqueous condition. Interestingly, the product installed with high sensitive mass tag could be detected without any purification. In the future, we envisioned that this Ns diazirine methodology will simplify the procedure for analysis in photoaffinity labeling.

2.7 Experimental procedures

Synthesis of 4-chloro-3-nitrobenzaldehyde, 13

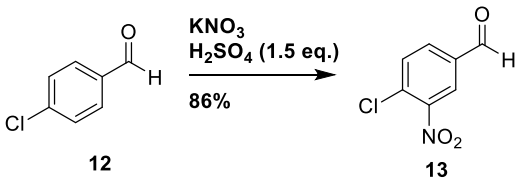

4-Chlorobenzaldehyde (2.018 g, 14.34 mmol) was stirred in 10 ml of H_2SO_4 for 20 minutes until it was fully dissolved. Potassium carbonate (2.180 g, 21.51 mmol) was then added into the mixture and stirred for 4 hours. The reaction mixture was added into H_2O at 0°C, extracted with ethyl acetate, dried over anhydrous Mg_2SO_4 and concentrated *in vacuo*. The residue was purified by silica gel column chromatography (eluent: chloroform/hexane = 2/1) to give 4-chloro-3-nitrobenzaldehyde, **13** (2.295 g, 86%) as white solid. ^{1}H NMR (500 MHz, $CDCl_3$) δ 10.06 (s,1H), 8.37 (s,1H), 8.07 (d, *J* = 2.0 Hz, 1H), 7.79 (s,1H). ^{13}C NMR ($CDCl_3$, 125 MHz) δ 188.6, 135.4, 133.0, 132.8, 126.3. HRMS (m/z): $[M+H]^+$ calculated for $C_7H_4ClNO_3$: 185.9943; found 185.9952.

Synthesis of 1-(4-chloro-3-nitrophenyl)-2,2,2-trifluoroethan-1-ol, 14

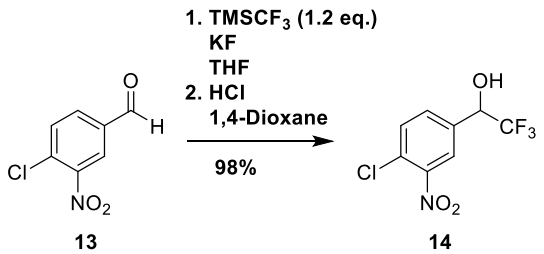

Potassium fluoride and trifluoromethylsilane (1.64 ml, 2.0 eq.) was added into a stirred solution of 4-chloro-3-nitrobenzaldehyde (1.0174 g, 5.48 mmol) and THF at 0°C. After 1 hour, the reaction mixture was filtered to remove the remaining KF and washed with 1,4-dioxane. Then 1M HCl was added and stirred overnight. Upon the completion of the reaction, THF and 1,4-dioxane was removed by using rotary evaporator, diluted with ethyl acetate, washed with H_2O, dried over $MgSO_4$ and evaporated once again. The crude product was purified using column chromatography (eluent: ethyl acetate/hexane = 1/3) to give 1-(4-chloro-3-nitrophenyl)-2,2,2-

trifluoroethan-1-ol, **14** (1.37g, 98%) as yellow oil. ^{1}H NMR (500 MHz, $CDCl_3$) δ 8.03 (d, *J* = 1.2 Hz, 1H), 7.66 (d, *J* = 10Hz, 1H), 7.60 (d, *J* = 6,4 Hz, 1H), 5.18 (q, J = 6.4 Hz, 1H), 3.51 (bs, 1H). ^{13} C NMR (126 MHz, $CDCl_3$) δ 147.84, 134.72, 132.43, 132.33, 128.26, 124.85, 124.14 (q, *J* = 283.5 Hz), 71.16 (q, *J* = 32.76 Hz). HRMS (m/z): $[M+H]^+$ calculated for $C_8H_5ClF_3NO_3$: 277.9802; found 277.9793.

Synthesis of 1-(4-chloro-3-nitrophenyl)-2,2,2-trifluoroethan-1-one, 15

14 **15**

2-Iodobenzoic acid (6.90 g, 23.92 mmol) was added portion wise in a stirred solution of 1-(4-chloro-3-nitrophenyl)-2,2,2-trifluoroethan-1-ol (2.04 g, 7.97 mmol) in ethyl acetate : DMSO (5:1) at room temperature. After 5 h of stirring, the reaction mixture was filtered to remove the IBX. The filtrate was then washed with H_2O, extracted with chloroform three times, dried and concentrated under reduced pressure. The remaining residue was purified using column chromatography (eluent: ethyl acetate/hexane = 1/2) to yield 1-(4-chloro-3-nitrophenyl)-2,2,2-trifluoroethan-1-one, **15** (1.69 g, 83%) as light yellow oil. ^{1}H NMR (500 MHz, $CDCl_3$) δ 8.46 (s, 1H), 8.12 (d, *J* = 10.0 Hz, 1H), 7.73 (d, *J* = 10.0 Hz, 1H). ^{13}C NMR ($CDCl_3$, 125 MHz) δ177.95 (q, *J* = 37.5 Hz), 134.63, 133.51, 133.16, 131.86, 129.1, 126.9, 124.7, 116.09 (q, *J* = 288.75 Hz). HRMS (m/z): $[M+H]^+$ calculated for $C_8H_3ClF_3NO_3$: 253.9826; found 253.9811.

Synthesis of (Z)-1-(4-chloro-3-nitrophenyl)-2,2,2-trifluoroethan-1-one oxime, 16

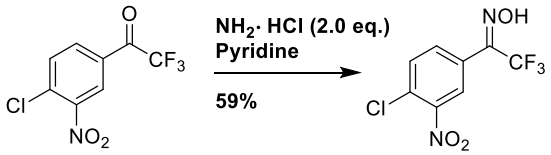

15 **16**

1-(4-chloro-3-nitrophenyl)-2,2,2-trifluoroethan-1-one (0.64 g, 2.52 mmol) was stirred in pyridine at room temperature. Then hydroxylamine hydrochloride was added and stirred for 5 h at 90^{o}C. The reaction mixture was quenched with H_2O. The organic layer was extracted with

ethyl acetate, dried over $MgSO_4$ and evaporated under reduced pressure. The crude product was purified using column chromatography (eluent: ethyl acetate/hexane = 1/2) to yield (Z)-1-(4-chloro-3-nitrophenyl)-2,2,2-trifluoroethan-1-one oxime, **16** (0.40 g, 59%) as yellow oil. ^{1}H NMR (500 MHz, $CDCl_3$) δ 8.92 (bs, 2H), 8.12 (S, 1H), 8.07 (S, 1H), 7.69 (s, 2H), 7.65 (s, 1H), 7.64 (s, 1H). ^{13}C NMR ($CDCl_3$, 125 MHz) δ 144.71 (q, *J* = 33.75 Hz), 133.18, 132.36, 132.18, 129. 96, 129.66, 129.22, 126.39, 125.43, 120.08 (q, *J* = 273.75 Hz). HRMS (m/z): $[M+H]^-$ calculated for $C_8H_4ClF_3N_2O_3$: 267.9887; found 267.9868.

Synthesis of (Z)-1-(4-chloro-3-nitrophenyl)-2,2,2-trifluoroethan-1-one O-tosyl oxime, 17

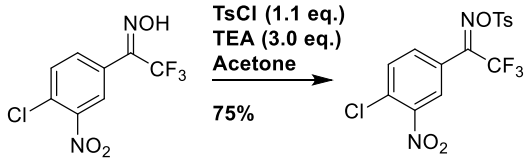

16 **17**

Triethylamine (0.054 ml, 0.39 mmol) and tosyl chloride (27.3 mg, 0.14 mmol) was added in a stirred solution of (Z)-1-(4-chloro-3-nitrophenyl)-2,2,2-trifluoroethan-1-one oxime (0.035 g, 0.13 mmol) and acetone at 0^{o}C. After 2 h of stirring, the reaction mixture was quenched with H_2O, extracted with ethyl acetate, dried over $MgSO_4$ and was evaporated under reduced pressure. The crude mixture was then purified by column chromatography (eluent: ethyl acetate/hexane = 1/4) to yield (Z)-1-(4-chloro-3-nitrophenyl)-2,2,2-trifluoroethan-1-one O-tosyl oxime, **17** (41.3 mg, 75%) as yellow oil. ^{1}H NMR (500 MHz, $CDCl_3$) δ 7.90 (s,1H), 7.88 (d, *J* = 8.3 Hz, 2H), 7.71 (d, *J* = 8.6 Hz, 2H), 7.59 (dd, *J* = 2.0, 8.0 Hz, 1H), 7.41 (d, *J* = 8.3 Hz, 2H), 2.50 (s,3H). ^{13}C NMR ($CDCl_3$, 125 MHz) δ 155.14, 150.45, 146.80, 133.08, 132.92, 131.06, 130.54, 130.23, 130.13, 129.36, 127.05, 125.75, 124.07, 120.23, 21.85. HRMS (m/z): $[M+H]^+$ calculated for $C_{15}H_{10}ClF_3N_2O_5S$: 432.0012; found 423.0023.

Synthesis of 3-(4-chloro-3-nitrophenyl)-3-(trifluoromethyl)diaziridine), 18

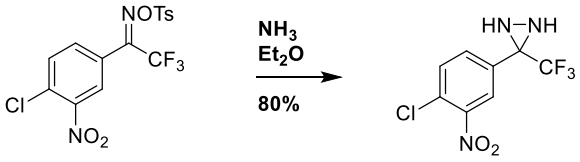

17 **18**

(Z)-1-(4-chloro-3-nitrophenyl)-2,2,2-trifluoroethan-1-one *O*-tosyl oxime (0.61 g, 1.45 mmol) was dissolved in diethyl ether in a pressure vessel. Ammonia gas was then bubbled and condensed till the volume increased. After stirring overnight, the reaction mixture was filtered and reduced under pressure using rotary evaporator. The crude mixture was purified using column chromatography (eluent: ethyl acetate/hexane = 1/3) to yield 3-(4-chloro-3-nitrophenyl)-3-(trifluoromethyl) diaziridine (0.30 g, 80%) as yellow oil. ^{1}H NMR (500 MHz, $CDCl_3$) δ 8.17 (d, *J* = 2.2 Hz, 1H), 7.81 (1H, dd, *J* = 2.2, 8.3 Hz), 7.65 (d, *J* = 8.6 Hz, 1H), 2.94 (d, *J* = 8.6 Hz, 1H), 2.28 (d, *J* = 8.6 Hz, 1H). ^{13}C NMR ($CDCl_3$, 125 MHz) δ 132.56, 131.99, 129.15, 125.40, 124.03 (q, *J* = 278.5), 56.89 (q, *J* = 36.5).

Synthesis of 3-(4-chloro-3-nitrophenyl)-3-(trifluoromethyl)-3H-diazirine, 19

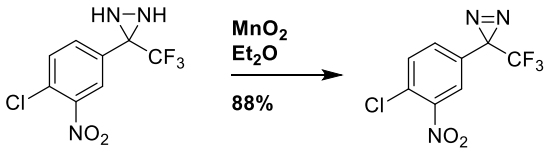

18 **19**

Manganese oxide was added to a stirred solution of 3-(4-chloro-3-nitrophenyl)-3-(trifluoromethyl) diaziridine (0.16 g, 0.59 mmol) and diethyl ether (5 ml) at room temperature. The reaction mixture was stirred for 1 h before it was filtered and concentrated using rotary evaporator. The crude mixture was then purified using column chromatography (eluent: ethyl acetate/hexane = 1/4) to yield 3-(4-chloro-3-nitrophenyl)-3-(trifluoromethyl)-3H-diazirine (0.12 g, 76%) as yellow oil. ^{1}H NMR (500 MHz, $CDCl_3$) δ 7.67 (d, *J* = 2.0 Hz, 1H), 7.63 (d, *J* = 8.6 Hz, 1H), 7.39 (dd, J = 6.8 Hz, 1.7 Hz, *J* = 1H). ^{13}C NMR ($CDCl_3$, 125 MHz) δ 136.87, 132.72, 120.78, 129.39, 128.95, 123.76 (q, *J* = 278.5 Hz), 29.69 (q, *J* = 36.5 Hz).

Synthesis of 3-(4-(benzylthio)-3-nitrophenyl)-3-(trifluoromethyl)-3H-diazirine, 20

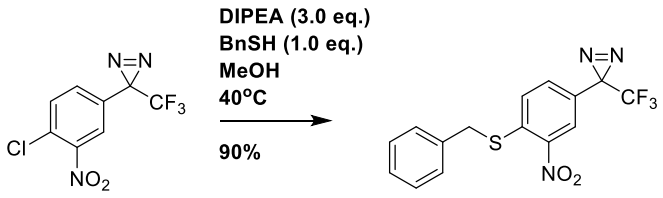

19 **20**

Diisopropylethylamine (100 μL, 3.0 eq) and benzyl mercaptan (20 μL, 1.0 eq) was added into a stirred solution of 3-(4-chloro-3-nitrophenyl)-3-(trifluoromethyl)-3*H*-diazirine (52.5 mg, 0.19 mmol) in methanol at room temperature. Then, the temperature of reaction solution was increased up to 40 °C and left stirred for 4 h. Upon the completion of the reaction, the mixture was cooled to room temperature and quenched with H_2O, extracted with ethyl acetate and dried over $MgSO_4$ and evaporated under vacuum. The reaction mixture was purified using column chromatography (ethyl acetate/*n*-hexane = 1:6) to yield 3-(4-(benzylthio)-3-nitrophenyl)-3-(trifluoromethyl)-3*H*-diazirine, **20** (62.8 mg, 90%) as yellow solid. ^{1}H NMR ($CDCl_3$, 500 MHz) δ 8.00 (d, J = 2.2Hz, 1H), 7.50 (d, J = 8.8 Hz, 1H), 7.39-7.25 (m, 6H).^{13}C NMR ($CDCl_3$, 125 MHz) δ 145.36, 140.57, 134.27, 130.95, 128.98, 128.04, 127.39, 125.87, 124.96, 121.69 (q, *J* = 272.5 Hz), 37.49, 27.85 (q, *J* = 40.0 Hz). HRMS (m/z): $[M+H]^+$ calculated for $C_{15}H_{10}F_3N_3O_2S$: 354.0513; found 354.0518.

Coupling of aminoethanol and nosyl diazirine 21

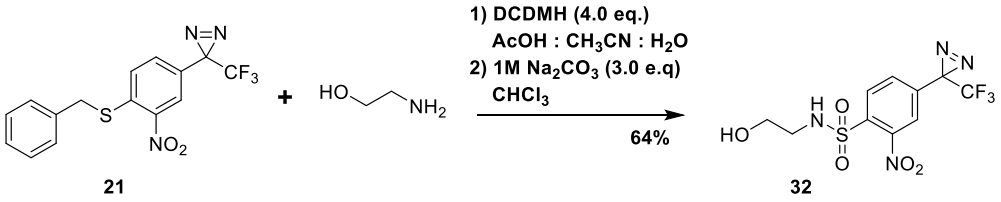

Acetic acid (0.15 ml) and H_2O (0.1 ml) was added into a stirred solution of 3-(4-(benzylthio)-3-nitrophenyl)-3-(trifluoromethyl)-3*H*-diazirine (90.9 mg, 0.26 mmol) in acetonitrile (4 mL). Then 2,4-dichloro-5,5-dimethylhydantoin (0.2 mg, 4.0 eq) was added at 0 °C for 2 h before evaporated under vacuum, extracted with dichloromethane, dried over $MgSO_4$ and evaporated under vacuum. Then the crude mixture was added into a stirred solution of aminoethanol (16.2 μl, 1.0 eq) in dichloromethane and 1M Na_2CO_3 (0.23 ml) at room temperature for overnight. Upon the completion of the reaction, it was evaporated to dryness and further purified using column chromatography (chloroform/methanol = 3:2) to give compound **61** (58 mg, 64%) as white solid. ^{1}H NMR ($CDCl_3$, 500 MHz) δ 8.19 (d, *J* = 8.3 Hz, 1H), 7.62 (s, 1 H), 7.55 (d, *J* = 8.7 Hz, 1H), 5.83 (t, *J* = 5.5 Hz, 1H), 3.75 (t, *J* = 5.0 Hz, 2H), 3.38 (q, *J* = 5.0 Hz, 2H). ^{13}C NMR ($CDCl_3$, 125 MHz) 148.75, 135.44, 134.74, 131.74, 130.39, 123.19, 123.13, 121.29 (q, *J*=273.75 Hz), 61.18, 45.73, 28.02 (q, *J* = 42.5 Hz) HRMS (m/z): $[M-H]^+$ calculated for $C_{10}H_8O_5N_4F_3S$: 353.01730; found 353.01788

Coupling of amine biotin 60 and nosyl diazirine 21

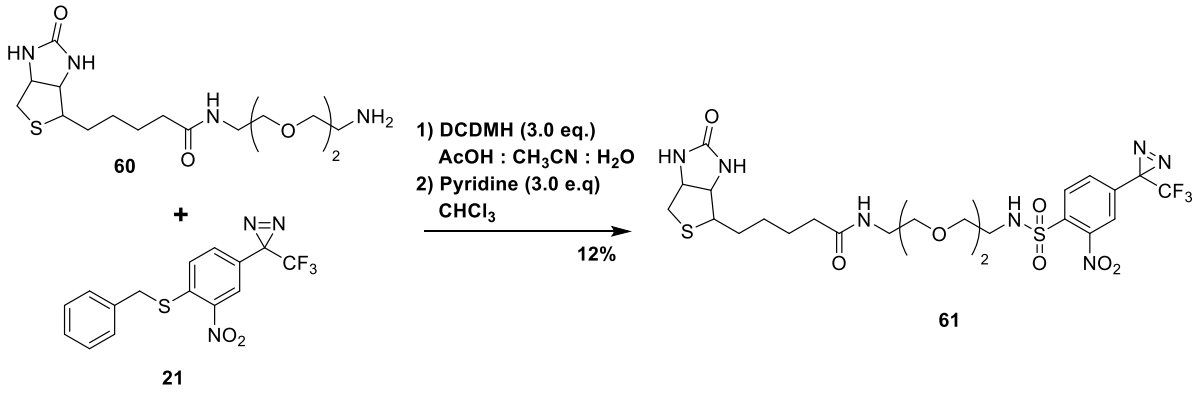

Acetic acid (37.5 µL) and H_2O (25 µL) was added into a stirred solution of 3-(4-(benzylthio)-3-nitrophenyl)-3-(trifluoromethyl)-3*H*-diazirine **21** in acetonitrile (1 mL). Then 2,4-Dichloro-5,5-dimethylhydantoin (13.8 mg, 2.0 eq) was added at 0 °C for 3 h before evaporated under vacuum, extracted with dichloromethane, dried over $MgSO_4$ and evaporated under vacuum. Then the crude mixture was added into a stirred solution of biotin linker[1] (15.5 mg, 1.0 eq) and pyridine (8.5 µL, 3.0 eq.) in dichloromethane at room temperature for overnight. Upon the completion of the reaction, it was evaporated to dryness and further purified using column chromatography (chloroform/methanol = 9:1) to give photoprobe **61** (3 mg, 12%). ^{1}H NMR ($CDCl_3$, 500 MHz) δ 8.21 (d, *J* = 8.5 Hz, 1H), 7.75 (d, *J* = 9.0 Hz, 1H), 7.73 (s, 1H), 4.49 (q, *J* = 5.0 Hz, 1H), 4.31 (q, *J* = 5.0 Hz, 1H), 3.56-3.54 (m, 6H), 3.52-3.50 (m, 6H), 3.37 (t, *J* = 5.5 Hz, 2H), 3.26 (t, *J* = 5.5 Hz, 2H), 3.22-3.19 (m, 1H), 2.93 (dd, *J* = 13.0 Hz, 5.5 Hz, 1H), 2.70 (d, *J* = 13.0 Hz, 1H), 2.22 (t, *J* = 7.5 Hz, 2H), 1.76 (m, 4H), 1.45-1.44 (m, 2H). ^{19}F NMR (CDCl3, 500 MHz) -66.75. HRMS (m/z): $[M+H]^+$ calculated for $C_{26}H_{36}F_3N_7O_9S_2$: 712.2050; found 712.2041.

Coupling of BODIPY^{TM} FL succimide ester and aminoethanthiol

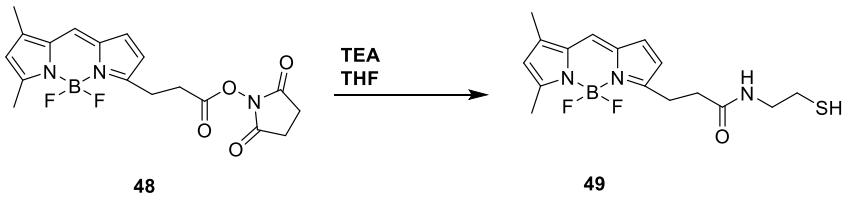

Aminoethanthiol hydrochloride (0.70 mg, 1.2 eq.) was added into a stirred solution of BODIPY^{TM} FL succimide ester, **48** (2 mg) with triethylamine (1.42 µl, 2 eq.) in THF at room

temperature for overnight. The reaction mixture was then evaporated and directly purified using column chromatography chromatography (eluent: chloroform/methanol = 9/1) to give aminoethanthiol BODIPY, **49** (0.4 mg, 22%). ^{1}H NMR ($CDCl_3$, 500 MHz) δ 7.10 (s, 1H), 6.89 (d, *J* = 4.3 Hz, 1H), 6.30 (d, *J* = 4.3 Hz, 1H), 6.14 (s, 1H), 6.06 (brs, 1H), 3.38 (q, *J* = 6.8 Hz, 1H), 3.28 (t, *J* = 7.5 Hz, 1H), 2.68 (t, *J* = 7.5 Hz, 1H), 2.58 (s, 3H), 2.56 (m, 2H), 2.27 (s, 3H). HRMS (m/z): $[M+H]^+$ calculated for $C_{16}H_{20}BF_2N_3OS$: 352.1431; found 352.1461.

Synthesis of pegylated NBD, 45

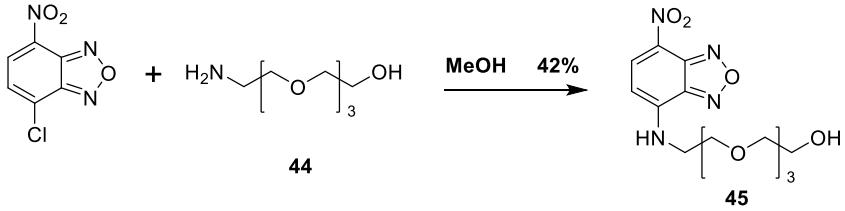

Amino hydroxy polyethylene glycol, **44** (28 mg, 0.079 mmol) was added into a stirred solution of NBDCl (17.2 mg, 1.1 eq.) in methanol at room temperature for overnight. The reaction mixture was then evaporated using a rotary evaporator and directly purified using column chromatography (eluent: ethyl acetate to ethyl acetate/methanol = 9/1) to give pegylated NBD **45** (11.7 mg, 42%). 1H NMR (500 MHz, CHLOROFORM-*d*) d ppm 3.65 - 3.78 (m, 14 H) 3.82 - 3.88 (m, 4 H) 6.14 (d, *J*=8.31 Hz, 1 H) 8.35 (br. s., 1 H) 8.47 (d, *J*=8.80 Hz, 1 H)

Mesylation of pegylated NBD, 45

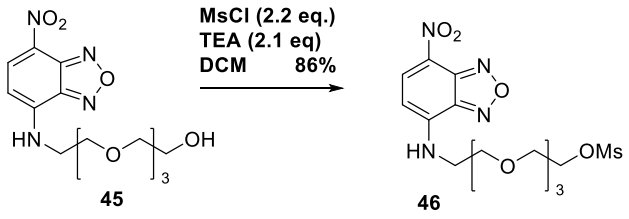

Mesyl chloride (5.6 µl, 2.2 eq.) and triethylamine (10 µl, 2.1 eq.) into a stirred solution of pegylated NBD, **45** (11.7 mg, 0.033 mmol) at room temperature for overnight. Upon the completion of the reaction, the reaction mixture was quenched with H_2O and dried over Mg_2SO_4. The crude mixture was then purified using column chromatography (eluent: chloroform/methanol = 9.5/0.5) to give mesylated compound **46** (12.3 mg, 86%). ^{1}H NMR (500 MHz, CD_3OD) d ppm 3.08 - 3.11 (m, 2 H) 3.59 - 3.70 (m, 10 H) 3.71 - 3.76 (m, 2 H) 4.25

- 4.42 (m, 3 H) 4.85 (d, *J*=2.20 Hz, 4 H), 6.43 (dd, *J*=8.80, 2.20 Hz, 1 H) 8.52 (d, *J*=8.55 Hz, 1 H)

Synthesis of compound 40

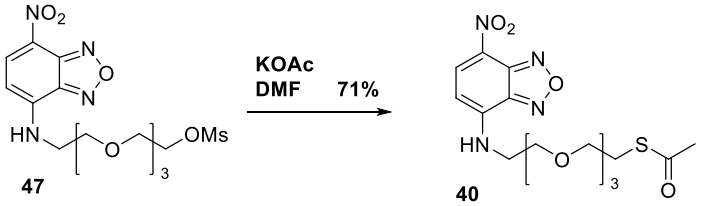

Potassium thioacetate (8 mg, 2.5 eq.) was added into a stirred solution of compound **46** in DMF. Upon completion of the reaction, DMF was removed using rotary evaporator before it was quenched with H_2O and dried over Mg_2SO_4. The crude mixture was purified using column chromatography (eluent:chloroform/H_2O/methanol = 8.0:1.5:0.5) to give the desired compound **40** (8.2 mg, 71%). ^{1}H NMR (500 MHz, $CDCl_3$) δ ppm 2.32 (s, 3 H) 3.07, (t, *J*=6.48 Hz, 2 H) 3.59 (t, *J*=6.60 Hz, 2 H) 3.64 - 3.76 (m, 12 H) 3.89 (t, *J*=5.01 Hz, 2 H), 6.20 (d, *J*=8.80 Hz, 1 H) 6.97 (br. s., 1 H) 8.49 (d, *J*=8.55 Hz, 1 H)

Synthesis of thiol NBD, 49

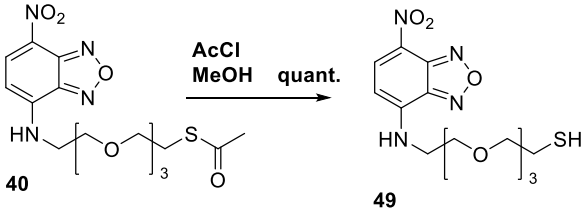

Acetic chloride was added dropwised into a stirred solution of compound **40** in MeOH for 2.5 h at 0^{O}C. The reaction mixture was evaporated using rotary evaporator and immediately used for the next step without any purification which gave us with compound **49** in quantitative yield. ^{1}H NMR (500 MHz,$CDCl_3$) δ ppm 1.59 (t, *J*=8.06 Hz, 1 H) 2.69 (q, *J*=6.76 Hz, 2 H) 3.63 (t, *J*=6.35 Hz, 2 H) 3.66 - 3.77 (m, 10 H) 3.89 (t, *J*=4.77 Hz, 2 H) 6.20 (d, *J*=8.55 Hz, 1 H) 6.94 (br. s., 1 H) 8.49 (d, *J*=8.55 Hz, 1 H).

Synthesis of methoxy coumarin amino ethanthiol, 51

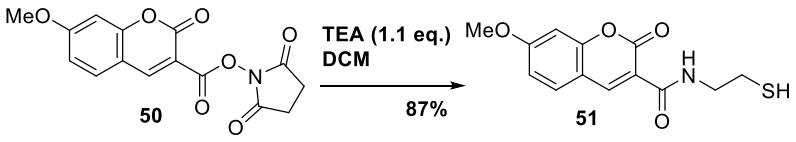

Amino ethanethiol hydrochloride (80 mg, 3.0 eq.) and triethyl amine (43.3 µl, 1.5 eq.) were added to a stirred solution of *N*-hydroxysuccimide methoxy coumarin, **58** (68.8 mg, 0.22 mmol) in DCM. Upon the completion of the reaction, the reaction mixture was quenched with 1N HCl and dried over $MgSO_4$. Compound **51** was proceeded with the next step without any purification. ^{1}H NMR (500 MHz, $CDCl_3$) δppm 1.47 (t, *J*=8.55 Hz, 1 H) 2.77 (q, *J*=7.09 Hz, 2 H) 3.65 (q, *J*=6.35 Hz, 2 H) 3.92 (s, 3 H) 6.86 (s, 1 H) 6.94 (dd,*J*=8.55, 1.71 Hz, 1 H) 7.58 (d, *J*=8.80 Hz, 1 H) 8.83 (s, 1 H) 9.05 (br. s., 1 H).

Ditosylation of polyethylene glycol

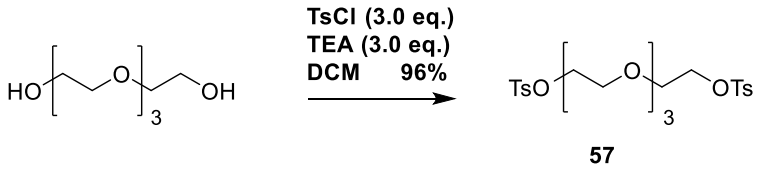

57

Tosyl chloride (1.0 g, 3.0 eq.) and triethylamine (0.73 ml, 3.0 eq.) was added into a stirred solution of polyethylene glycol (1.3 ml, 1.74 mmol) in DCM at 0^{o}C. The reaction mixture was left stirring at room temperature for 3h until the reaction was completed. It was quenched with H_2O, diluted in ethyl acetate and dried over $MgSO_4$. The crude was purified using column chromatography (eluent: ethyl acetate/hexane = 3/1) and gave us with ditosyl PEG, **57** (0.84 g, 96%). ^{1}H NMR ($CDCl_3$, 500 MHz) δ ppm 7.79 (d, *J*=8.31 Hz, 4 H), 7.34 (d, *J*=8.07 Hz, 4 H), 4.15 (t, *J*=4.8 Hz, 4H), 3.68 (t, *J*=5.0 Hz, 4H), 3.57-3.55 (m, 8H), 2.44 (s, 6H)

Azidation of compound 57

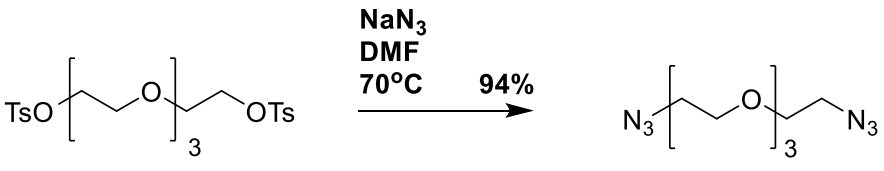

57

Sodium azide (0.21g, 5.0 eq.) was added into a stirred solution of ditosyl PEG, **57** (0.32 g, 0.64 mmol) in DMF and left stirring at 80°C for 6 h. Upon completion of the reaction, it was evaporated using rotary evaporator and directly purified using column chromatography (eluent: ethyl acetate) which afforded us with diazide, **58** (0.15g, 94%). ^{1}H NMR ($CDCl_3$, 500 MHz) δ ppm 3.39 (t, *J*=5.01 Hz, 4 H) 3.66 - 3.70 (m, 12 H).

Reduction of diazide linker

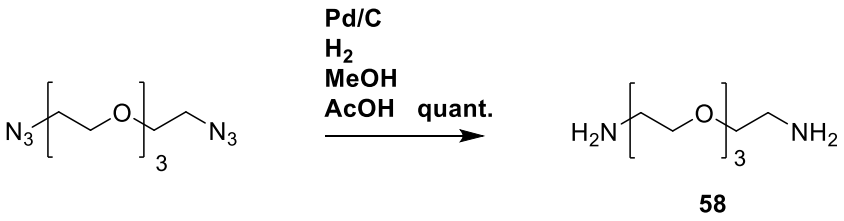

58

Pd/C (87.5 mg, 0.5 eq.) was added into a stirred solution of diazide, in methanol before hydrogen was inserted through balloon. After stirring for overnight at room temperature, the reaction mixture was filtered through celite and evaporated using rotary evaporator. The compound, **58** was obtained quantitatively without any purification required. ^{1}H NMR ($CDCl_3$, 500 MHz) δ ppm 2.79 - 2.88 (m, 4 H) 3.51 - 3.59 (m, 4 H) 3.61 - 3.71 (m, 9 H).

Coupling reaction between diamine linker, 58 and NHS activated biotin, 59

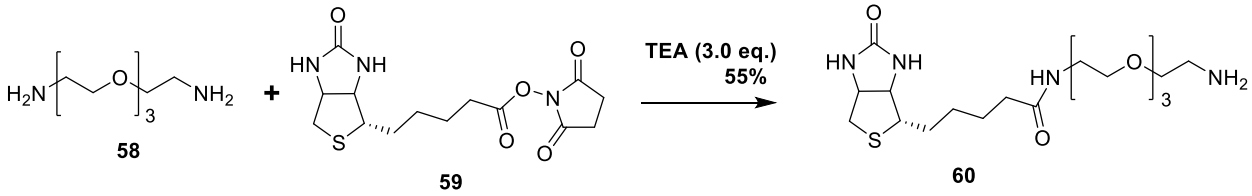

58 **59** **60**

Triethylamine (0.75 ml, 5.0 eq.) and NHS activated biotin, **59** (0.41g, 1.1 eq.) was added to a stirred solution of diamine linker, **58** (0.21 g, 1.09 mmol) in DMF at room temperature and left stirring for 3 h. Upon the completion of the reaction, DMF was removed using rotary evaporator and directly purified using column chromatography (eluent: chloroform/MeOH = 8/2) which gave us with compound amine linker biotin, **60** (0.17g, 35%). ^{1}H NMR ($CDCl_3$, 500 MHz) δ ppm 4.48 - 4.53 (m, 1 H), 4.30 (dd, *J*=7.9, 4.5 Hz, 1 H), 3.67 - 3.63 (m, 9 H), 3.60 (t, *J*=5.3 Hz, 2 H), 3.55 (t, *J*=5.5 Hz, 2 H), 3.37 (t, *J*=6.4 Hz, 3 H), 3.24-3.20 (m, 1 H),2.93-2.91 (m, 1H), 2.72 (d, *J*=12.4 Hz, 1 H), 2.23 (t, *J*=8.8 Hz, 2 H), 1.77-1.57 (m, 4 H), 1.49-1.44 (m, 2 H)

Monotosylation of polyethylene glycol (PEG)

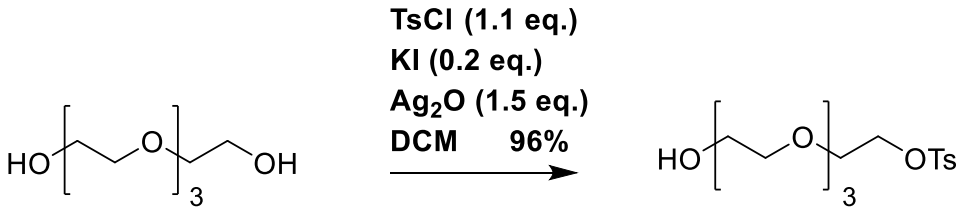

Tosyl chloride (1.12 g, 1.1 eq.), Ag_2O (2.02 g, 1.5 eq.) and KI (0.19 g, 0.2 eq.) was added into a stirred solution of polyethylene glycol (1.0 ml, 5.81 mmol) in DCM at 0^{o}C. The reaction mixture was left stirring at room temperature for overnight until the reaction was completed. It was quenched with H_2O, diluted in ethyl acetate and dried over $MgSO_4$. The crude was purified using column chromatography (eluent: chloroform/MeOH = 9.5/0.5) and gave us with mono-tosyl PEG (0.96 g, 96%). ^{1}H NMR ($CDCl_3$, 500 MHz) δ ppm 7.79 (d, *J*=8.0 Hz, 2H), 7.33 (d, *J*=8.0 Hz, 2H), 4.16-4.14 (m, 2H), 3.69-3.67 (m, 2H), 3.66-3.61 (m, 4H), 3.60-3.58 (m, 6H), 2.58 (br.s, 1H), 2.44 (s, 3H) ^{13}C NMR ($CDCl_3$, 125 MHz) 144.75, 132.91, 129.73, 127.91, 127.88, 72.40, 70.65, 69.19, 68.62, 61.64, 21.59

Azidation of mono-tosylated polyethylene glycol

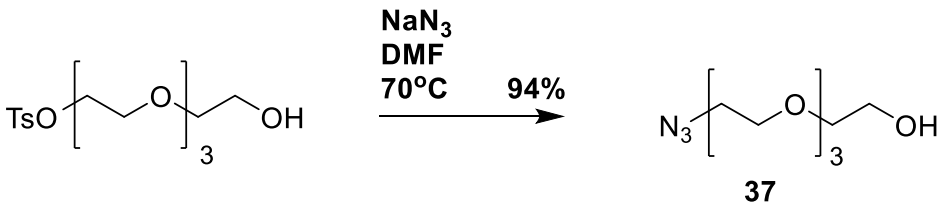

Sodium azide (1.31g, 2.0 eq.) was added into a stirred solution of mono-tosyl PEG (3.52 g, 0.01 mol) in DMF and left stirring at 90^{o}C for 5 h. Upon completion of the reaction, it was evaporated using rotary evaporator and directly purified using column chromatography (eluent: ethyl acetate) which afforded us with mono-azide, **37** (1.89g, 86%). ^{1}H NMR ($CDCl_3$, 500 MHz) δ ppm 3.72-3.69 (m, 2H), 3.67-3.65 (m, 10H), 3.59 (t, *J*=4.8 Hz, 2H), 3.38 (t, *J*=4.8Hz, 2H), 2.66 (br.s, 1H)

Mesylation of azide hydroxyl polyethylene glycol

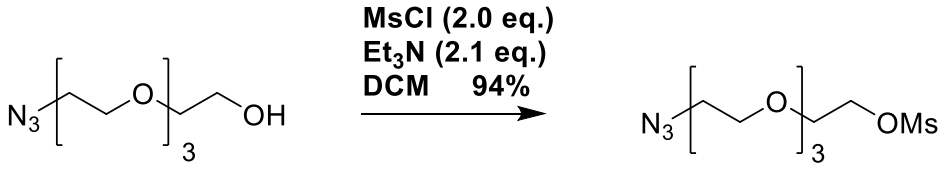

Mesyl chloride (0.83 g, 2.0 eq.) and triethylamine (1.38 ml, 2.1 eq.) was added into a stirred solution of polyethylene glycol (1.18 ml, 5.38 mmol) in DCM at 0^{o}C. The reaction mixture was left stirring at room temperature for overnight until the reaction was completed. It was quenched with H_2O, diluted in ethyl acetate and dried over $MgSO_4$. The crude was purified using column chromatography (eluent: ethyl acetate/hexane = 3/1) and gave us with compound azide mesyl polyethylene glycol (1.50 g, 94%). ^{1}H NMR ($CDCl_3$, 500 MHz) δ ppm 4.36 (t, *J*=4.8 Hz, 2H), 3.76 (t, *J*=4.8 Hz, 2H), 3.67-3.64 (m, 10H), 3.37 (t, *J*=4.8Hz, 2H), 3.06 (s, 3H)

Insertion of thioacetate functionality

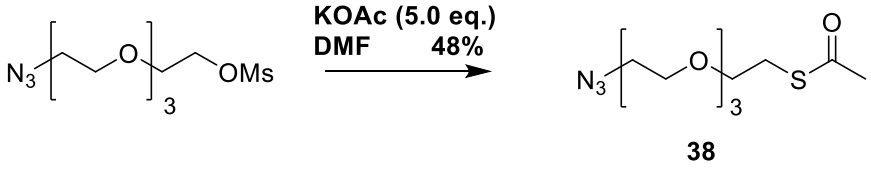

38

Potassium thioacetate (3.3 g, 5.0 eq.) was added into a stirred solution of azide mesyl polyethylene glycol in DMF. Upon completion of the reaction, DMF was removed using rotary evaporator before it was quenched with H_2O and dried over Mg_2SO_4. The crude mixture was purified using column chromatography (eluent : ethyl acetate : hexane = 2/1) to give the desired compound **38** (0.77 g, 48%). ^{1}H NMR (500 MHz, $CDCl_3$) δ ppm 3.68-3.58 (m, 14H), 3.38 (t, *J*=4.8Hz, 2H), 3.08 (t, *J*=4.8 Hz, 2H), 2.33 (s, 3H).

Reduction of azide mesylated linker

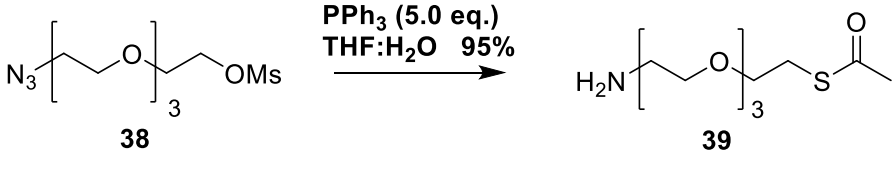

38 **39**

Triphenylphosphine (0.5 g, 5.0 eq.) was added into a stirred solution of compound **38** in THF:$H_2$0 at room temperature and was left stirring at 60^{o}C for 2.5 h. Upon completion of the

reaction, the mixture was evaporated using rotary evaporator and diluted in ethyl acetate and H_2O. The aqueous phase was again evaporated using rotary evaporator and diluted with DCM before it was dried over $MgSO_4$. The crude mixture, **39** (92.4 mg, 95%) was used in the next reaction without any purification. ^{1}H NMR (500 MHz, CD_3OD) δ ppm 3.68-3.61 (m, 10H), 3.55 (t, *J* =5.4 Hz, 2H), 3.36 (t, *J*=6.4 Hz, 2H), 1.96 (s, 3H)

Coupling reaction between NBDCl and thioacetate amine linker, 39

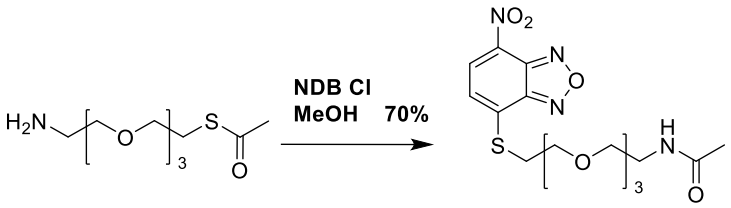

39 **40**

NBD Cl (11.4 mg, 1.1 eq.) and triethylamine (7.2 µl, 1.0 eq.) were added to a stirred solution of compound **39** in MeOH at room temperature for 30 min. The mixture was then evaporated with rotary evaporator before it was purified using column chromatography (eluent: ethyl acetate:MeOH = 9/1) to give NBD thioacetate, **40** (15 mg, 70%) ^{1}H NMR (500 MHz, CD_3OD) δ ppm 8.41 (d, *J*=8.8 Hz, 1H), 7.34 (d, *J*=8.8 Hz, 1H), 6.05 (s, 1H), 3.91 (t, *J*=6.4 Hz, 2H), 3.68-3.67 (m, 2H), 3.63-3.61 (m, 6H), 3.56 (t, *J*=6.0 Hz, 2H), 3.52 (t, *J*=6.0 Hz, 2H), 3.45-3.42 (m, 2H), 1.98 (s, 3H).

Coupling reaction between fluorescein and amine thioacetate linker 42

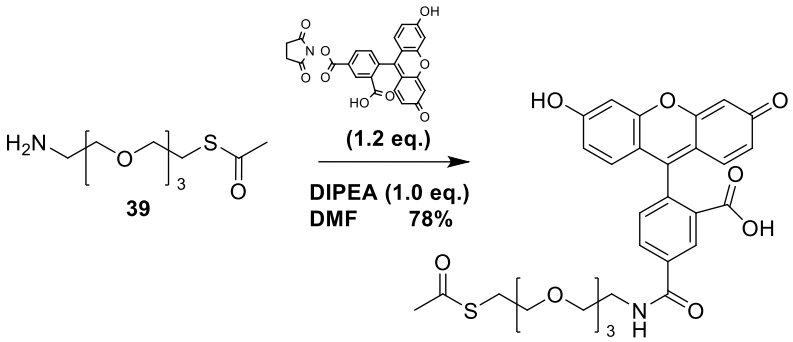

39 **42**

Diluted thioacetate linker, **39** in DMF was added into a stirred solution of fluorescein (10.5 mg, 0.002 mmol) and DIPEA (4.1 µl. 1.0 eq.) in DMF. The reaction mixture was stirred at room temperature for overnight and evaporated using rotary evaporator upon completion of reaction. The crude was the purified using column chromatography (eluent: ethyl acetate: hexane: H_2O

= 8/1/1) to give fluorescein thioacetate linker, **42** (10.46 mg, 78%). ^{1}H NMR (500 MHz, CD_3OD) δ ppm 8.54 (s, 1H), 8.31 (d, *J*=4.8 Hz, 1H), 8.25 (d, *J*=4.8 Hz, 1H), 8.14 (d, *J*=4.8 Hz), 7.69 (s, 1H), 7.36 (d, *J*=4.8 Hz, 1H), 6.72 (d, *J*=2.0 Hz, 1H), 6.70 (d, *J*=2.8 Hz, 1H), 6.85 (d, *J*=4.0 Hz, 1H), 6.63 (s, 1H), 6.57 (2, 1H), 6.55 (m, 1H), 3.75 (t, *J* = 6.4 Hz, 2H), 3.70-3.65 (m, 8H), 3.63-3.59 (m, 7H), 3.55 (t, *J*=5.6 Hz, 4H), 3.40 (t, *J*=6.4 Hz, 2H), 3.39 (t, *J* = 6.4 Hz, 2H), 3.35 (t, *J*=6.4 Hz, 2H), 3.28 (t, *J*=6.4 Hz, 2H), 1.95 (s, 3H), 1.93 (s, 3H)

General procedure for exchangeable reaction via Meisenheimer complex

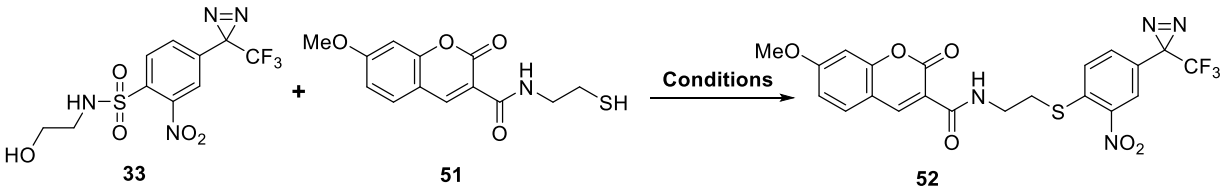

Methoxy coumarin thiol (1.5 eq.) and the base (3.0 eq.) were added into a stirred solution of sulfonamide **33**. Each reaction mixture was stirred at room temperature. Upon the completion of the reaction, the reaction mixture was quenched with H_2O and dried over $MgSO_4$. The crude was the purified using column chromatography (only dichloromethane) to give desired compound **52** as white solid. ^{1}H NMR (500 MHz, $CDCl_3$) δ ppm 9.13 (br.s, 1 H) 8.85 (s, 1 H), 8.00 (s, 1 H) 7.92 (d, *J*=8.6 Hz, 1 H) 7.61 (d, *J*=1.8 Hz, 1H) 7.52 (d, J=8.6 Hz, 1 H), 6.97 (dd, *J*= 8.6 Hz 1.8 Hz, 1 H), 6.88 (s, 1 H), 3.93 (s, 3 H), 3.72 (q, *J*=7.3 Hz, 2 H), 3.28 (t, *J*=7.3 Hz, 1 H). ^{13}C NMR ($CDCl_3$, 125 MHz) 165.20, 162.89, 161.77, 156.82, 148.59, 139.31, 131.14, 131.06, 127.50, 126.04, 124.33, 114.30, 114.15, 112.30, 100.38, 56.10, 38.57, 30.76. HRMS (m/z): $[M+H]^+$ calculated for $C_{21}H_{15}O_6N_4F_3NaS$: 531.05566: found 531.05582.

Bodipy-Ns diazirine, 55

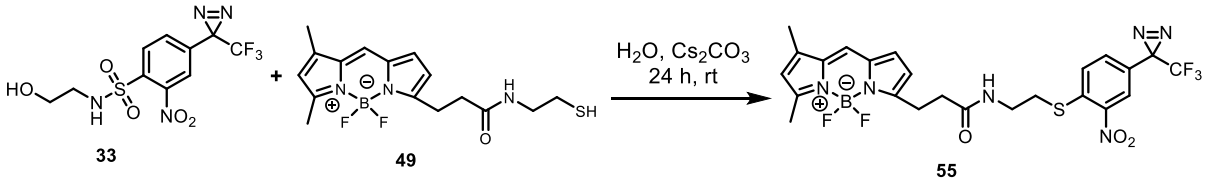

BODIPY aminoethanethiol (5.3 mg, 2.0 eq.) and Cs_2CO_3 (7.3 mg, 3.0 eq.) were added into a stirred solution of sulfonamide **33** (2.7 mg, 7.4 µmol) in THF. The reaction mixture was stirred at room temperature for 2 h. Upon the completion of the reaction, the reaction mixture was

quenched with H_2O and dried over $MgSO_4$. The crude was the purified using column chromatography (only dichloromethane) to give compound **55** (3.5 mg, 81%) as orange oil. ^1H NMR (500 MHz, $CDCl_3$) δ ppm 7.98 (s, 1 H) 7.76 (d, *J*=8.90 Hz, 1 H) 7.47 (d, *J*=8.90 Hz, 1 H) 7.08 (s, 1H), 6.86 (d, *J*=3.9 Hz, 1H) 6.29 (d, *J*=3.9 Hz, 1 H), 6.25 (brs, 1 H), 6.14 (s, 1 H), 3.44 (q, *J*=6.5 Hz, 2 H), 3.27 (t, *J*=7.5 Hz, 2 H), 3.02 (t, *J*=7.3 Hz, 2 H), 2.70 (t, *J*=7.3 Hz, 2H), 2.57 (3H, s), 2.27 (3H,s). 13C NMR (CDCl3, 125 MHz) 172.42, 161.43, 151.33, 139.46, 131.14, 128.13, 127.37, 125.92, 124.25, 123.90. 120.72, 117.25, 38.04, 35.73, 30.92, 29.71, 24.84, 11.34. HRMS (m/z): [M+Na]+ calculated for $C_{24}H_{22}BF_5N_6O_3SNa$: 602.14158; found 602.14204

N,N,N-trimethyl-2-((2-nitro-4-(3-(trifluoromethyl)-3H-diazirin-3-yl)phenyl)thio)ethan-1-aminium, 54

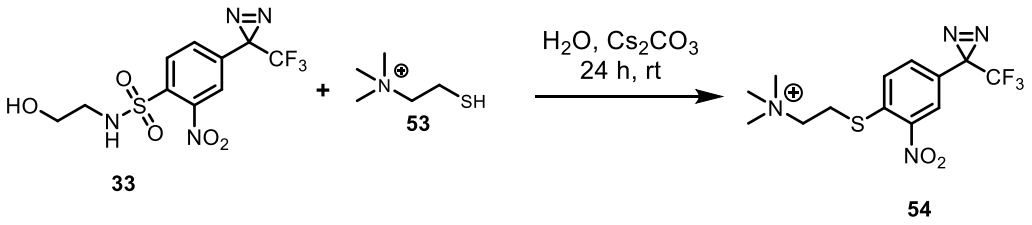

2-mercapto-*N,N,N*-trimethylethan-1-aminium (7.6 mg, 1.5 eq.) and Cs_2CO_3 (41.2 mg, 3.0 eq.) was added into a stirred solution of sulfonamide **33** (15 mg, 0.042 mmol) in water at room temperature and was stirred for 24 h. Upon the completion of the reaction, the reaction mixture was directly subjected to ESI mass without purification. HRMS (m/z): [M]+ calculated for $C_{13}H_{16}O_2N_4F_3S$: 349.09406; found 349.09413.

N,N-dimethyl-2-((2-nitro-4-(3-(trifluoromethyl)-3H-diazirin-3-yl)phenyl)thio)ethan-1-amine, 56

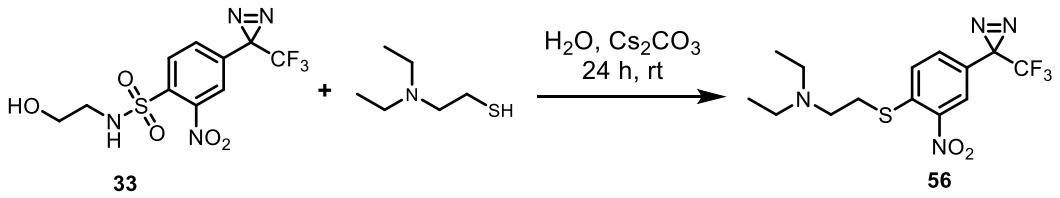

2-(Dimethylamino) ethane-1-thiol hydrochloride (14.3 mg, 2.0 eq.) and Cs_2CO_3 (41.3 mg, 3.0 eq.) was added into a stirred solution of sulfonamide **33** (15.4 mg, 0.042 mmol) in THF at room temperature for overnight. Upon the completion of the reaction, the reaction mixture was quenched with H_2O and dried over $MgSO_4$. The crude was the purified using column

chromatography (ethyl acetate/chloroform = 1:1) to give compound **56** (11.8 mg, 78%) as white solid. ^{1}H NMR (500 MHz, $CDCl_3$) δ ppm 7.99 (d, *J*=1.7 Hz, 1 H), 7.53 (d, *J*=8.5 Hz, 1 H,) 7.42 (d, *J*=8.5 Hz, 1 H), 3.09 (t, *J*=7.8 Hz, 2 H), 2.80 (t, *J*=7.8 Hz, 2 H), 2.61 (q, *J*=7.1 Hz, 4 H), 1.06 (t, *J*=7.1 Hz, 6H). ^{13}C NMR ($CDCl_3$, 125 MHz) 140.61, 127.43, 127.22, 125.64, 124.36, 124.22, 120.61, 50.83, 47.06, 30.09, 11.67. HRMS (m/z): $[M+H]^+$ calculated for $C_{14}H_{18}O_2N_4F_3S$: 363.10971; found 363.10992.

Coupling reaction between biotin linker 60 and benzyl mercaptan diazirine 21

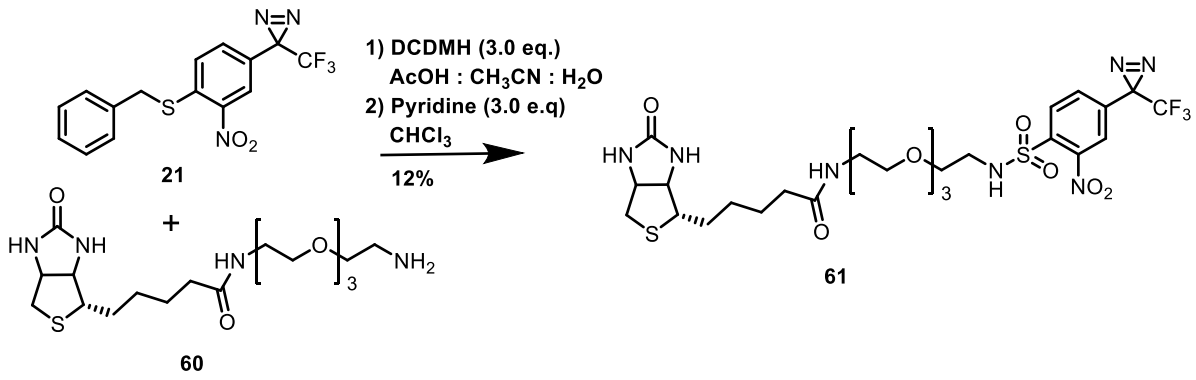

Acetic acid (37.5 µL) and H_2O (25 µL) was added into a stirred solution of 3-(4-(benzylthio)-3- nitrophenyl)-3-(trifluoromethyl)-3*H*-diazirine21 in acetonitrile (1 mL). Then 2,4-Dichloro-5,5- dimethylhydantoin (13.8 mg, 2.0 eq.) was added at 0 °C for 3 h before evaporated under vacuum, extracted with dichloromethane, dried over $MgSO_4$ and evaporated under vacuum. Then the crude mixture was added into a stirred solution of biotin linker **60** (15.5 mg, 1.0 eq) and pyridine (8.5 µL, 3.0 eq.) in dichloromethane at room temperature for overnight. Upon the completion of the reaction, it was evaporated to dryness and further purified using column chromatography (chloroform/methanol = 9:1) to give photoprobe **61**(3 mg, 12%). ^{1}H NMR ($CDCl_3$, 500 MHz) δ 8.21 (d, *J* = 8.5 Hz, 1H), 7.76 (d, *J* = 9.0 Hz, 1H), 7.73 (s, 1H), 4.49 (q, *J* = 5.0 Hz, 1H), 4.31 (q, *J* = 5.0 Hz, 1H), 3.56-3.54 (m, 6H), 3.52- 3.50 (m, 6H), 3.37 (t, *J* = 5.5 Hz, 2H), 3.26 (t, *J* = 5.5 Hz, 2H), 3.22-3.19 (m, 1H), 2.93 (dd, *J* = 13.0 Hz, 5.5 Hz, 1H), 2.70 (d, *J* = 13.0 Hz, 1H), 2.22 (t, *J* = 7.5 Hz, 2H), 1.67-1.57 (m, 4H), 1.45-1.44 (m, 2H). ^{19}F NMR ($CDCl^3$, 500 MHz) -66.75. HRMS (m/z): [M+H]+ calculated for $C_{26}H_{36}F_3N_7O_9S_2$: 712.2050; found 712.2041.

Photocross-linking of photoprobe 33 to BSA

Efficiency of photoaffinity labeling of biotinylated BSA with photoprobe 33 was generally performed as follows. A buffered solution (15 µl) of BSA-biotin (30 nM, 20 nM, 10 nM, 4 nM) was incubated with photoprobe **33** (15 µl, 5 µM) in PBS buffer with 5% DMSO for 10 min before it was irradiated at 0 ^{o}C for 2 min with 365 nm UV light. After photolysis, the resulting mixtures were treated with 10 µl of 4x SDS sample buffer (0.5 M Tris-HCl, 1M DTT, 10% SDS, 20% glycerol, pH 6.8) and subjected to SDS-PAGE. The gel was transferred onto a PVDF membrane and stained with Coomassie Brilliant Blue. Photocross-linked products were detected by chemiluminescence method using avidin-HRP conjugate. The labeling efficiency was calculated based on the intensity of the bands.

Photoaffinity labelling and installation of the BODIPY-thiol on photocross-linked product

BSA (15 µl, 5 µM) was incubated with photoprobe **61** (15 µl, 5 µM) at 4^{o}C for 10 min before it was irradiated under 360-nm light in ice for 2 min. Solution of $CsCO_3$ (15 µl, 500 µM) and BODIPY-SH (15 µl, 500 µM) were added into the photocross-linked mixture. The resulting mixture was incubated with shaking at 50^{o}C for 1 min, 5 min, 15 min, 30 min (each sample). Next, the mixtures were filtered using Amicon ultra-0.5 30K centrifugal filters to remove excess of SH-BODIPY and $CsCO_3$ and followed by washing for 3 times with distilled H_2O. The concentrates were then treated with 10 µl of 4x SDS sample buffer (0.5 M Tris-HCl, 1M DTT, 10% SDS, 20% glycerol, pH 6.8) each, heated for 10 min at 95^{o}C and subjected to SDS-PAGE. The gel was scanned using fluorescent image analyzer (LAS 4000, Fujifilm) and stained with Coomasie Brilliant Blue. Photoaffinity labeling and the cleavage of the photocross-linked product was confirmed by the increment of the intensity of fluorescence band observed.

2.7 NMR Spectra

nitration_pure

Acquisition Time (sec)	2.0487	*Date*	Jun 28 2017	*Date Stamp*	Jun 28 2017	*File Name*	H:\s_20170628_01 (nitration_1H)\data\cdcl3_01.fid\fid		
Frequency (MHz)	500.61	*Nucleus*	1H	*Number of Transients*	8	*Original Points Count*	16409	*Points Count*	32768
Pulse Sequence	s2pul	*Receiver Gain*	42.00	*Solvent*	CHLOROFORM-d			*Spectrum Offset (Hz)*	3006.0486
Spectrum Type	STANDARD	*Sweep Width (Hz)*	8009.61	*Temperature (degree C)*	25.000				

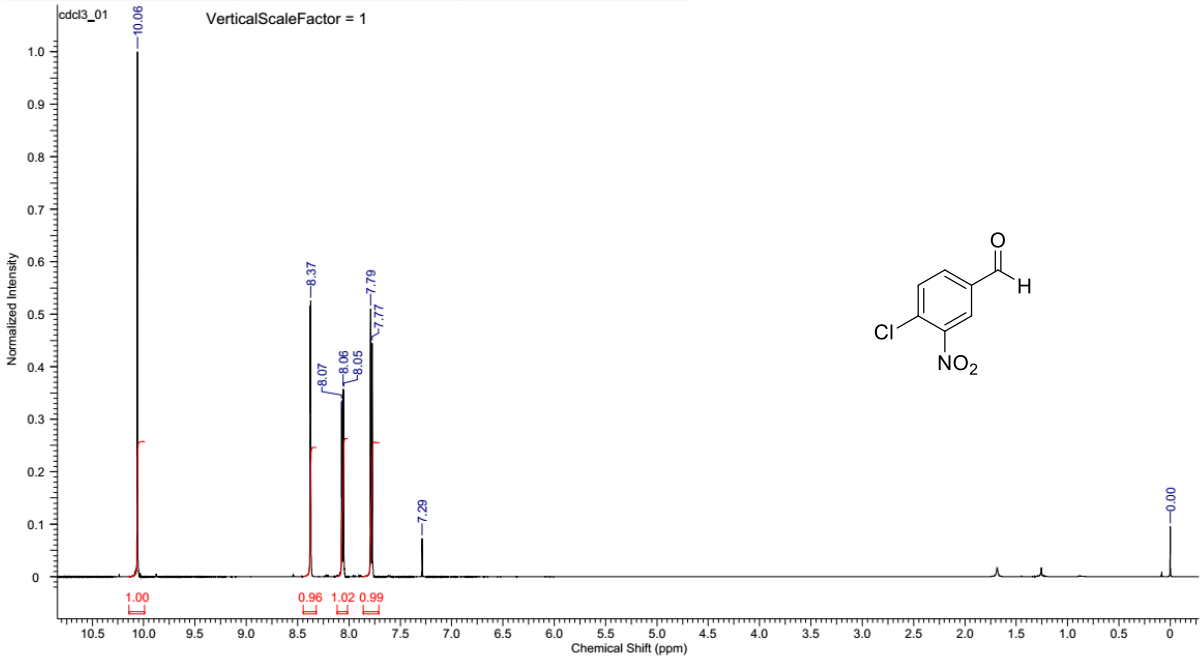

28-Jun-2017 9:10:45 AM
nitration_pure

Acquisition Time (sec)	1.3005	*Date*	Jun 28 2017	*Date Stamp*	Jun 28 2017	*File Name*	H:\s_20170628_02 (nitration_13C)\data\cdcl3_01.fid\fid		
Frequency (MHz)	125.89	*Nucleus*	13C	*Number of Transients*	1000	*Original Points Count*	39289	*Points Count*	65536
Pulse Sequence	s2pul	*Receiver Gain*	30.00	*Solvent*	CHLOROFORM-d			*Spectrum Offset (Hz)*	13217.1172
Spectrum Type	STANDARD	*Sweep Width (Hz)*	30211.48	*Temperature (degree C)*	25.000				

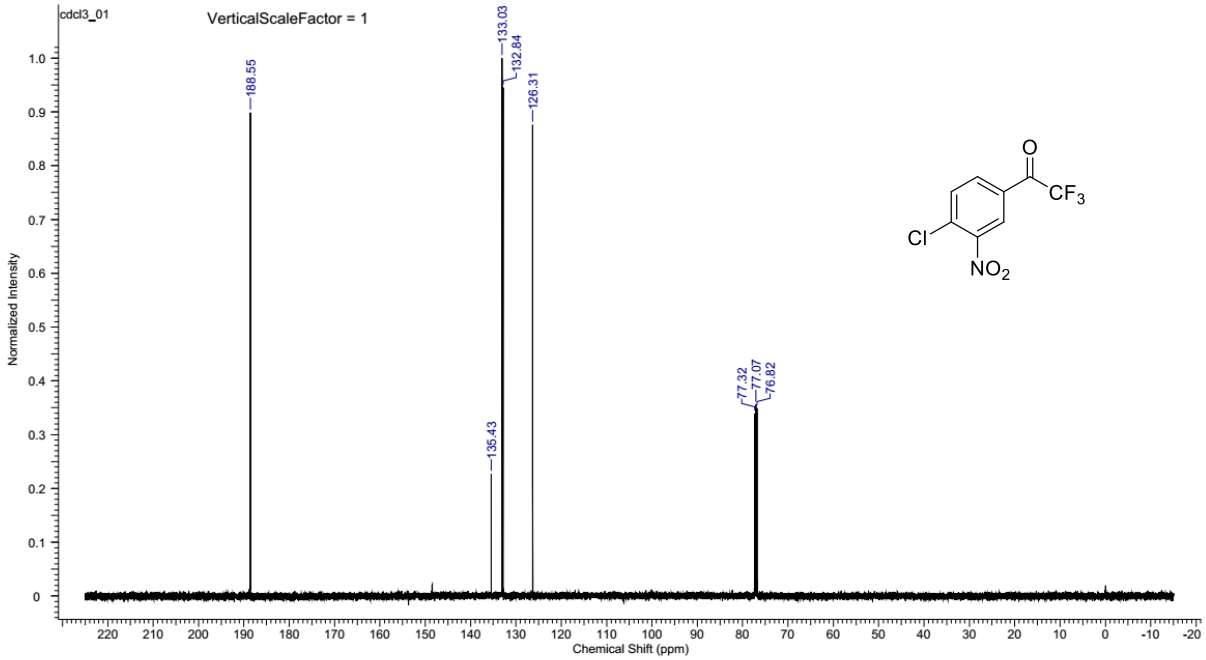

Acquisition Time (sec)	2.0487	*Date*	Apr 7 2019	*Date Stamp*	Apr 7 2019	*File Name*	E:\s_20190407_03 (OH CF3_pure_1H)\data\cdcl3_01.fid\fid		
Frequency (MHz)	500.45	*Nucleus*	1H	*Number of Transients*	8	*Original Points Count*	16404	*Points Count*	32768
Pulse Sequence	s2pul	*Receiver Gain*	20.00	*Solvent*	CHLOROFORM-d			*Spectrum Offset (Hz)*	3003.5532
Spectrum Type	STANDARD	*Sweep Width (Hz)*	8007.21	*Temperature (degree C)*	25.000				

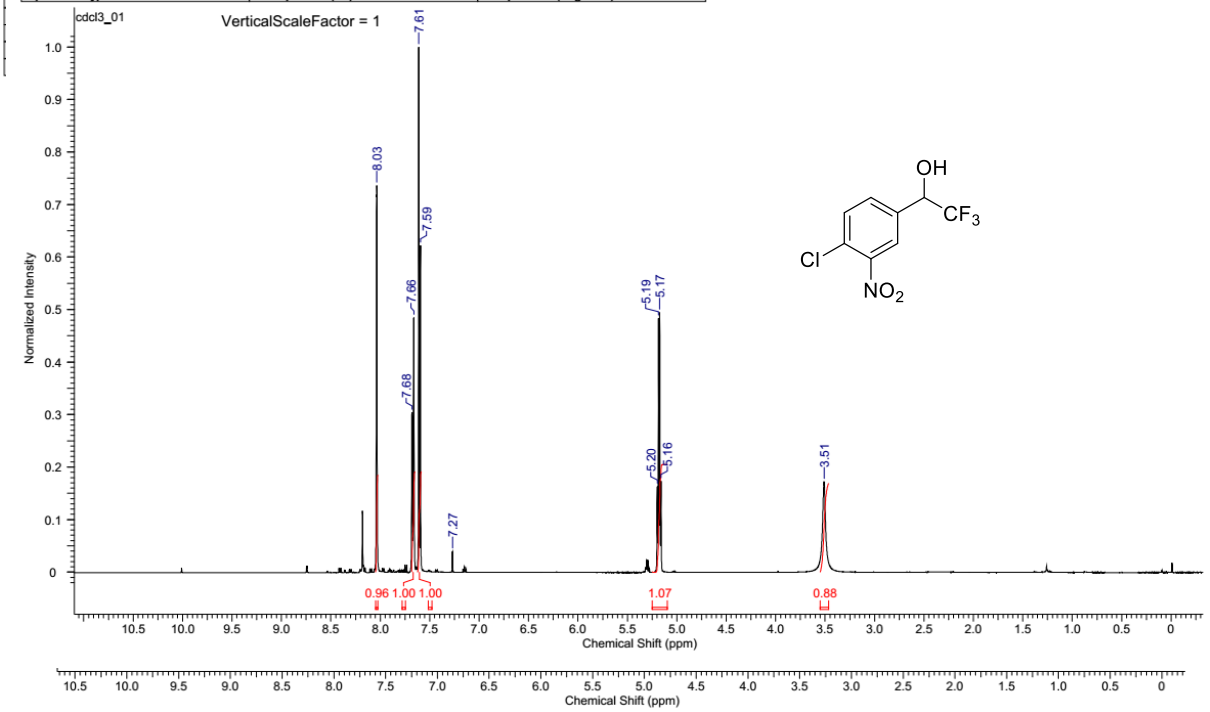

Acquisition Time (sec)	1.3005	*Date*	Apr 5 2019	*Date Stamp*	Apr 5 2019	*File Name*	E:\s_20190405_03 (OH CF3_1H)\data\cdcl3_01.fid\fid		
Frequency (MHz)	125.85	*Nucleus*	13C	*Number of Transients*	1000	*Original Points Count*	39274	*Points Count*	65536
Pulse Sequence	s2pul	*Receiver Gain*	30.00	*Solvent*	CHLOROFORM-d			*Spectrum Offset (Hz)*	13238.2285
Spectrum Type	STANDARD	*Sweep Width (Hz)*	30200.08	*Temperature (degree C)*	25.000				

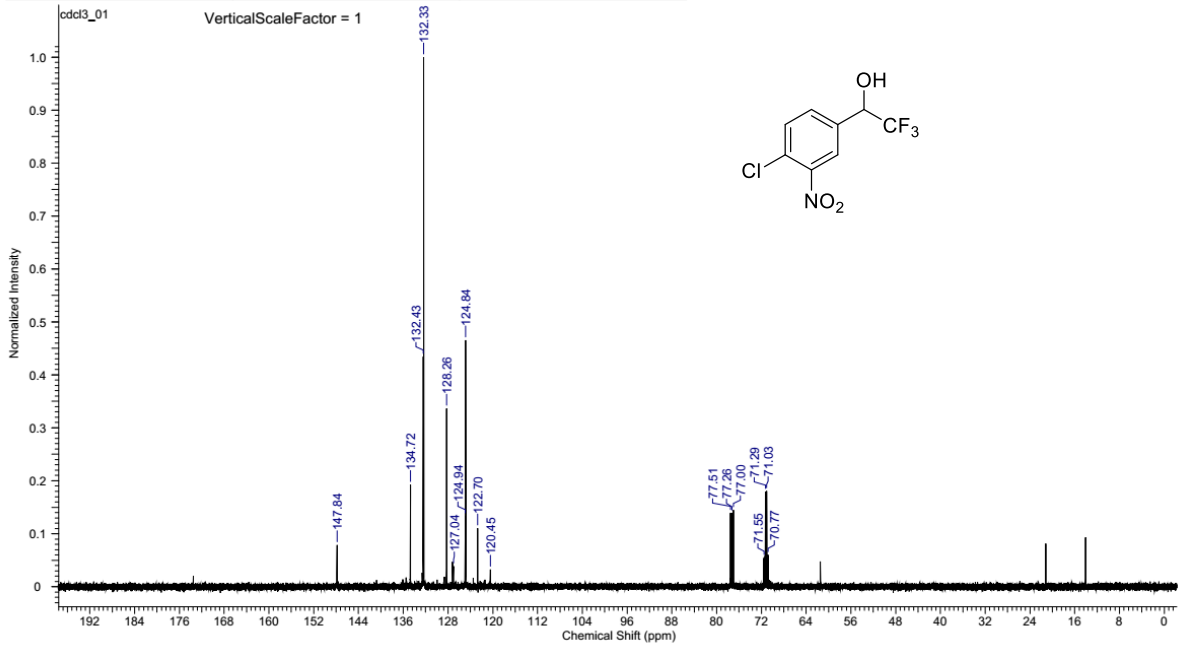

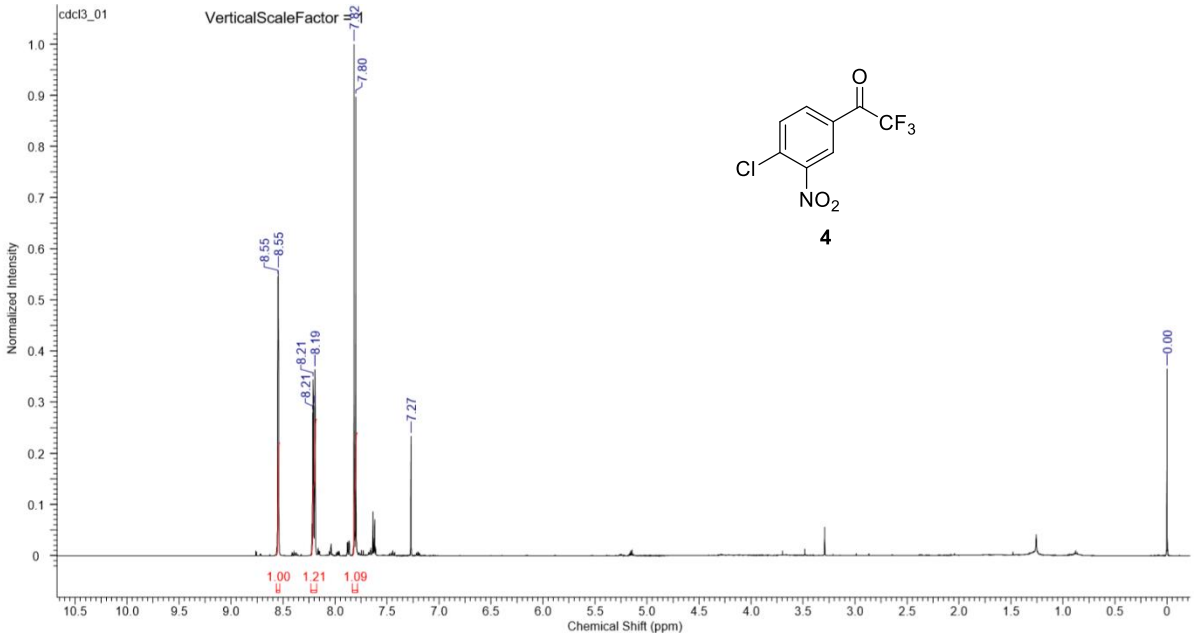
cdcl3_01
VerticalScaleFactor = 1
Normalized Intensity
Chemical Shift (ppm)
8.55
8.55
8.21
8.21
8.19
7.80
7.27
0.00
1.00
1.21
1.09
O
CF3
Cl
NO2
4

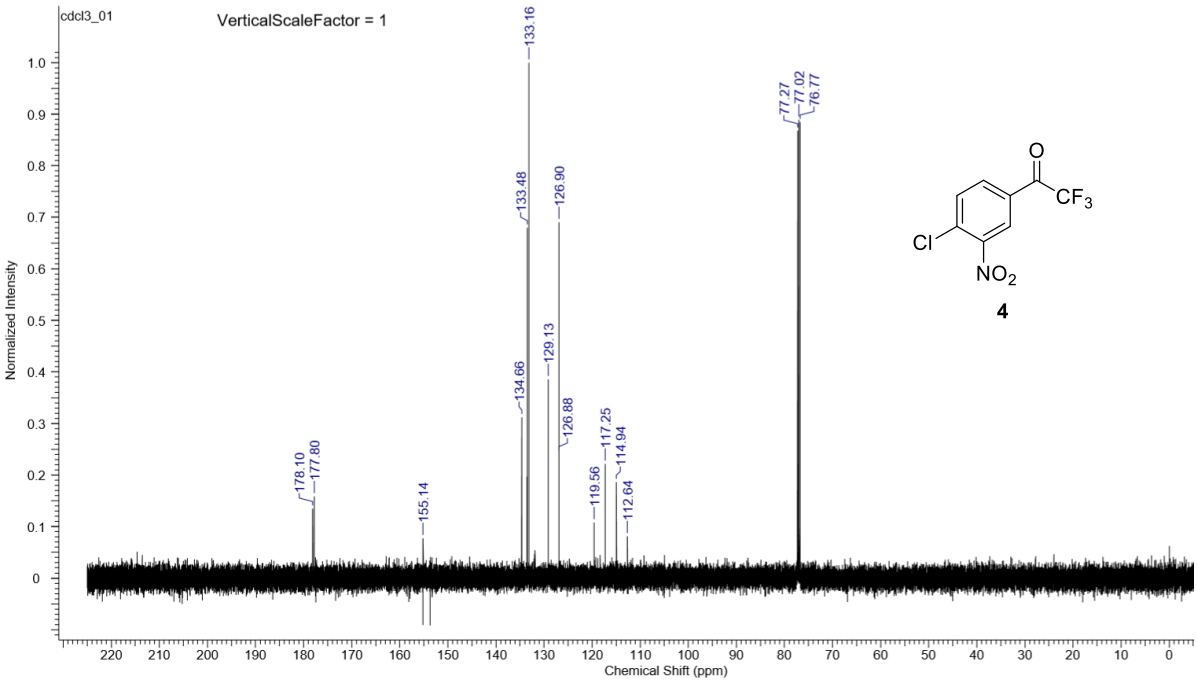
cdcl3_01
VerticalScaleFactor = 1
Normalized Intensity
Chemical Shift (ppm)
133.16
133.48
126.90
129.13
134.66
126.88
117.25
114.94
119.56
112.64
178.10
177.80
155.14
77.27
77.02
76.77
O
CF3
Cl
NO2
4

tosylation 1H

Acquisition Time (sec)	2.0487	*Date*	Jun 29 2017	*Date Stamp*	Jun 29 2017		
File Name	C:\Users\user\Dropbox\PHD\Group meeting\Experimental part\NMR_pure compounds\s_20170629_03 (tosylation_1H)\data\cdcl3_01.fid\fid						
Frequency (MHz)	500.61	*Nucleus*	1H	*Number of Transients*	8	*Original Points Count*	16409
Points Count	32768	*Pulse Sequence*	s2pul	*Receiver Gain*	44.00	*Solvent*	CHLOROFORM-d
Spectrum Offset (Hz)	2994.0713	*Spectrum Type*	STANDARD	*Sweep Width (Hz)*	8009.61	*Temperature (degree C)*	25.000

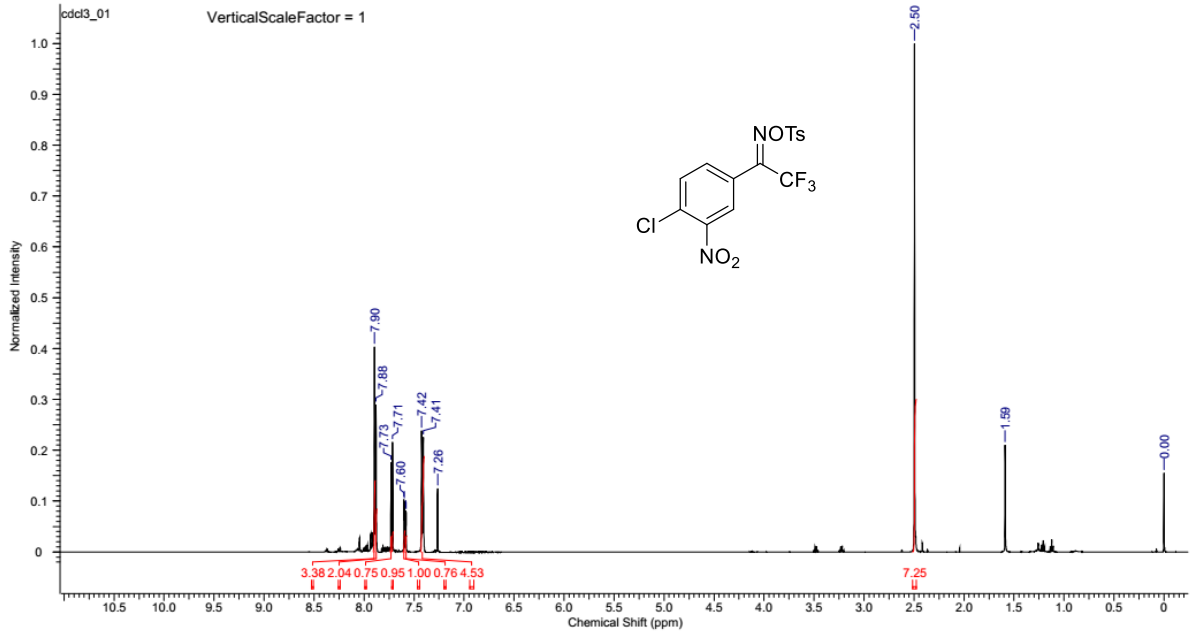

tosylation 13C

Acquisition Time (sec)	1.3005	*Date*	Jun 29 2017	*Date Stamp*	Jun 29 2017		
File Name	C:\Users\user\Dropbox\PHD\Group meeting\Experimental part\NMR_pure compounds\s_20170629_04 (tosylation_13C)\data\cdcl3_01.fid\fid						
Frequency (MHz)	125.89	*Nucleus*	13C	*Number of Transients*	1000	*Original Points Count*	39289
Points Count	65536	*Pulse Sequence*	s2pul	*Receiver Gain*	30.00	*Solvent*	CHLOROFORM-d
Spectrum Offset (Hz)	13217.1172	*Spectrum Type*	STANDARD	*Sweep Width (Hz)*	30211.48	*Temperature (degree C)*	25.000

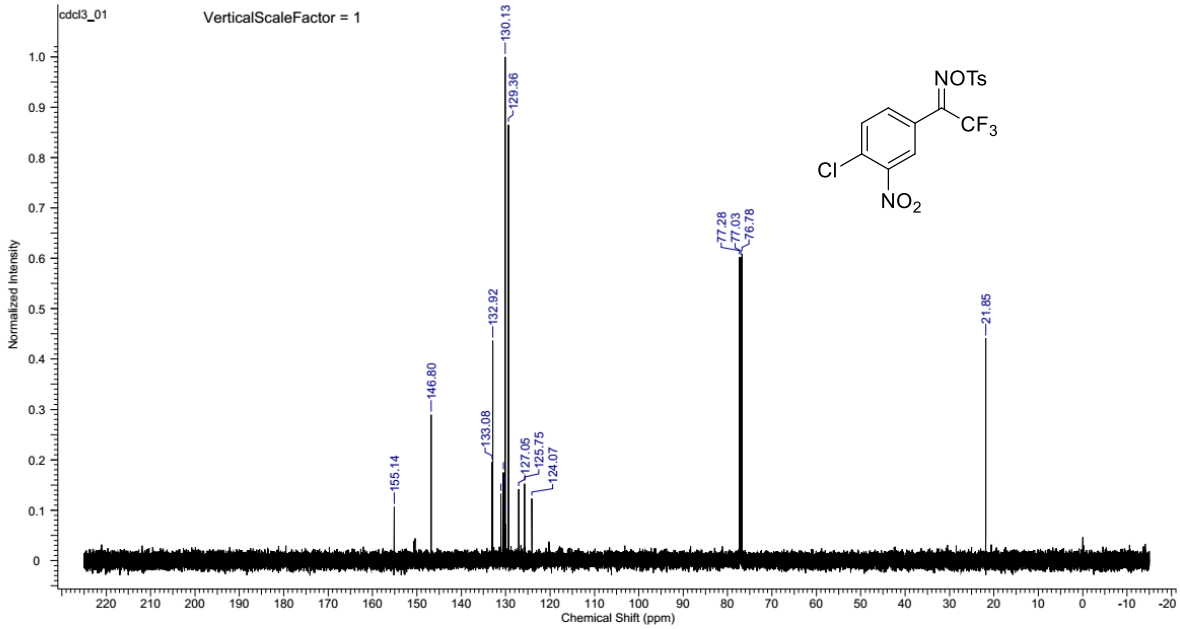

diaziridine 1H

Acquisition Time (sec)	2.0487	**Date**	Mar 28 2019			**Date Stamp**	Mar 28 2019
File Name	E:\s_20190328_05\data\cdcl3_01.fid\fid			**Frequency (MHz)**	500.45	**Nucleus**	1H
Original Points Count	16404	**Points Count**	32768	**Pulse Sequence**	s2pul	**Receiver Gain**	42.00
Spectrum Offset (Hz)	3000.0144	**Spectrum Type**	STANDARD			**Sweep Width (Hz)**	8007.21

Number of Transients	8		
Solvent	CHLOROFORM-d		
Temperature (degree C)	25.000		

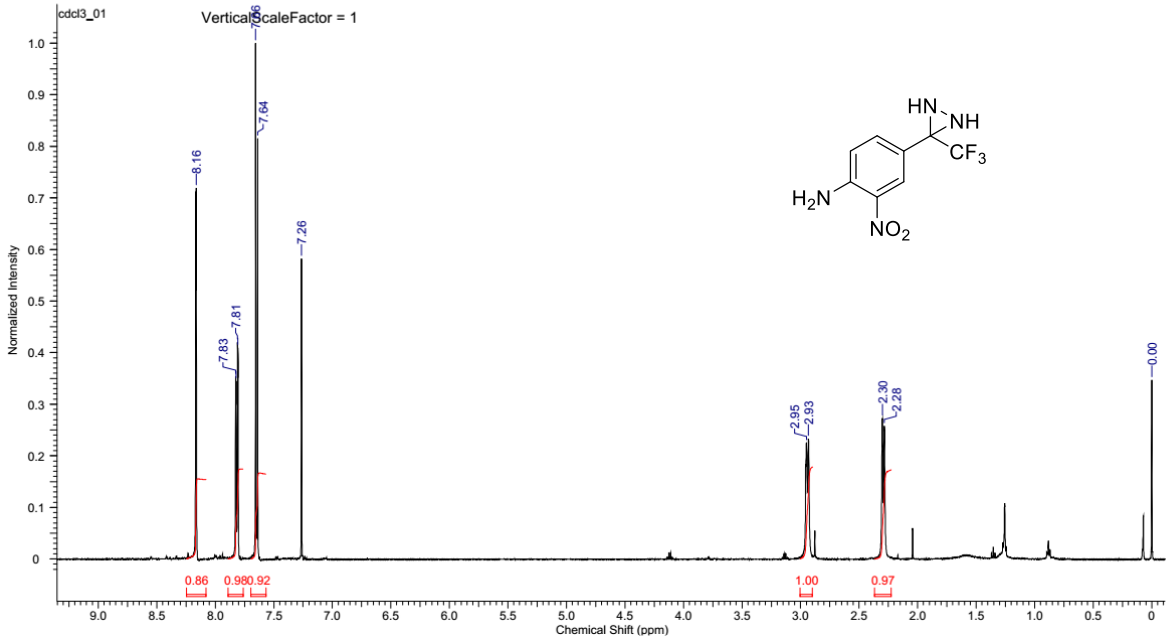

diaziridine 13C

Acquisition Time (sec)	1.3005	**Date**	Mar 28 2019	**Date Stamp**	Mar 28 2019	**File Name**	E:\s_20190328_04\data\cdcl3_01.fid\fid
Frequency (MHz)	125.85	**Nucleus**	13C	**Number of Transients**	1000	**Original Points Count**	39274
Pulse Sequence	s2pul	**Receiver Gain**	30.00	**Solvent**	CHLOROFORM-d		
Spectrum Type	STANDARD	**Sweep Width (Hz)**	30200.08	**Temperature (degree C)**	25.000		

Points Count	65536
Spectrum Offset (Hz)	13213.0635

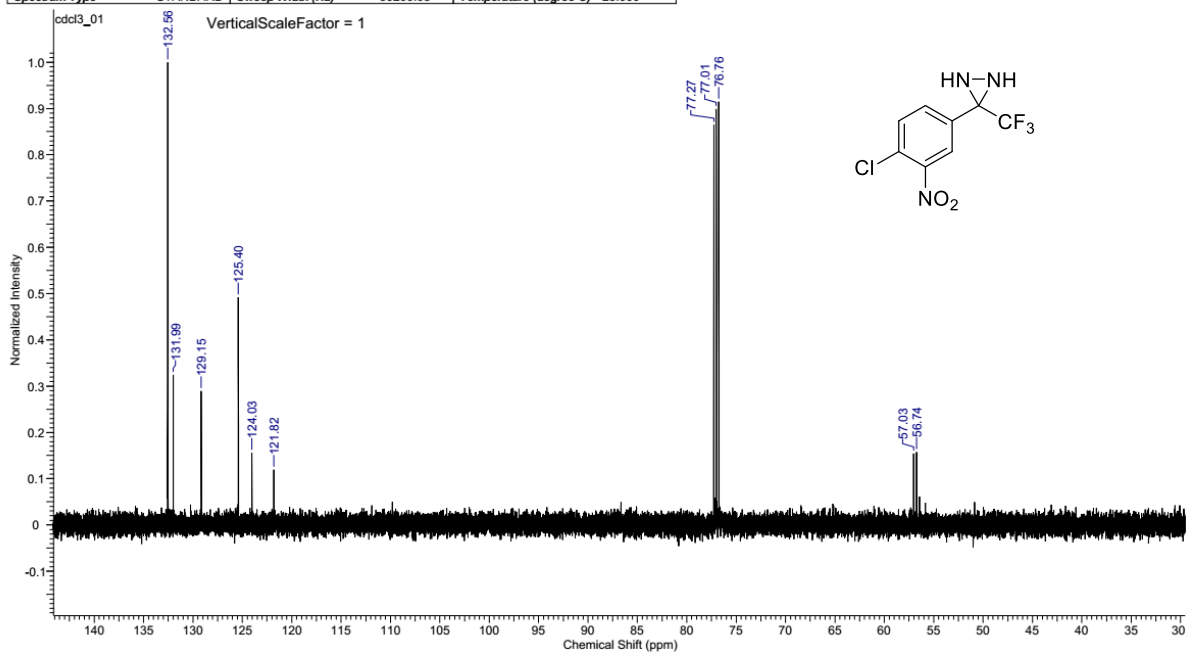

DIAZIRINE CI

Acquisition Time (sec)	2.0487	*Date*	Apr 2 2019	*Date Stamp*	Apr 2 2019	*File Name*	E:\s_20190402_07\data\cdcl3_01.fid\fid		
Frequency (MHz)	500.45	*Nucleus*	1H	*Number of Transients*	8	*Original Points Count*	16404	*Points Count*	32768
Pulse Sequence	s2pul	*Receiver Gain*	36.00	*Solvent*	CHLOROFORM-d			*Spectrum Offset (Hz)*	2999.0371
Spectrum Type	STANDARD			*Sweep Width (Hz)*	8007.21	*Temperature (degree C)*	25.000		

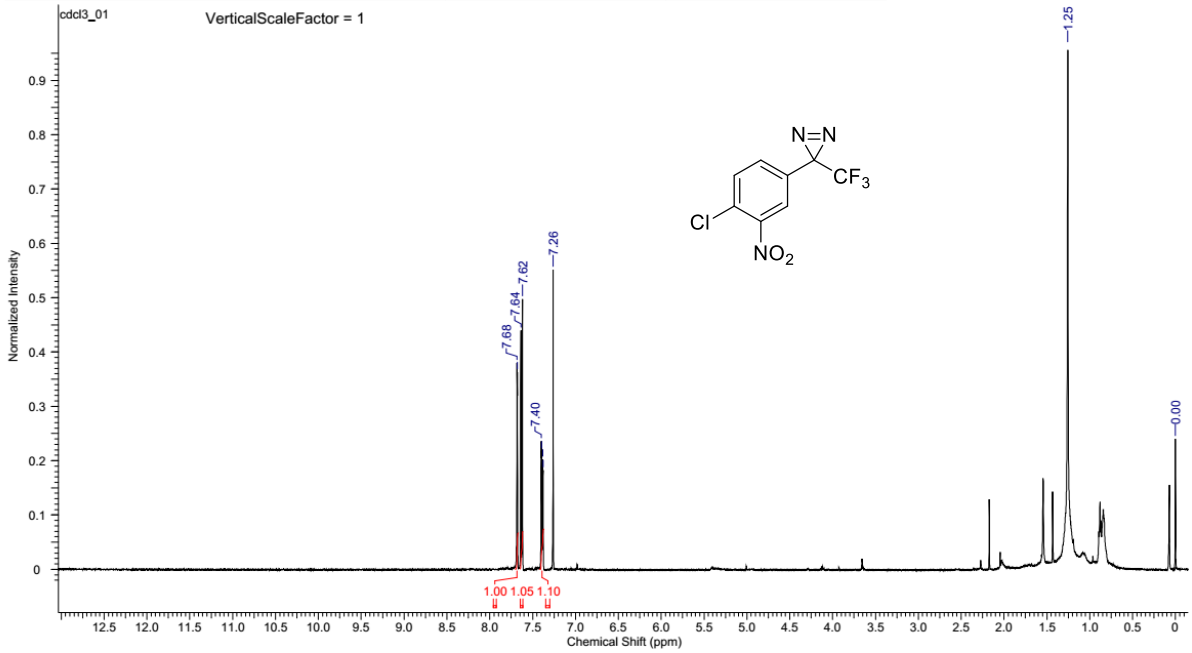

DIAZIRINE CI 13C

Acquisition Time (sec)	1.3005	*Date*	Apr 2 2019	*Date Stamp*	Apr 2 2019	*File Name*	E:\s_20190402_08\data\cdcl3_01.fid\fid		
Frequency (MHz)	125.85	*Nucleus*	13C	*Number of Transients*	1500	*Original Points Count*	39274	*Points Count*	65536
Pulse Sequence	s2pul	*Receiver Gain*	30.00	*Solvent*	CHLOROFORM-d			*Spectrum Offset (Hz)*	13213.0635
Spectrum Type	STANDARD			*Sweep Width (Hz)*	30200.08	*Temperature (degree C)*	25.000		

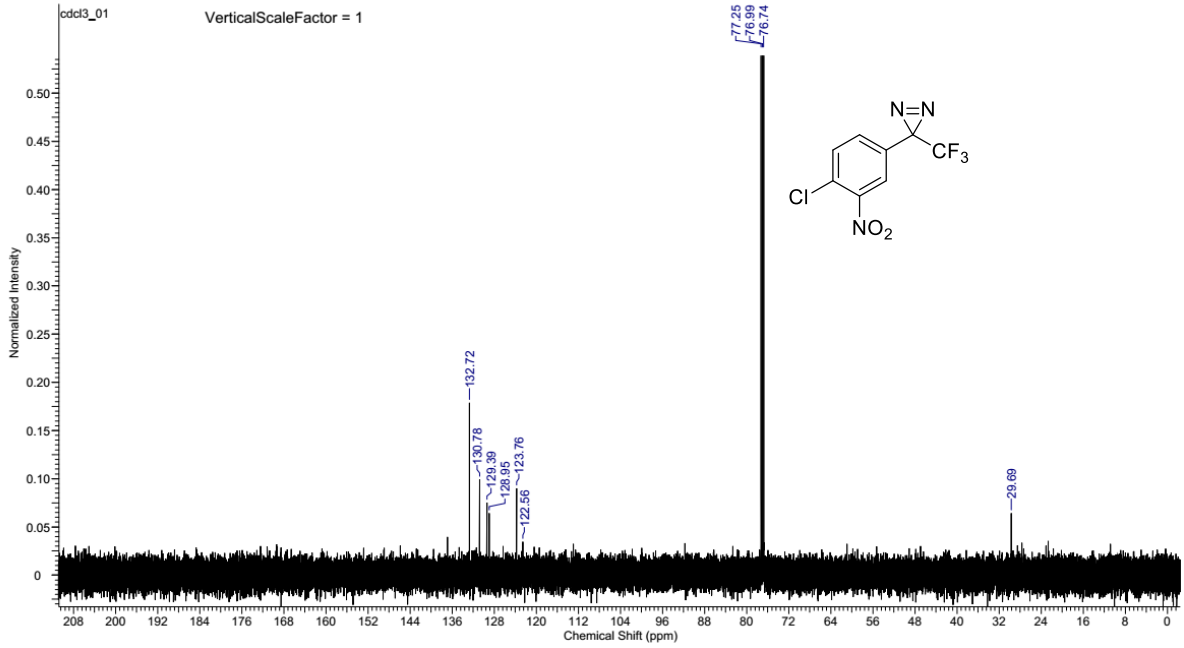

diazirine BnSH 1H

Acquisition Time (sec)	2.0487	*Date*	Jun 30 2017	*Date Stamp*	Jun 30 2017		
File Name	C:\Users\user\Dropbox\PHD\NMR_2\s_20170630_01 (diazirineBnSH_1H)\data\cdcl3_01.fid\fid					*Frequency (MHz)*	500.61
Nucleus	1H	*Number of Transients*	8	*Original Points Count*	16409	*Points Count*	32768
Pulse Sequence	s2pul	*Receiver Gain*	36.00	*Solvent*	CHLOROFORM-d		
Spectrum Offset (Hz)	2986.9827	*Spectrum Type*	STANDARD	*Sweep Width (Hz)*	8009.61	*Temperature (degree C)*	25.000

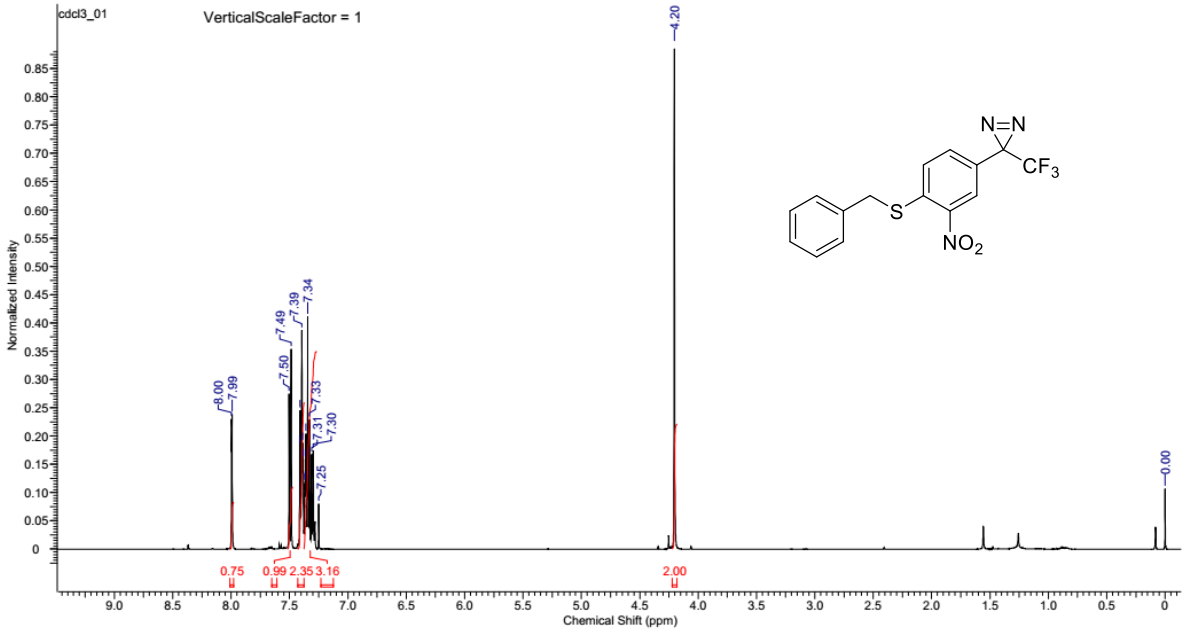

diazirine BnSH 13C

Acquisition Time (sec)	1.3005	*Date*	Jun 30 2017	*Date Stamp*	Jun 30 2017		
File Name	C:\Users\user\Dropbox\PHD\NMR_2\s_20170630_02 (diazirineBnSH_13C)\data\cdcl3_01.fid\fid					*Frequency (MHz)*	125.89
Nucleus	13C	*Number of Transients*	1000	*Original Points Count*	39289	*Points Count*	65536
Pulse Sequence	s2pul	*Receiver Gain*	30.00	*Solvent*	CHLOROFORM-d		
Spectrum Offset (Hz)	13217.1172	*Spectrum Type*	STANDARD	*Sweep Width (Hz)*	30211.48	*Temperature (degree C)*	25.000

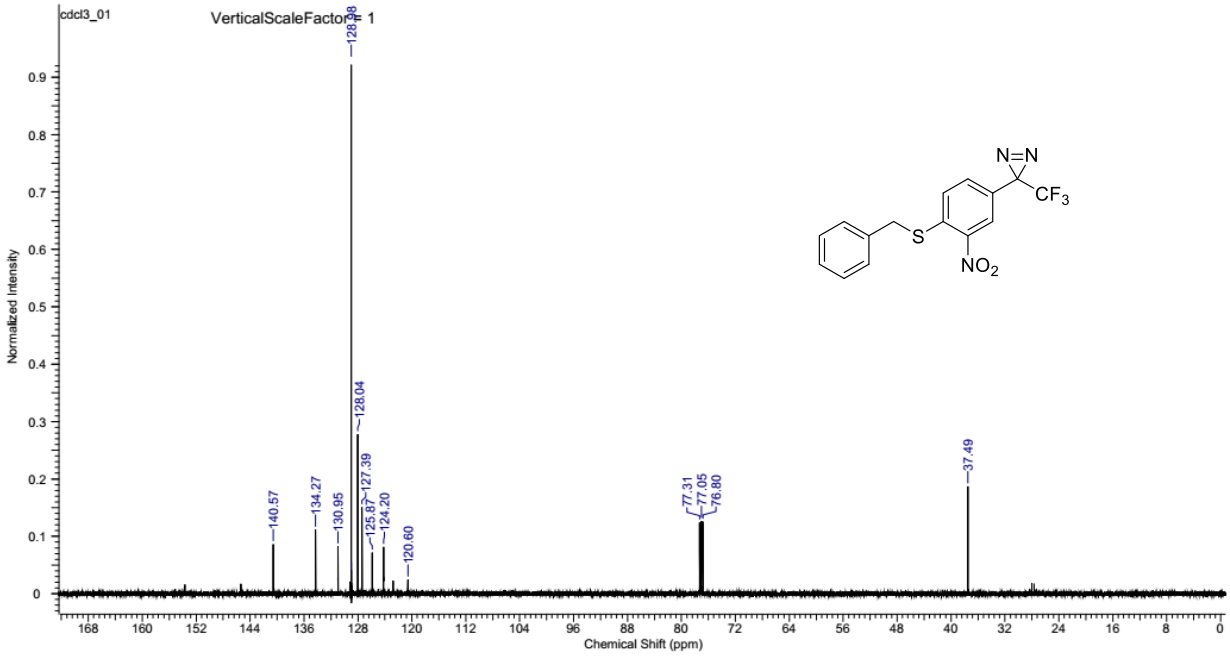

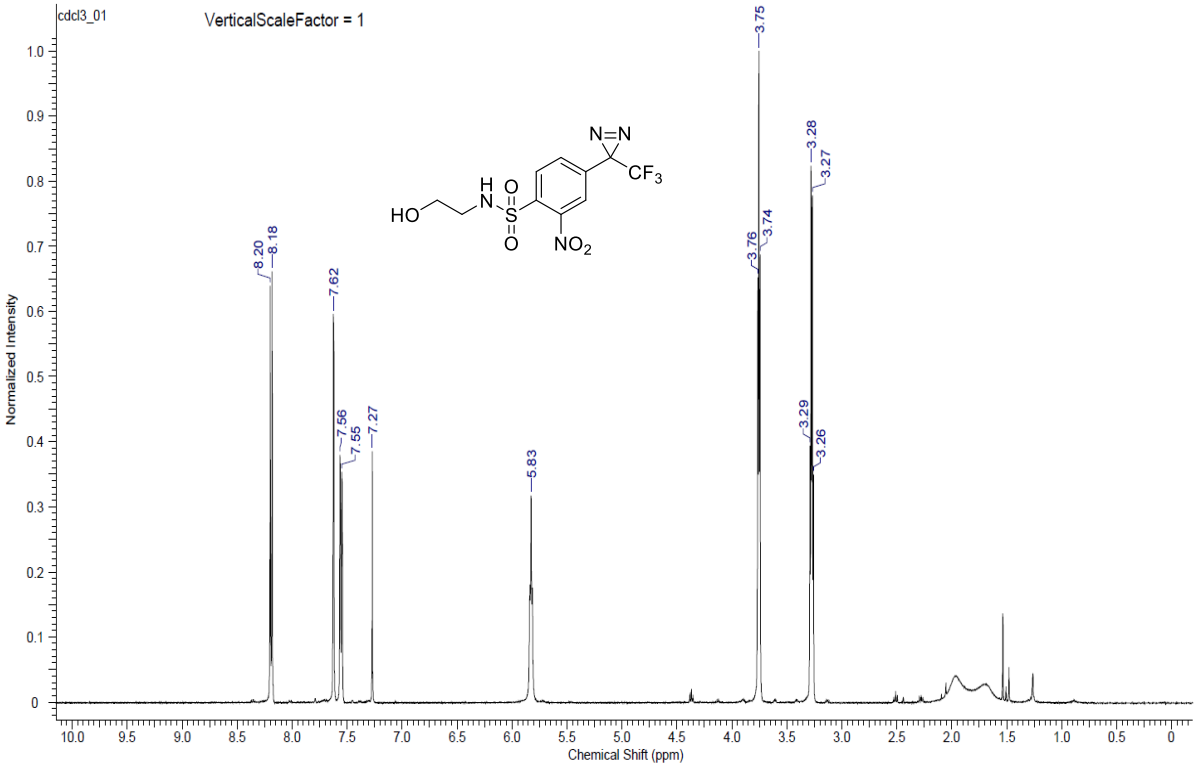
cdcl3_01
VerticalScaleFactor = 1
Normalized Intensity
Chemical Shift (ppm)
8.20
8.18
7.62
7.56
7.55
7.27
5.83
3.75
3.76
3.74
3.29
3.28
3.27
3.26
HO
N=N
CF3
NO2

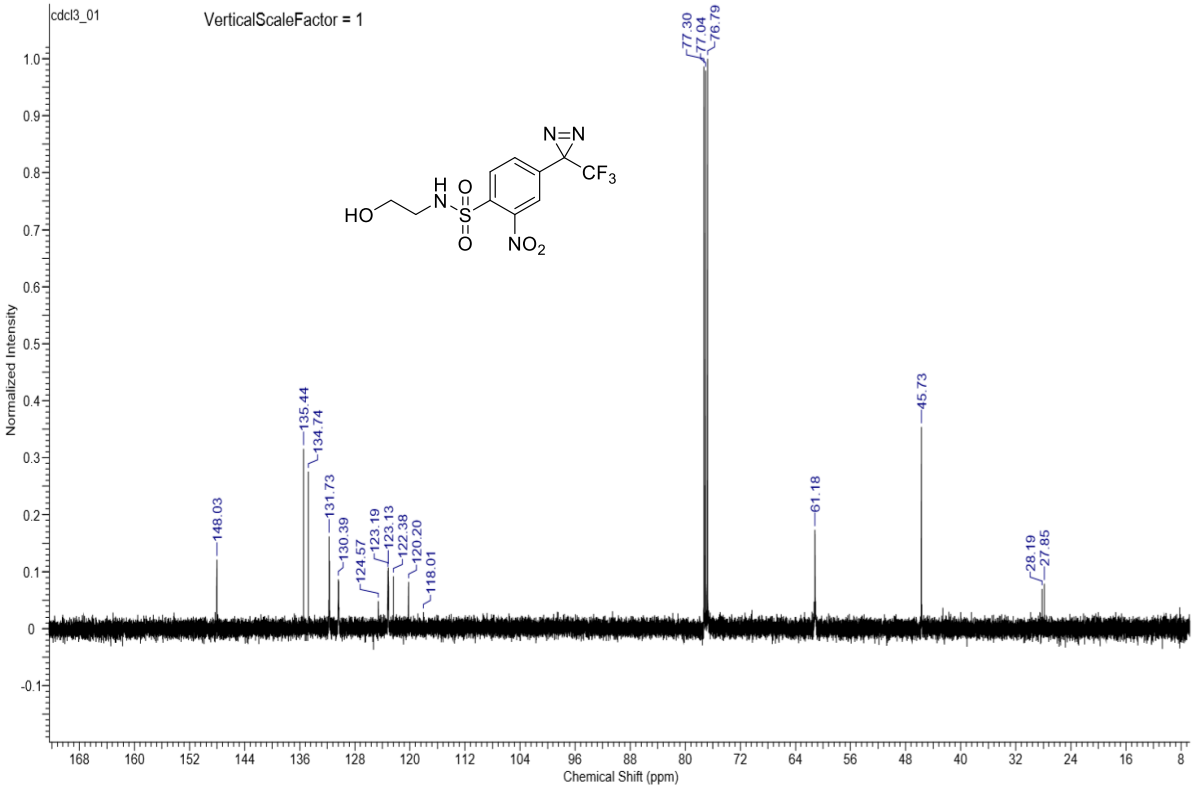
cdcl3_01
VerticalScaleFactor = 1
Normalized Intensity
Chemical Shift (ppm)
77.30
77.04
76.79
148.03
135.44
134.74
131.73
130.39
124.57
123.19
123.13
122.38
120.20
118.01
61.18
45.73
28.19
27.85
HO
N=N
CF3
NO2

13/5/2019 3:28:41 PM
3-168 NBD aminohydroxy PEG

Acquisition Time (sec)	2.0486	**Date**	Dec 29 2018			**Date Stamp**	Dec 29 2018
File Name	E:\s_20181229_04 (3-168)\data\cdcl3_01.fid\fid			**Frequency (MHz)**	500.48	**Nucleus**	1H
Original Points Count	16405	**Points Count**	32768	**Pulse Sequence**	s2pul	**Receiver Gain**	54.00
Spectrum Offset (Hz)	2996.1602	**Spectrum Type**	STANDARD	**Sweep Width (Hz)**	8008.01	**Temperature (degree C)**	25.000

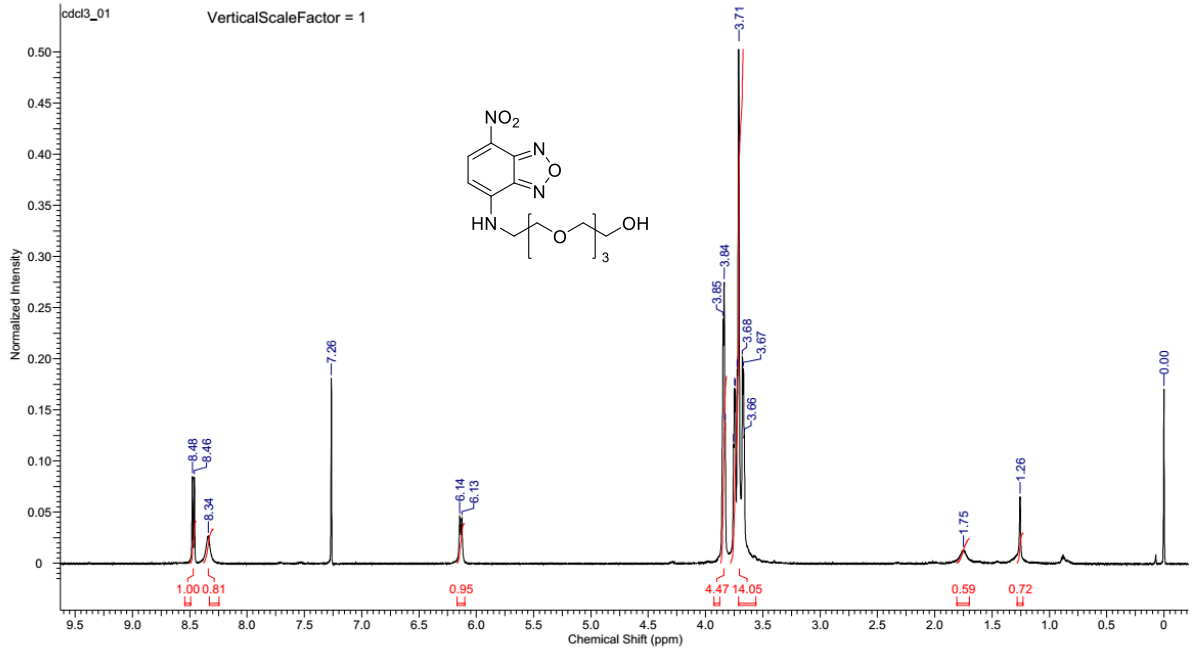

14/5/2019 2:50:00 PM
3-177

Acquisition Time (sec)	2.0487	**Date**	Jan 8 2019	**Date Stamp**	Jan 8 2019	**File Name**	E:\s_20190108_05 (3-177)\data\cd3od_01.fid\fid
Frequency (MHz)	500.47	**Nucleus**	1H	**Number of Transients**	8	**Original Points Count**	16404
Points Count	32768	**Pulse Sequence**	s2pul	**Receiver Gain**	48.00	**Solvent**	METHANOL-d4
Spectrum Offset (Hz)	3002.7734	**Spectrum Type**	STANDARD	**Sweep Width (Hz)**	8007.21	**Temperature (degree C)**	25.000

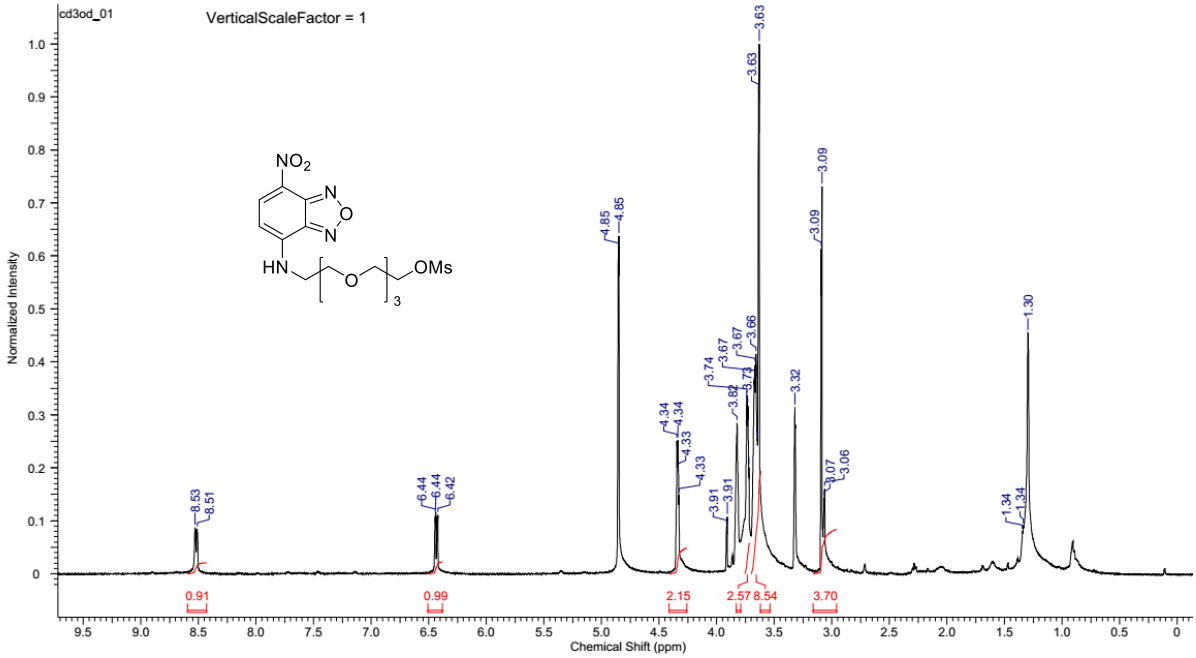

3-178 NBD thioacetate

Acquisition Time (sec)	2.0487	*Date*	Jan 10 2019	*Date Stamp*	Jan 10 2019	*File Name*	E:\s_20190110_01 (3-178)\data\cdcl3_01.fid\fid		
Frequency (MHz)	500.47	*Nucleus*	1H	*Number of Transients*	8	*Original Points Count*	16404	*Points Count*	32768
Pulse Sequence	s2pul	*Receiver Gain*	56.00	*Solvent*	CHLOROFORM-d			*Spectrum Offset (Hz)*	3001.2041
Spectrum Type	STANDARD	*Sweep Width (Hz)*	8007.21	*Temperature (degree C)*	25.000				

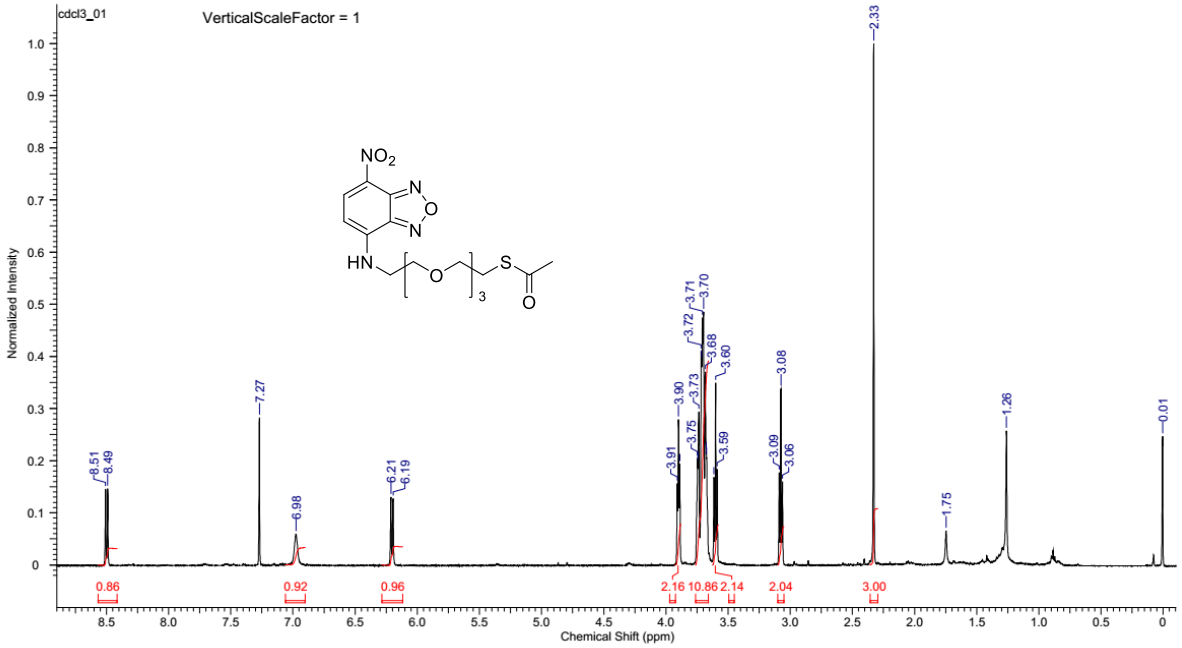

3-179 NBD thiol PEG

Acquisition Time (sec)	2.0487	*Date*	Jan 10 2019	*Date Stamp*	Jan 10 2019	*File Name*	E:\s_20190110_05 (3-179)\data\cdcl3_01.fid\fid		
Frequency (MHz)	500.47	*Nucleus*	1H	*Number of Transients*	8	*Original Points Count*	16404	*Points Count*	32768
Pulse Sequence	s2pul	*Receiver Gain*	54.00	*Solvent*	CHLOROFORM-d			*Spectrum Offset (Hz)*	3000.2268
Spectrum Type	STANDARD	*Sweep Width (Hz)*	8007.21	*Temperature (degree C)*	25.000				

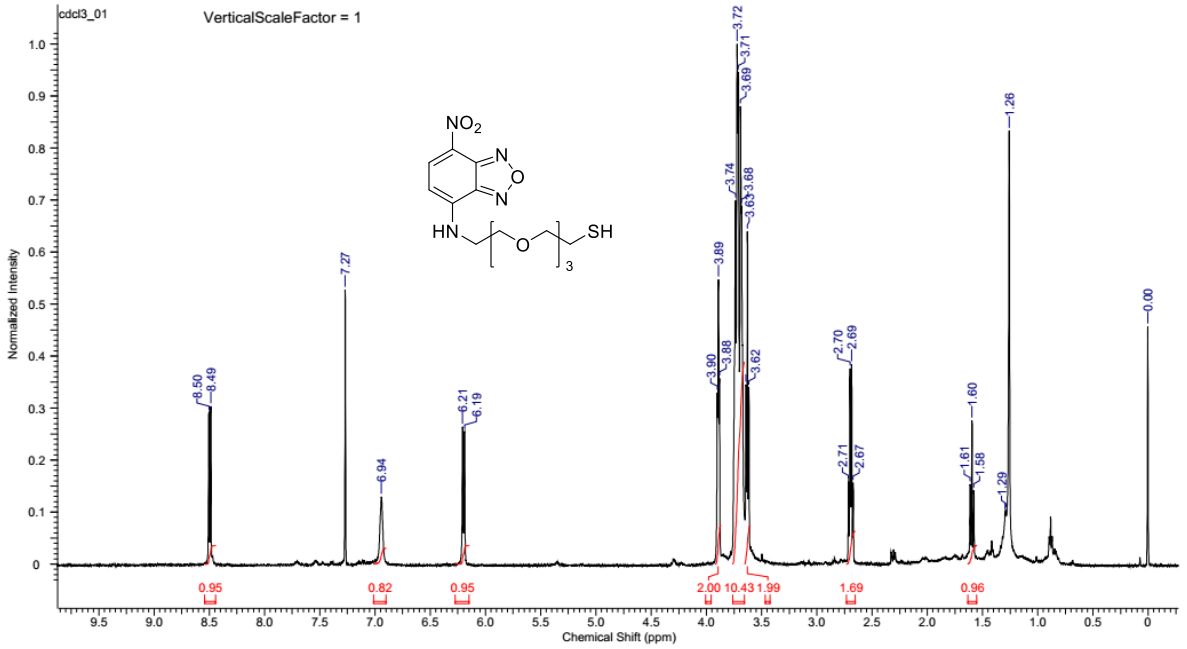

ditosylation

Acquisition Time (sec)	2.0487	**Date**	Jun 30 2017	**Date Stamp**	Jun 30 2017		
File Name	C:\Users\user\Dropbox\PHD\NMR_2\s_20170630_03 (tditosylation)\data\cdcl3_01.fid\fid					**Frequency (MHz)**	500.61
Nucleus	1H	**Number of Transients**	8	**Original Points Count**	16409	**Points Count**	32768
Pulse Sequence	s2pul	**Receiver Gain**	44.00	**Solvent**	CHLOROFORM-d		
Spectrum Offset (Hz)	2997.1660	**Spectrum Type**	STANDARD	**Sweep Width (Hz)**	8009.61	**Temperature (degree C)**	25.000

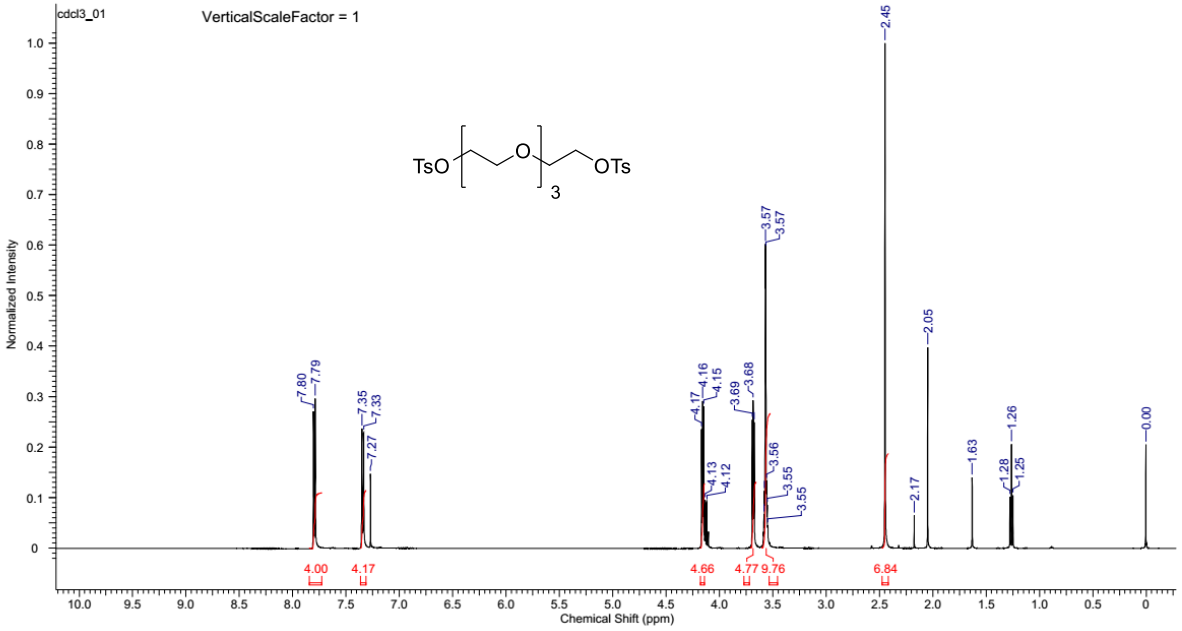

16/5/2019 1:27:43 PM
DIAZIDE

Acquisition Time (sec)	2.0487	**Date**	May 30 2017	**Date Stamp**	May 30 2017		
File Name	C:\Users\user\Dropbox\PHD\NMR_2\s_20170530_02 (2_16_crude)\data\cdcl3_01.fid\fid					**Frequency (MHz)**	500.62
Nucleus	1H	**Number of Transients**	8	**Original Points Count**	16409	**Points Count**	32768
Pulse Sequence	s2pul	**Receiver Gain**	44.00	**Solvent**	CHLOROFORM-d		
Spectrum Offset (Hz)	3003.7317	**Spectrum Type**	STANDARD	**Sweep Width (Hz)**	8009.61	**Temperature (degree C)**	25.000

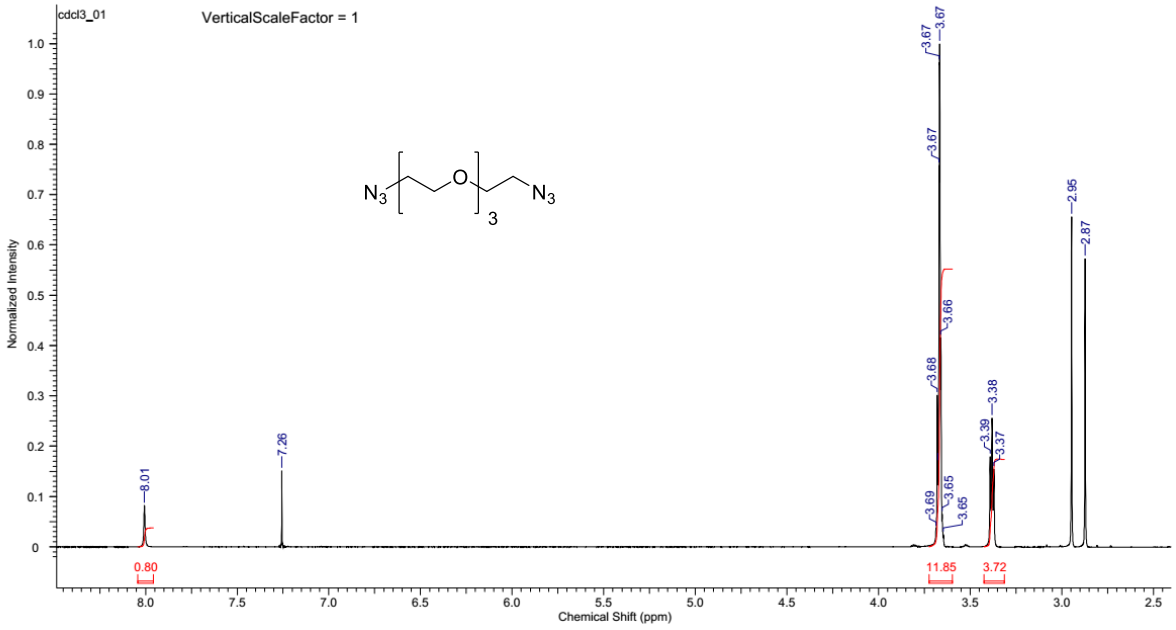

diazide

Acquisition Time (sec)	2.0487	Date	Sep 15 2017	Date Stamp	Sep 15 2017		
File Name	C:\Users\user\Dropbox\PHD\NMR_2\s_20170915_01\data\cdcl3_01.fid\fid				Frequency (MHz)	500.58	Nucleus	1H
Number of Transients	8	Original Points Count	16409	Points Count	32768	Pulse Sequence	s2pul	Receiver Gain	36.00
Solvent	CHLOROFORM-d			Spectrum Offset (Hz)	3002.3542	Spectrum Type	STANDARD	Sweep Width (Hz)	8009.61
Temperature (degree C)	25.000								

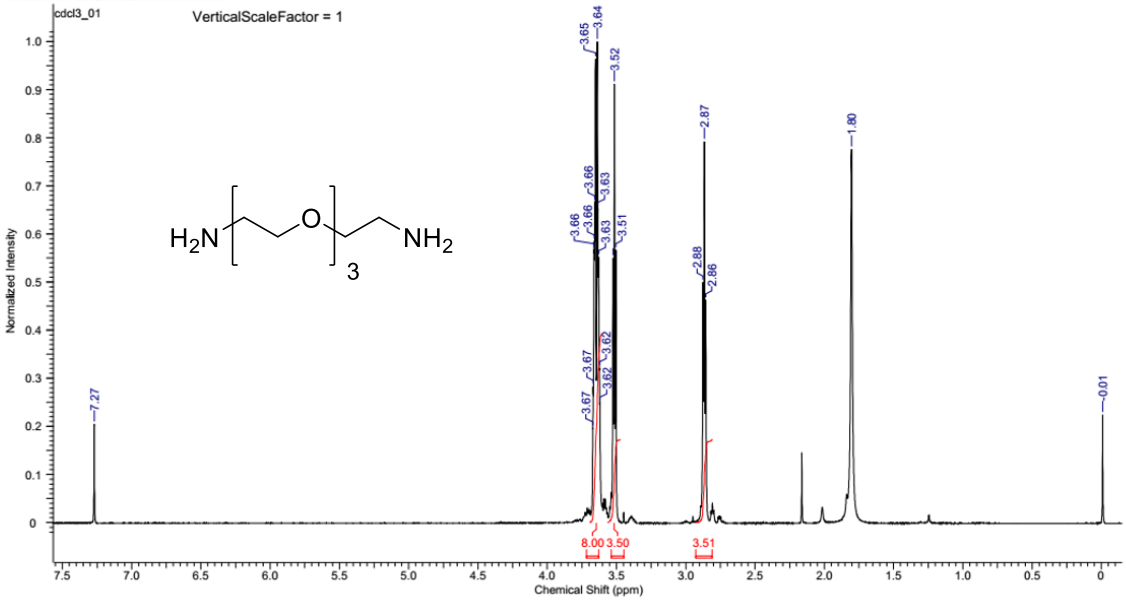

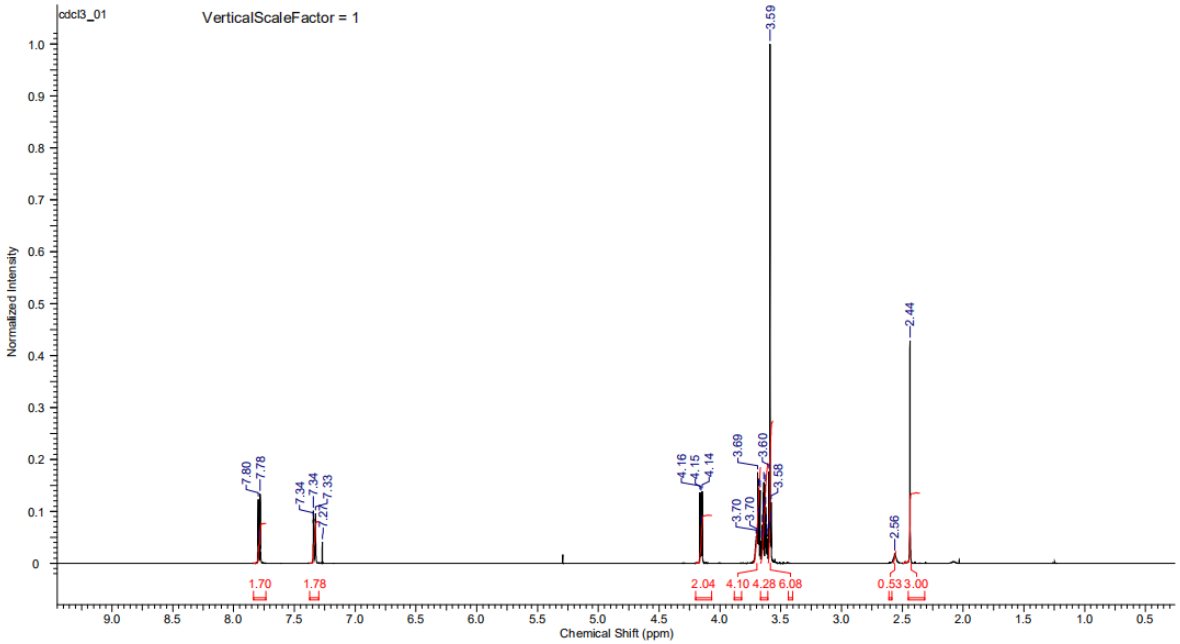

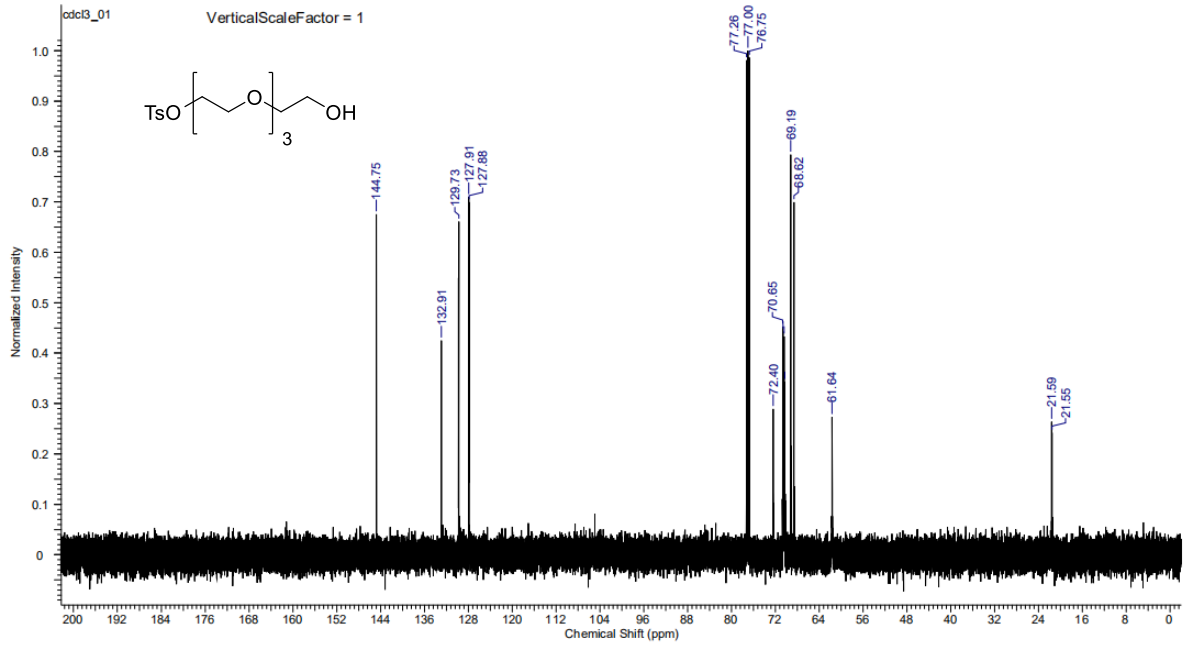
cdcl3_01
VerticalScaleFactor = 1
TsO
O
OH
3
77.26
77.00
76.75
69.19
68.62
144.75
129.73
127.91
127.88
132.91
70.65
72.40
61.64
21.59
21.55
Normalized Intensity
Chemical Shift (ppm)

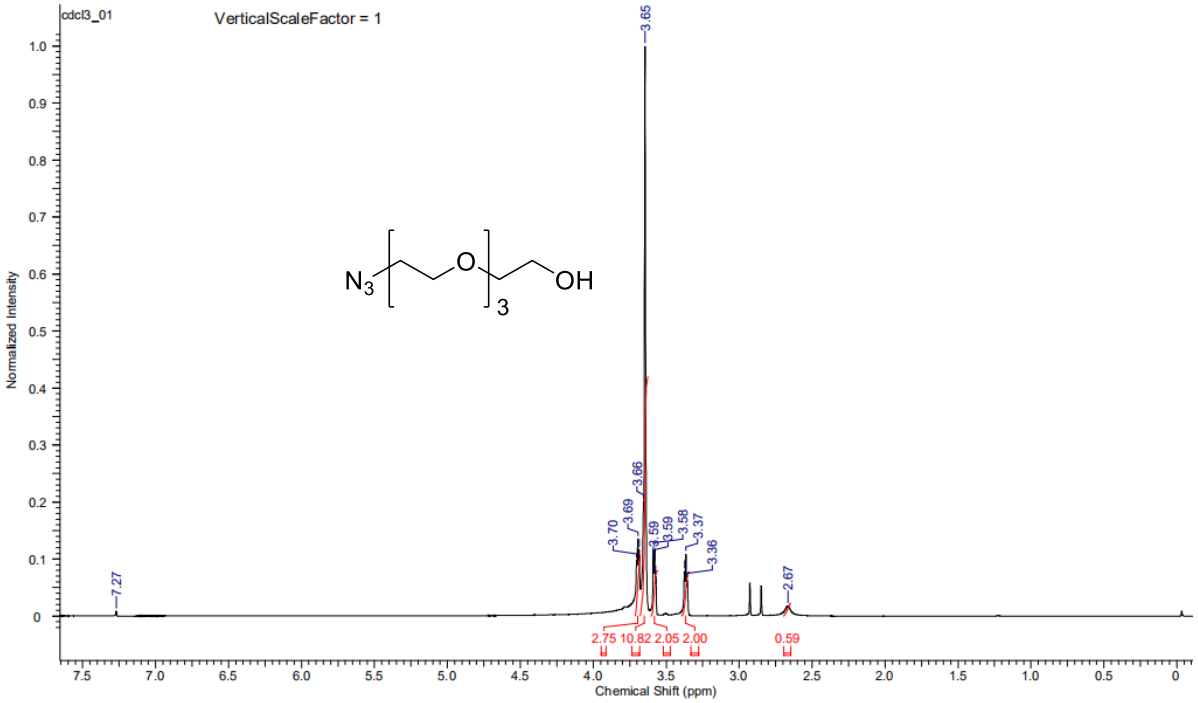
cdcl3_01
VerticalScaleFactor = 1
N3
O
OH
3
3.65
3.66
3.69
3.70
3.59
3.58
3.37
3.36
7.27
2.67
2.75 10.82 2.05 2.00
0.59
Normalized Intensity
Chemical Shift (ppm)

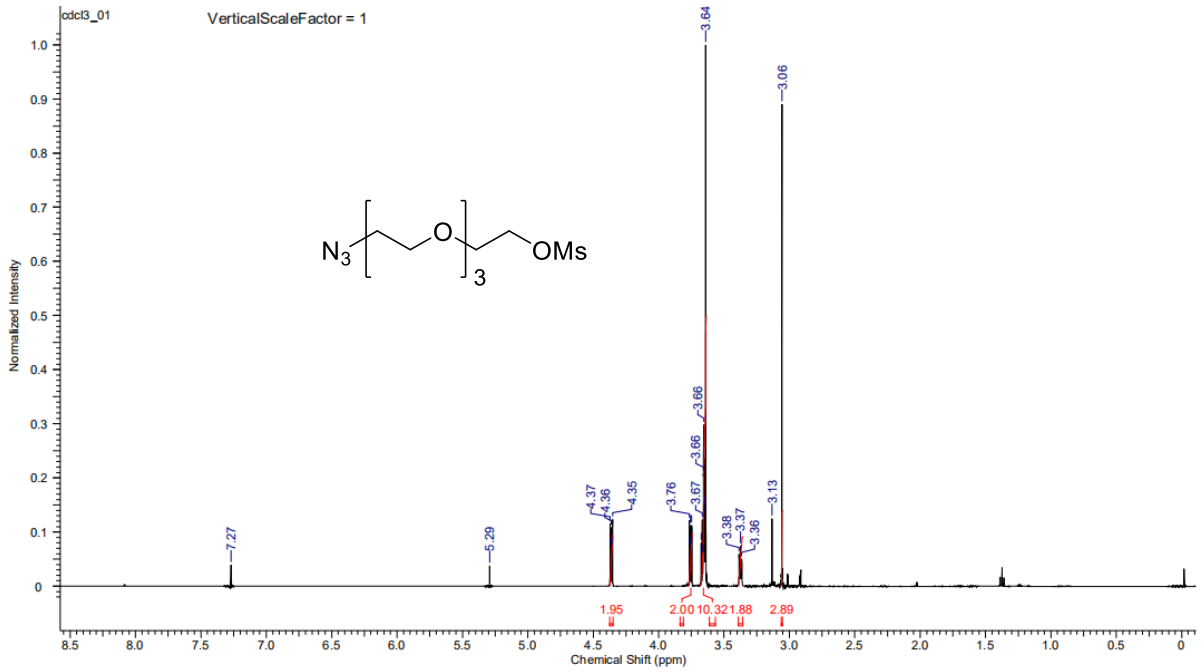
cdcl3_01
VerticalScaleFactor = 1
Normalized Intensity
Chemical Shift (ppm)
N3
O
OMs
3
7.27
5.29
4.37
4.36
4.35
3.76
3.67
3.66
3.64
3.38
3.37
3.36
3.13
3.06
1.95
2.00
10.32
1.88
2.89

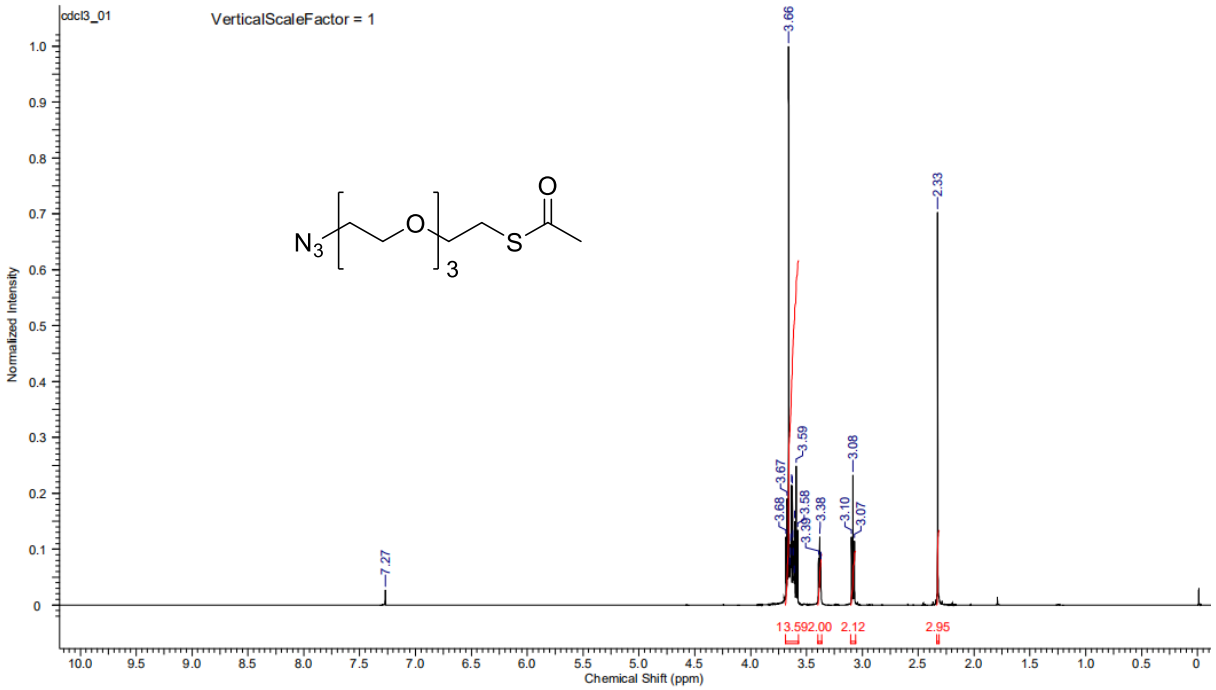
cdcl3_01
VerticalScaleFactor = 1
Normalized Intensity
Chemical Shift (ppm)
N3
O
S
O
3
7.27
3.68
3.67
3.59
3.58
3.38
3.10
3.08
3.07
3.66
2.33
13.59
2.00
2.12
2.95

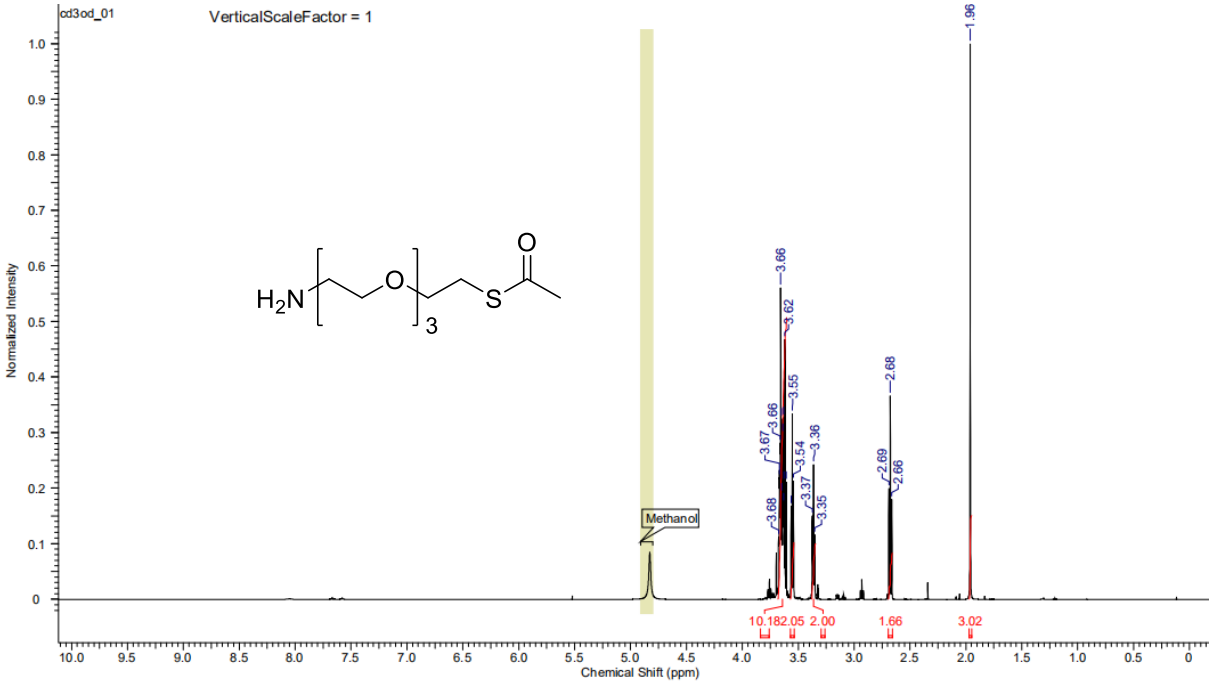
cd3od_01
VerticalScaleFactor = 1
Normalized Intensity
Chemical Shift (ppm)
Methanol
1.96
3.66
3.62
3.55
3.68
3.67
3.66
3.54
3.36
3.37
3.35
2.68
2.69
2.66
10.18
2.05
2.00
1.66
3.02
H2N
O
S
3

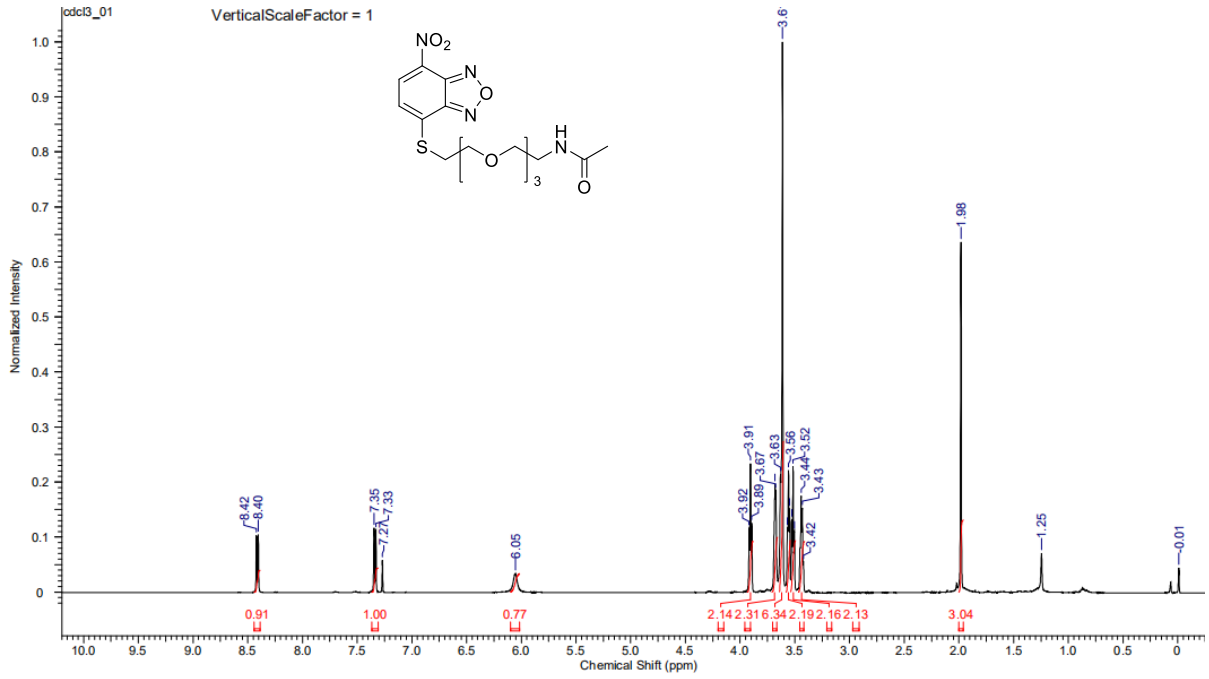
cdcl3_01
VerticalScaleFactor = 1
Normalized Intensity
Chemical Shift (ppm)
NO2
N
O
S
H
3.6
1.98
1.25
0.01
8.42
8.40
7.35
7.33
7.27
6.05
3.91
3.67
3.63
3.56
3.52
3.44
3.43
3.92
3.89
3.42
0.91
1.00
0.77
2.14
2.31
6.34
2.19
2.16
2.13
3.04

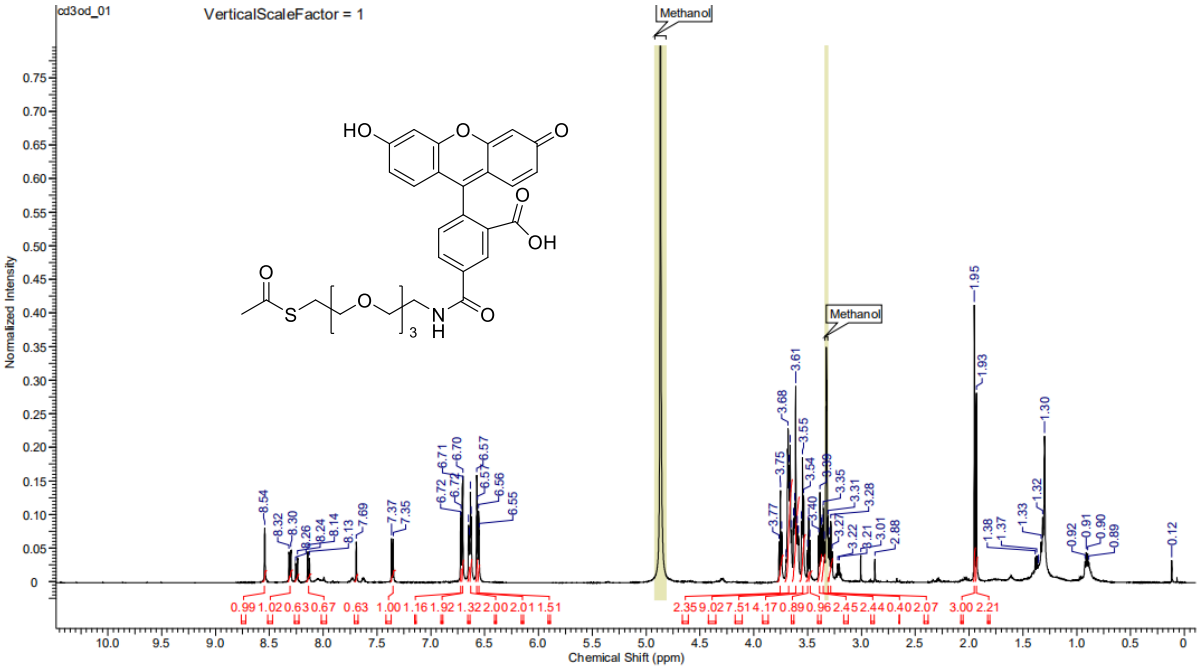
od3od_01
VerticalScaleFactor = 1
Methanol
Methanol
HO
O
O
O
OH
O
S
O
O
N
H
O
3
Normalized Intensity
Chemical Shift (ppm)

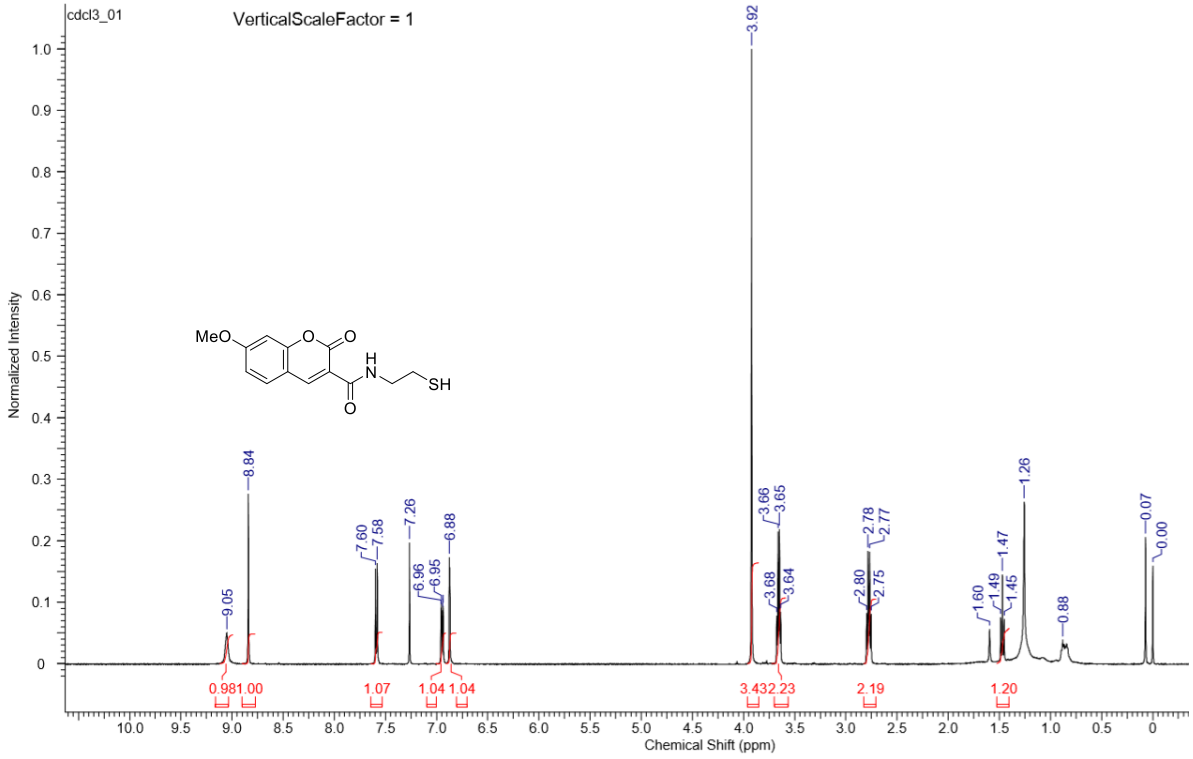
cdcl3_01
VerticalScaleFactor = 1
MeO
O
O
H
N
SH
O
Normalized Intensity
Chemical Shift (ppm)

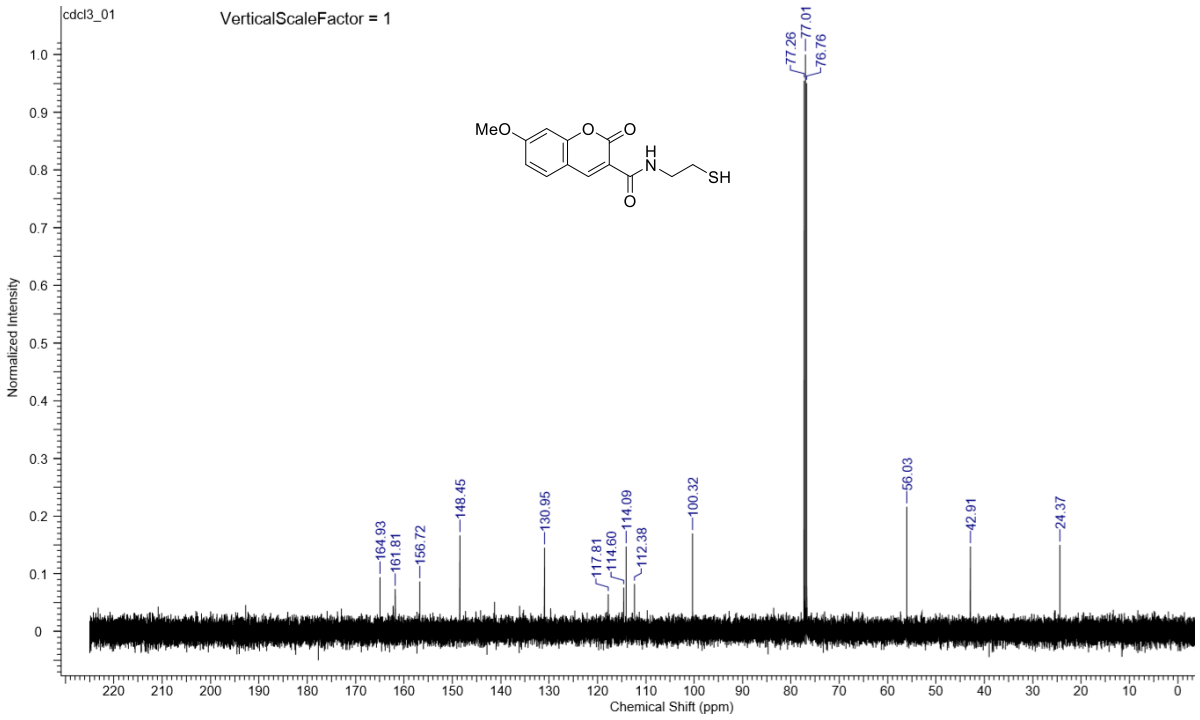
cdcl3_01
VerticalScaleFactor = 1
MeO
O
O
H
N
SH
O
77.26
77.01
76.76
164.93
161.81
156.72
148.45
130.95
117.81
114.60
114.09
112.38
100.32
56.03
42.91
24.37
Normalized Intensity
Chemical Shift (ppm)

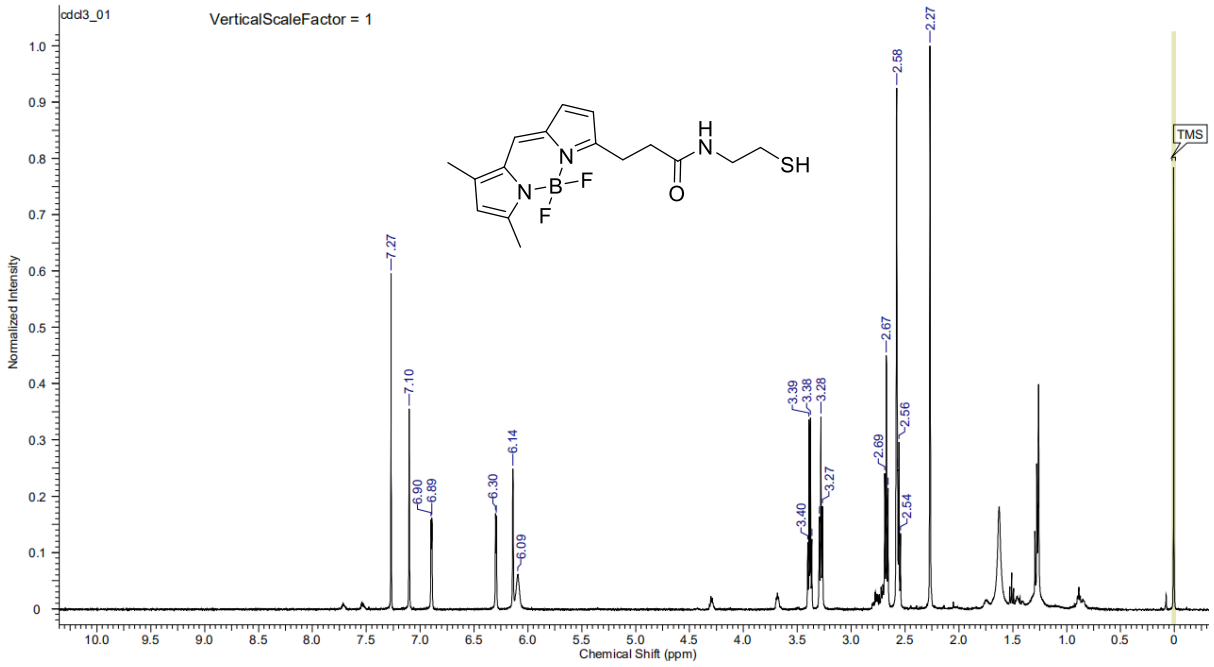
cdcl3_01
VerticalScaleFactor = 1
N
N
B
F
F
H
N
SH
O
TMS
7.27
7.10
6.90
6.89
6.30
6.14
6.09
3.40
3.39
3.38
3.28
3.27
2.69
2.67
2.58
2.56
2.54
2.27
Normalized Intensity
Chemical Shift (ppm)

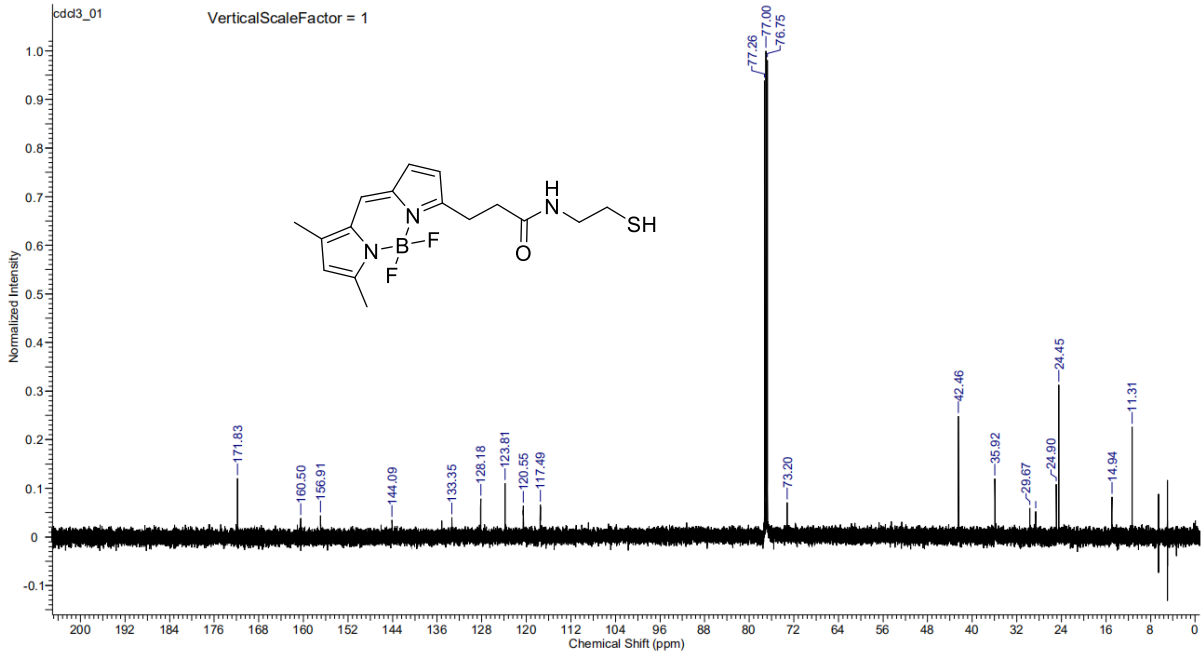
cdd3_01
VerticalScaleFactor = 1
Normalized Intensity
Chemical Shift (ppm)
77.26
77.00
76.75
171.83
160.50
156.91
144.09
133.35
128.18
123.81
120.55
117.49
73.20
42.46
35.92
29.67
24.90
24.45
14.94
11.31
H
N
O
SH
N
B
F
F

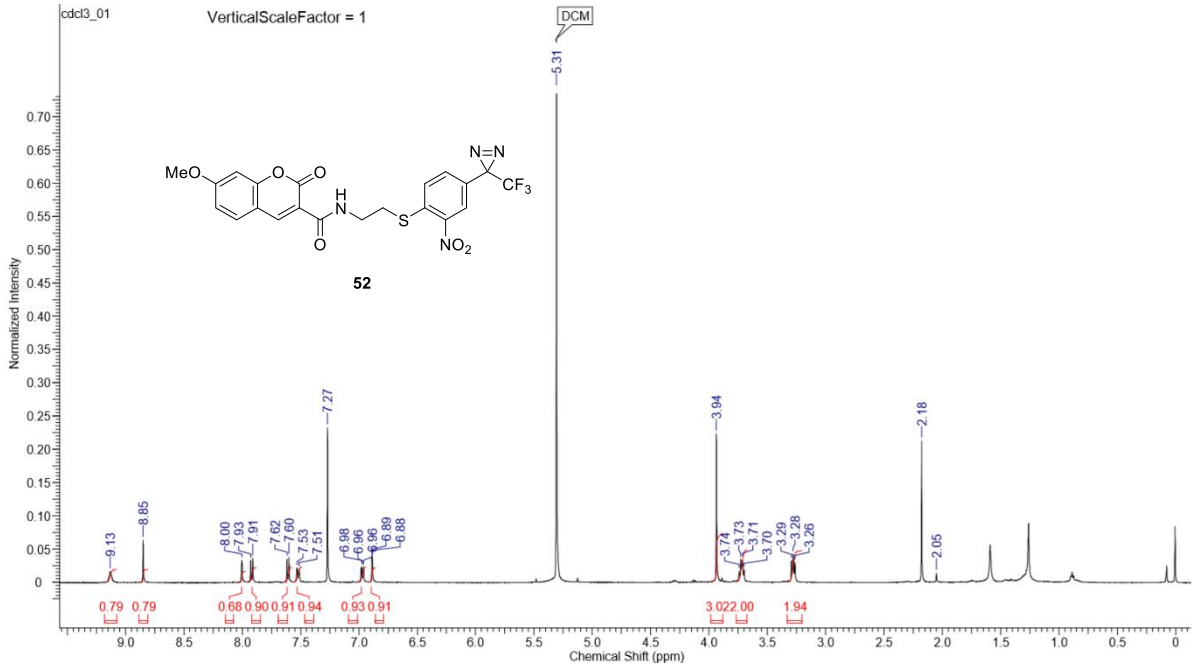
cdcl3_01
VerticalScaleFactor = 1
DCM
Normalized Intensity
Chemical Shift (ppm)
MeO
O
O
H
N
O
S
N=N
CF3
NO2
52
5.31
7.27
3.94
2.18
9.13
8.85
8.00
7.93
7.91
7.62
7.60
7.53
7.51
6.98
6.96
6.96
6.89
6.88
3.74
3.73
3.71
3.70
3.29
3.28
3.26
2.05
0.79
0.79
0.68
0.90
0.91
0.94
0.93
0.91
3.02
2.00
1.94

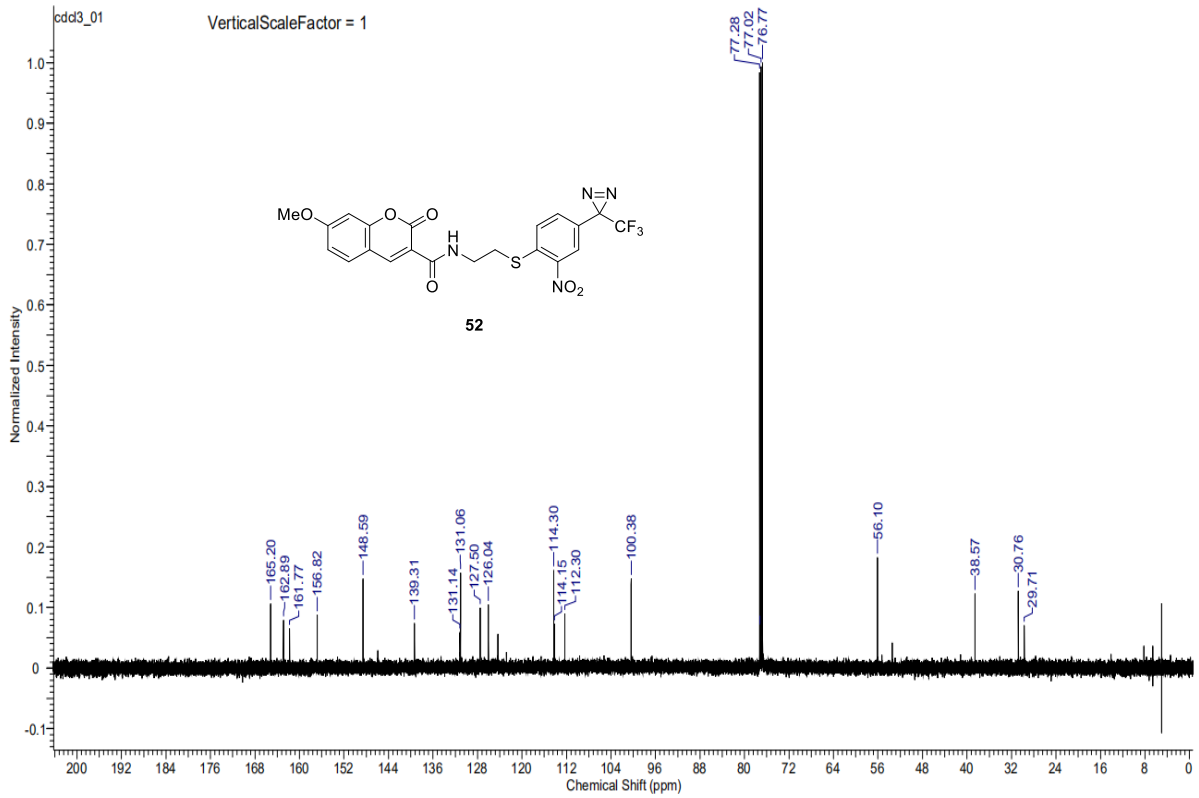
cdcl3_01
VerticalScaleFactor = 1
MeO
O
O
H
N
O
S
N=N
CF3
NO2
52
Normalized Intensity
Chemical Shift (ppm)
77.28
77.02
76.77
165.20
162.89
161.77
156.82
148.59
139.31
131.14
131.06
127.50
126.04
114.30
114.15
112.30
100.38
56.10
38.57
30.76
29.71

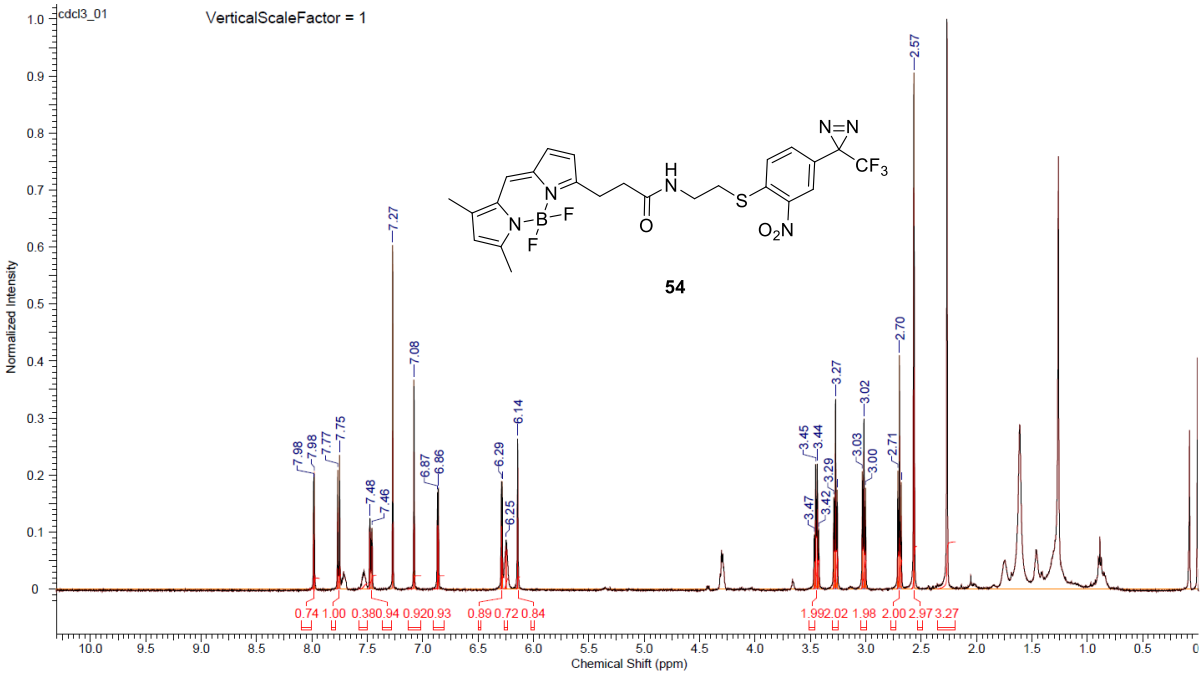
cdcl3_01
VerticalScaleFactor = 1
N
B
F
F
H
N
O
S
N=N
CF3
O2N
54
Normalized Intensity
Chemical Shift (ppm)
7.98
7.98
7.77
7.75
7.48
7.46
7.27
7.08
6.87
6.86
6.29
6.25
6.14
3.45
3.44
3.47
3.42
3.29
3.27
3.03
3.02
3.00
2.71
2.70
2.57
0.74 1.00 0.38 0.94 0.92 0.93 0.89 0.72 0.84 1.99 2.02 1.98 2.00 2.97 3.27

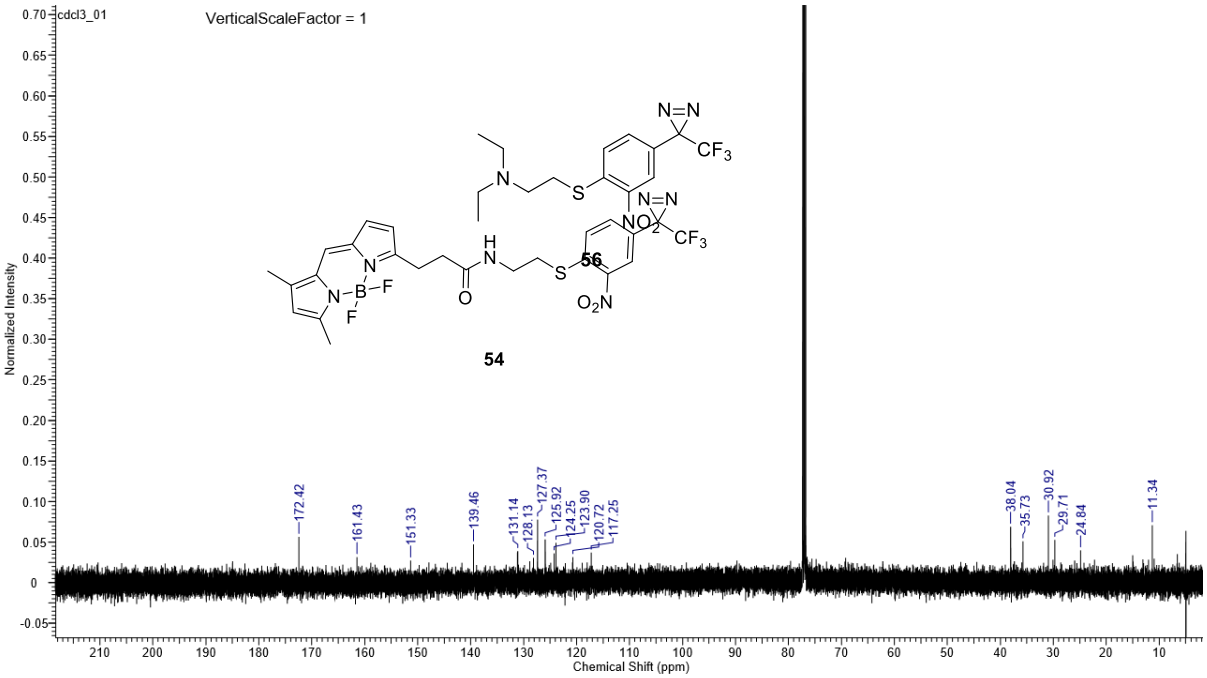
cdcl3_01
VerticalScaleFactor = 1
Normalized Intensity
Chemical Shift (ppm)
172.42
161.43
151.33
139.46
131.14
128.13
127.37
125.92
124.25
123.90
120.72
117.25
38.04
35.73
30.92
29.71
24.84
11.34
56
54

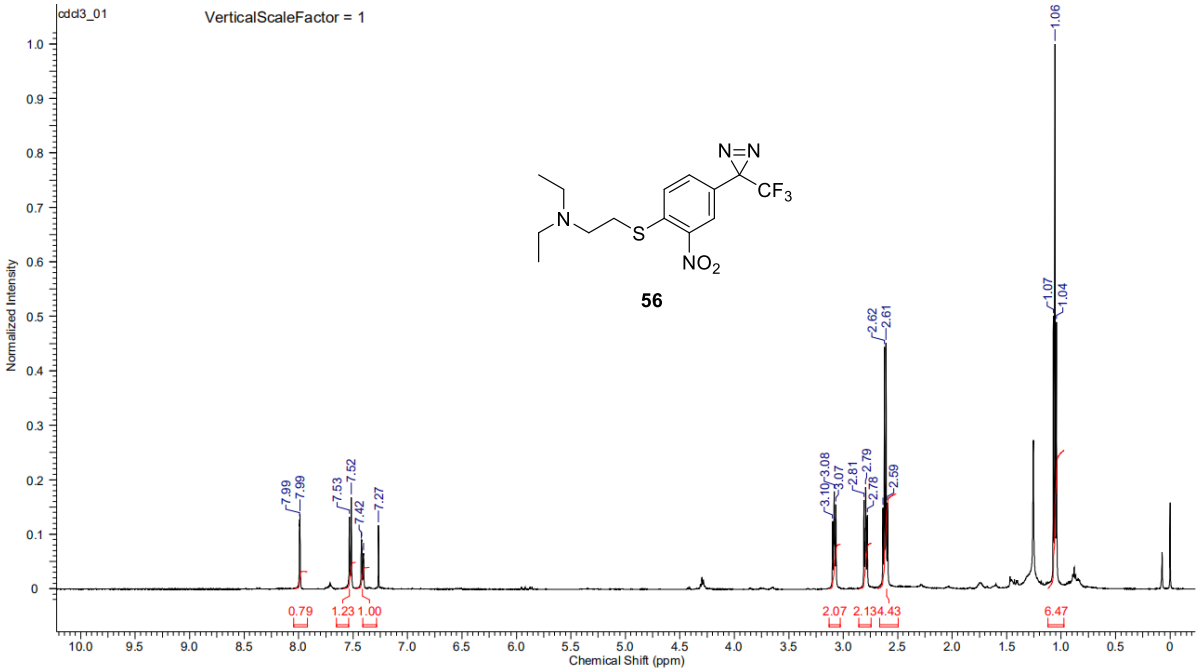
cdcl3_01
VerticalScaleFactor = 1
Normalized Intensity
Chemical Shift (ppm)
7.99
7.99
7.53
7.52
7.42
7.27
3.10
3.08
3.07
2.81
2.78
2.79
2.59
2.62
2.61
1.07
1.04
1.06
0.79
1.23
1.00
2.07
2.13
4.43
6.47
56

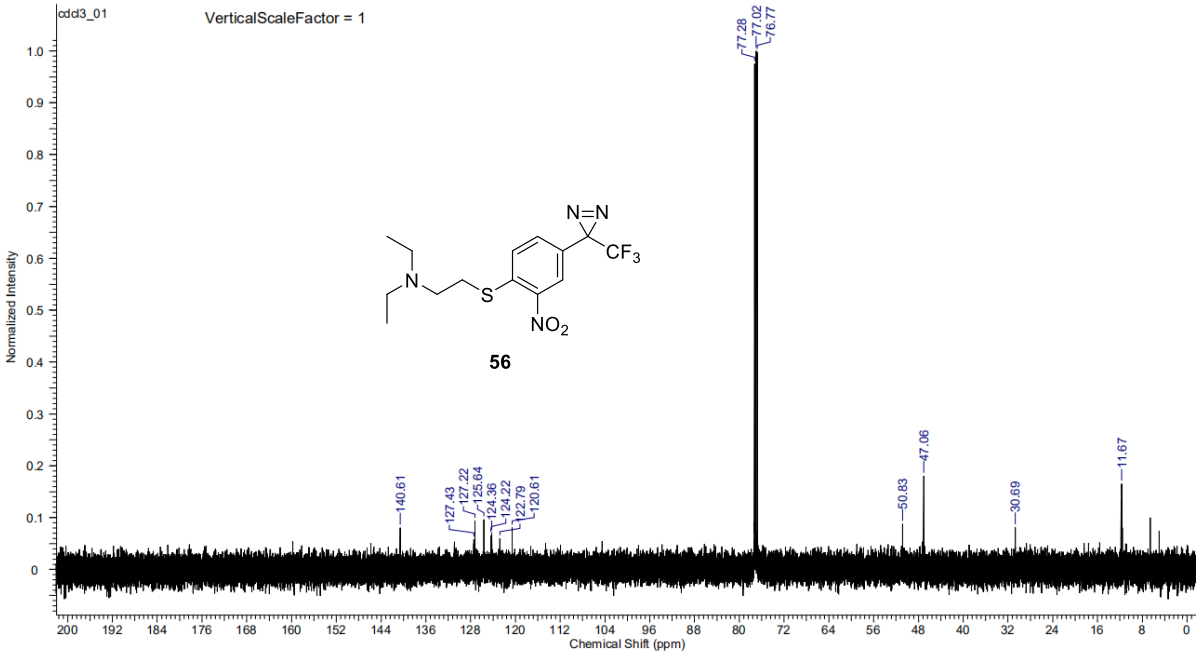

17/5/2019 9:50:18 AM
DIAZIDE

Acquisition Time (sec)	2.0487	*Date*	Oct 3 2017	*Date Stamp*	Oct 3 2017		
File Name	C:\Users\user\Dropbox\PHD\NMR_2\s_20171003_04 (2_94)\data\cd3od_01.fid\fid					*Frequency (MHz)*	500.59
Number of Transients	8	*Original Points Count*	16409	*Points Count*	32768	*Pulse Sequence*	s2pul
Solvent	METHANOL-d4			*Spectrum Offset (Hz)*	3003.4644	*Spectrum Type*	STANDARD
Temperature (degree C)	25.000						

Nucleus	1H		
Receiver Gain	60.00		
Sweep Width (Hz)	8009.61		

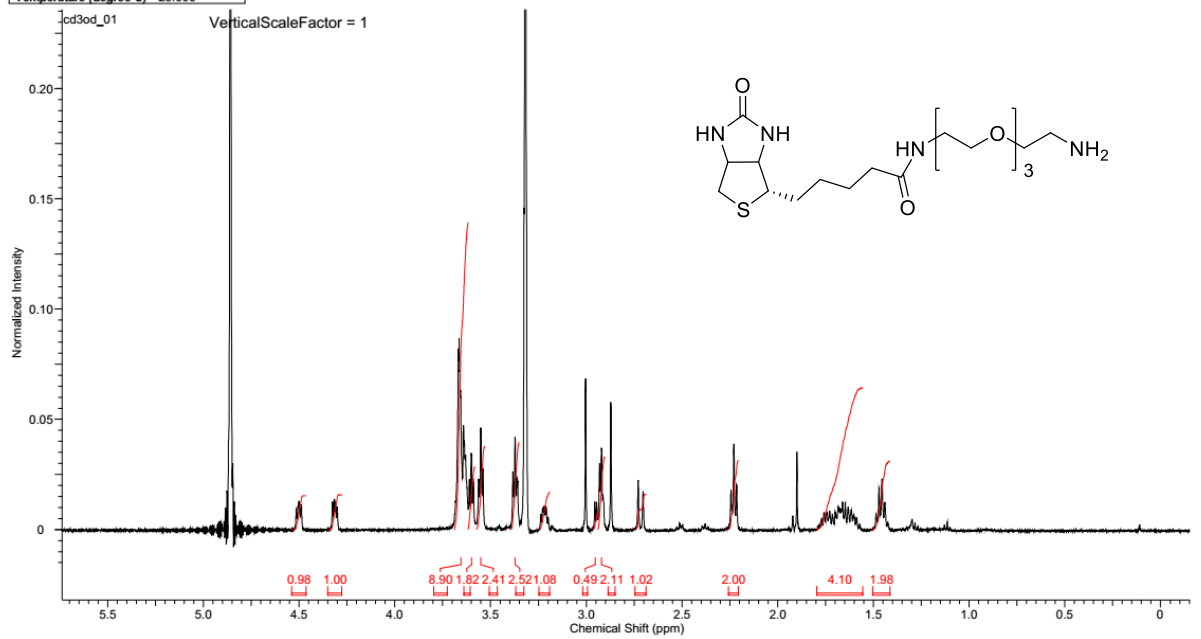

biotin DA

Acquisition Time (sec)	2.0487	Date	Mar 4 2019	Date Stamp	Mar 4 2019	File Name	E:\s_20190304_04 (biotin DA)\data\cd3od_01.fid\fid
Frequency (MHz)	500.46	Nucleus	1H	Number of Transients	8	Original Points Count	16404
Pulse Sequence	s2pul	Receiver Gain	20.00	Solvent	METHANOL-d4	Points Count	32768
Spectrum Type	STANDARD	Sweep Width (Hz)	8007.21	Temperature (degree C)	25.000	Spectrum Offset (Hz)	3020.4041

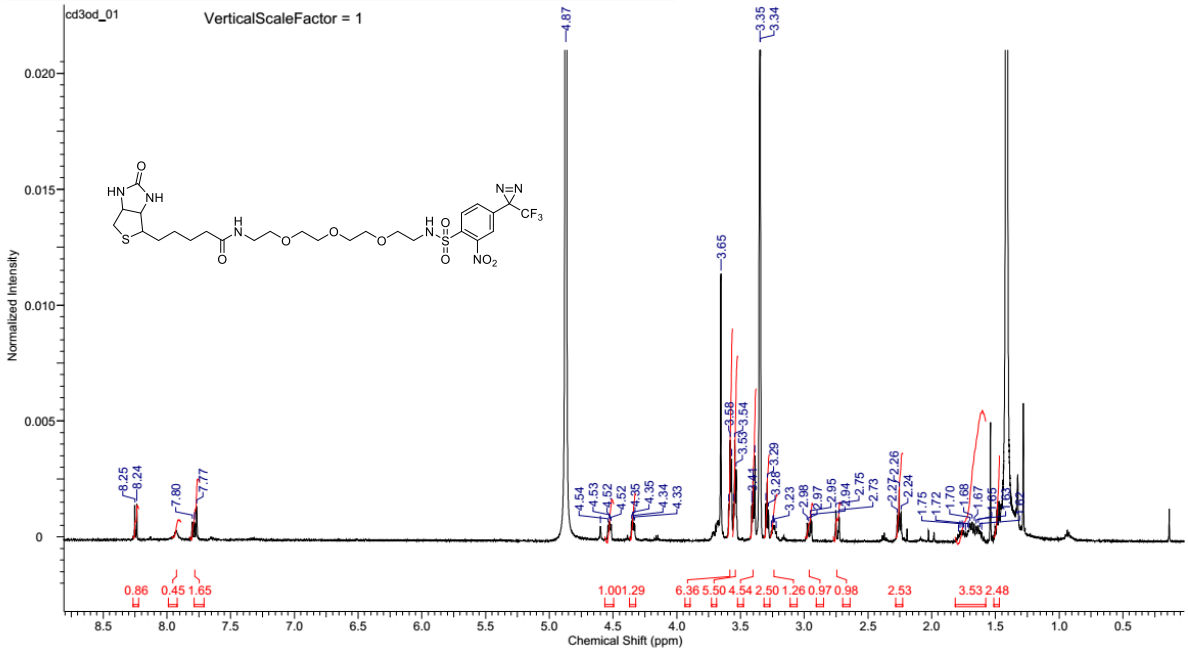

DA biotin 19F

Acquisition Time (sec)	1.0000	Date	Apr 3 2019	Date Stamp	Apr 3 2019	File Name	E:\s_20190403_03 (biotin DA 19F)\data\cd3od_01.fid\fid
Frequency (MHz)	470.83	Nucleus	19F	Number of Transients	16	Original Points Count	94229
Pulse Sequence	s2pul	Receiver Gain	46.00	Solvent	METHANOL-d4	Points Count	131072
Spectrum Type	STANDARD	Sweep Width (Hz)	94228.51	Temperature (degree C)	25.000	Spectrum Offset (Hz)	-61216.4492

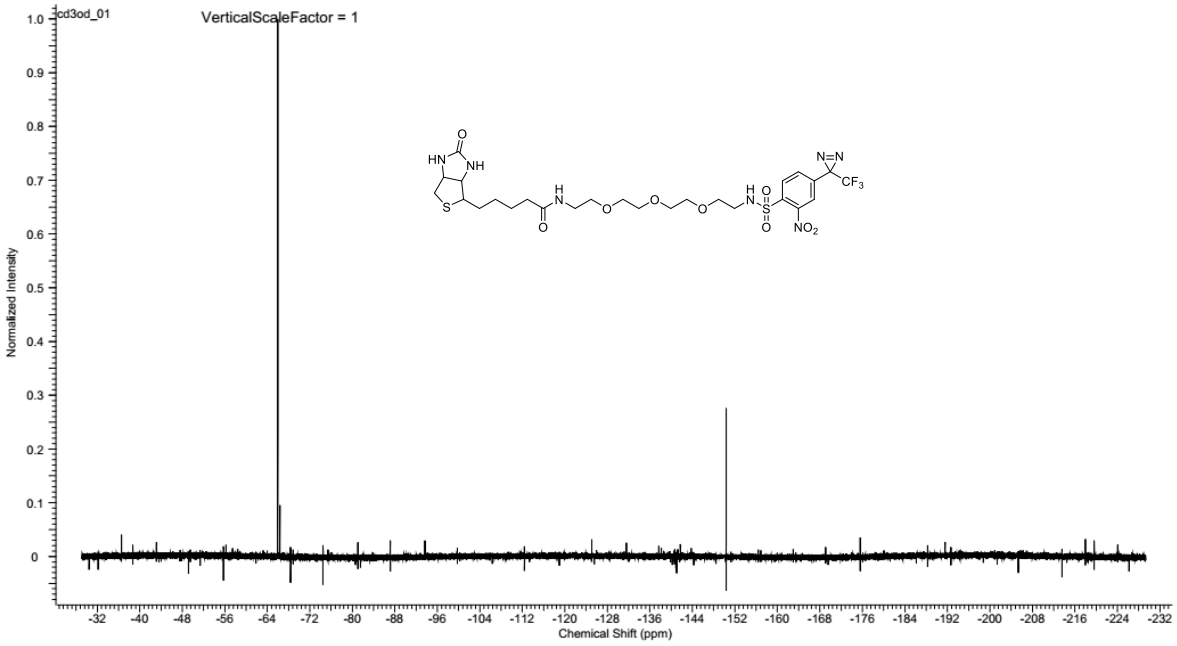

2.8 References

1. Lapinsky, D. J. Tandem photoaffinity labeling-bioorthogonal conjugation in medicinal chemistry. *Bioorganic Med. Chem.* **20**, 6237–6247 (2012).

2. Hashimoto, M. & Hatanaka, Y. Recent progress in diazirine-based photoaffinity labeling. *European Journal of Organic Chemistry* (2008). doi:10.1002/ejoc.200701069

3. Fukuyama, T., Jow, C. K. & Cheung, M. 2- and 4-Nitrobenzenesulfonamides: Exceptionally versatile means for preparation of secondary amines and protection of amines. *Tetrahedron Lett.* **36**, 6373–6374 (1995).

4. Tanaka, Y., Ishihara, T. & Konno, T. A new entry for the oxidation of fluoroalkyl-substituted methanol derivatives: Scope and limitation of the organoiodine(V) reagent-catalyzed oxidation. *J. Fluor. Chem.* **137**, 99–104 (2012).

5. More, J. D. & Finney, N. S. A simple and advantageous protocol for the oxidation of alcohols with o-iodoxybenzoic acid (IBX). *Org. Lett.* **4**, 3001–3003 (2002).

6. Ho, D. K. H., Chan, L., Hooper, A. & Brennan, P. E. A general and mild two-step procedure for the synthesis of aryl and heteroaryl sulfonamides from the corresponding iodides. *Tetrahedron Lett.* **52**, 820–823 (2011).

7. Pu, Y. M., Christesen, A. & Ku, Y. Y. A simple and highly effective oxidative chlorination protocol for the preparation of arenesulfonyl chlorides. *Tetrahedron Lett.* **51**, 418–421 (2010).

8. Cal, M., Jaremko, M., Jaremko, Ł. & Stefanowicz, P. One-pot efficient synthesis of N α-urethane-protected β- And γ-amino acids. *Amino Acids* **44**, 1085–1091 (2013).

9. Ge, S.-S. *et al.* Current advances of carbene-mediated photoaffinity labeling in medicinal chemistry. (2018). doi:10.1039/c8ra03538e

10. Hosoya, T. *et al.* Novel bifunctional probe for radioisotope-free photoaffinity labeling: Compact structure comprised of photospecific ligand ligation and detectable tag anchoring units. *Org. Biomol. Chem.* **2**, 637–641 (2004).

11. Brunner, J., Senn, H. & Richards, F. M. 3-Trifluoromethyl-3-phenyldiazirine. A new carbene generating group for photolabeling reagents. *J. Biol. Chem.* **255**, 3313–3318 (1980).

Chapter 3

Photolabeling of Methoxtrexate

Abstract

Methotrexate (MTX), an analogue of folic acid is a widely used drug used for the treatment of cancer, autoimmune diseases and induction of abortion with misoprostol. This analogue also is a known inhibitor for DHFR, an enzyme that reduces dihydrofolic acid to tetrahydrofolic acid. Herein in this chapter, we utilize MTX as a bioactive ligand to further confirm the feasibility of the Ns-diazirine. Since it was reported by Fresheim et al. that the α-carboxylate moiety of MTX plays a crucial role in binding interaction with DHFR, the γ-carboxylate moiety was modified by coupling it with the previously synthesized amine linker. It was then undergo the key step of the synthetic strategy, which is the oxidation chlorination using dichloro-dimethyl hydantoin. After successfully synthesized the MTX photolabel probe, the probe was incubated in DHFR and subjected to phoirradiation and SDS-Page. Finally, the MTX-labeled DHFR was identified by using modified thiol BODIPY as the identification tag. The fluorescence detection band of the DHFR cross-linked was observed at 21 KDa.

.

Chapter 3 Photolabeling of Methotrexate

3.1 Introduction of Methotrexate

In order to prove the feasibility of our approach, methotrexate (MTX) was used as a bioactive ligand. Methotrexate is a widely known inhibitor for dihydrofolate reductase (DHFR) and drug used to treat a range of diseases including cancer, rheumatoid arthritis and psoriasis. Faber and co-workers mentioned that aminopterin, a folic acid analogue which was first discovered by Subbarao, could be used to treat acute lymphoblastic leukaemia in children (Scheme 1). Since then, the development of folic acid analogue continues rapidly as it was proved that folic acid supply could worsen the leukaemia and deficiency of folic acid could im=prove the curative action of folic acid analogs [1]. In 1950, MTX replaced aminopterin, which is known as the most toxic anti tumor treatment for leukaemia. The first result of the pre-clinical and clinical studies in 1956 showed that MTX exhibit a better therapeutic margin than aminopterin[2]. Also, in the same year, a report on efficacy of MTX in choriocarcinoma was established too. Based on these results, this drug was further explored for many other cancers either alone or in combination with many other drugs, and extensively studied for other noncancer indications in the 1970s. Finally, in 1988 and 2002, this drug has been approved by US Food and Drug Administration (FDA) for the treatment of rheumatoid arthritis (RA) and Crohn's disease, respectively.

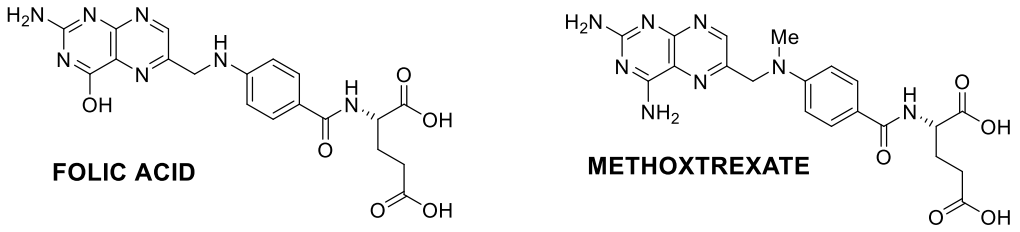

Scheme 1. Structure of folic acid and methotrexate

As a known analogue for folate, MTX is a powerful competitive inhibitor for dihydrofolate reductase (DHFR). DHFR is responsible for converting folates to their active form of tetrahydrofolate, a substrate of thymidylate synthase (TS). TS is used to convert deoxyuridine monophosphate to deoxythymidine-5'-monophosphate resulting in DNA synthesis [3]. The other mechanism is the poly glutamated form of MTX directly inhibits thymidylate synthase (TS) (Fig. 1). Thus far, comprehensive studies have been done on Methotrexate which includes its

crystal structure and structure activity relationship (SAR) with DHFR [4,5]. Previous studies on the α- and γ-carboxyl-modified MTX derivatives indicate that free α-carboxylate plays an essential role in MTX binding with DHFR. These studies also showed that the modification of γ-carboxyl group of MTX did not significantly alter the drug's binding to DHFR[6]. Hence, we modified Methotrexate by coupling γ-carboxylic acid with an amine linker.

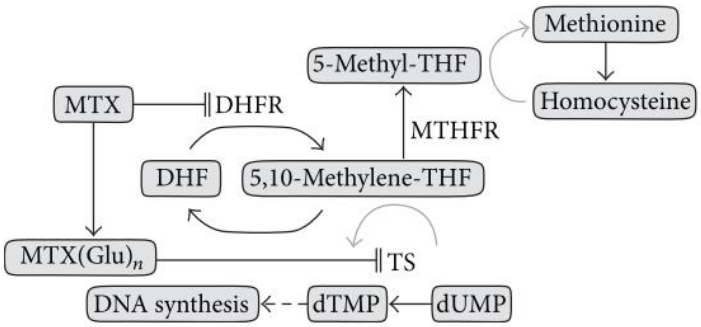

Fig. 1 Schematic representation of methotrexate action. MTX inhibits folic metabolism through two mechanisms: MTX inhibits DHFR, which leads to the depletion of THF compounds, resulting in impairment of purine and thymidine synthesis. Polyglutamated MTX inhibits TS directly, which causes depletion of DNA synthesis. MTX: methotrexate; DHFR: dihydrofolate reductase; DHF: dihydrofolate; THF: tetrahydrofolate; TS: thymidylate synthase; MTHFR: methylenetetrahydrofolate reductase; MTX $(Glu)_n$: MTX glutamates; dTMP: deoxythymidine monophosphate; dUMP: deoxyuridine monophosphate.

3.2 Synthesis of MTX photoaffinity probe

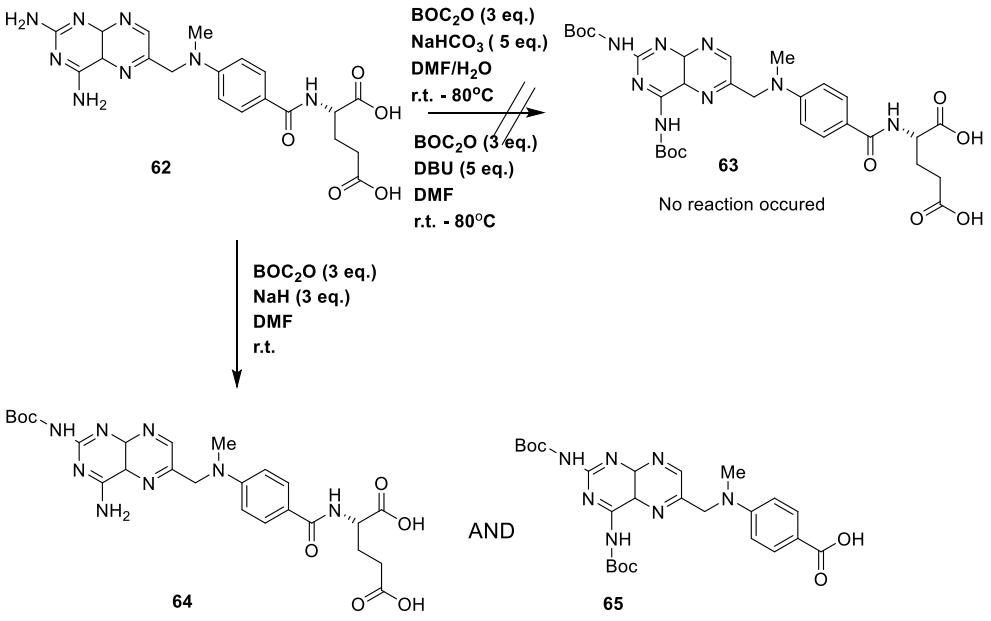

Scheme 2. Protection of methotrexate

Firstly, an attempt of protecting both the amine group on the pteridine ring of Methotrexate was carried out in the presence two different bases such as $NaHCO_3$ and DBU. However, after stirring the reaction mixture for overnight at 80°C, no desired product was observed. Hence, the base was changed to a stronger base which is NaH and the reaction mixture was left stirring overnight at room temperature. Unfortunately, based on the crude NMR spectra, we concluded that instead of the desired di-boc protected MTX, **63**, di-protected MTX without the glutamic part, **65** and mono-protected MTX were obtained, **64** (Scheme 2).

Based on this observation, the synthetic strategy was changed by coupling the MTX with a linker without having to protect the free amine first. The carboxylic acid at the γ-position was selectively activated using NHS before being coupled with the amine linker as reported by Martin *et al.* using EDC and DCC as peptide coupling agent and DMAP as catalyst. The reaction mixture was stirred for overnight at 80°C as the reaction proceeded slowly at room temperature. Despite that, formation of an acid anhydride in the glutamoyl moiety of MTX, **66** was favoured [7]. This product was confirmed only by ESI-mass spectrometry. So, the anhydride was then opened by amine linker, which gave us with the desired product, **68** but in low yield (Scheme 3).

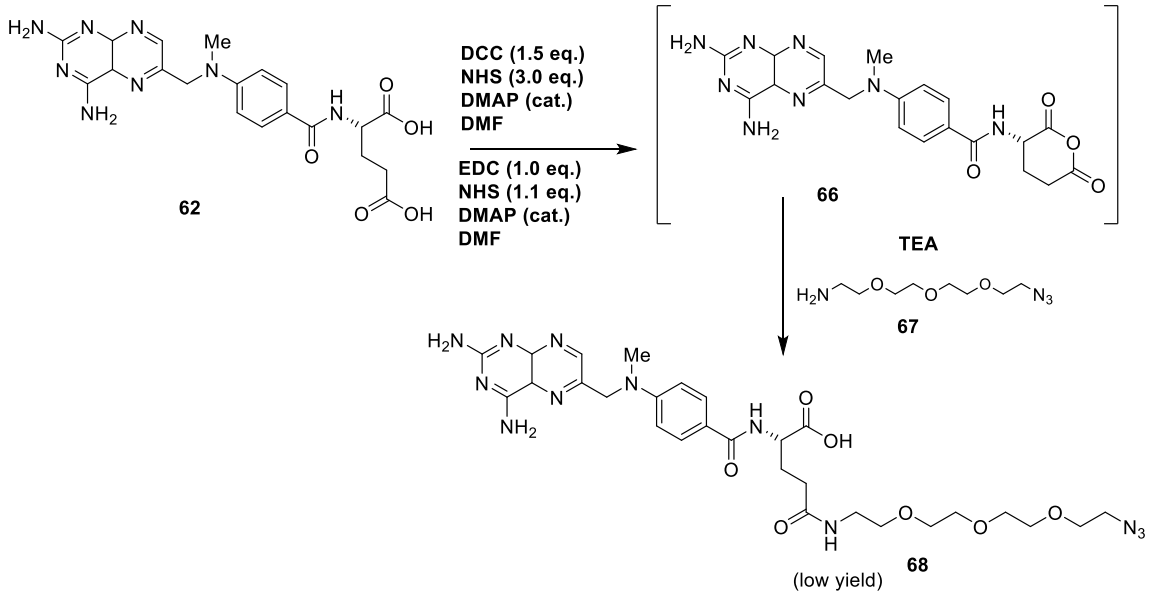

Scheme 3. Coupling reaction of MTX with amine linker

Knowing this, we then directed our strategy by directly coupled the carboxylic acid and amine linker without any activation step. Di-amine linker was synthesized from polyethylene glycol via 3 steps before it was converted to mono-boc protected compound, **68** which gave us 41% (Scheme 14). Next, compound **69** was coupled with commercially available MTX using DCC as the peptide coupling agent. This reaction gave us with a mixture of the α- and γ- amide in total of 77%, in which 43% of the compound is a pure regioselected γ-amide. Next, we proceeded with the deprotection of Boc using TFA. Although the reaction proceeded, the purification of the desired product was difficult. Then we decided to continue with the coupling reaction. Unfortunately, the final desired compound was not observed.

In order to circumvent this problem, the synthetic strategy was once again changed by forming a diazirine sulfoamide via oxidative chlorination which afforded us with 75% yield, followed by deprotection of Boc (Scheme 4). Next is the coupling reaction between diazirine amine linker, **70** and MTX. But the reaction did not proceed well as we expected and only a mixture of by product was obtained. We hypothesized that the diazirine was not stable enough to tolerate the coupling reaction condition.

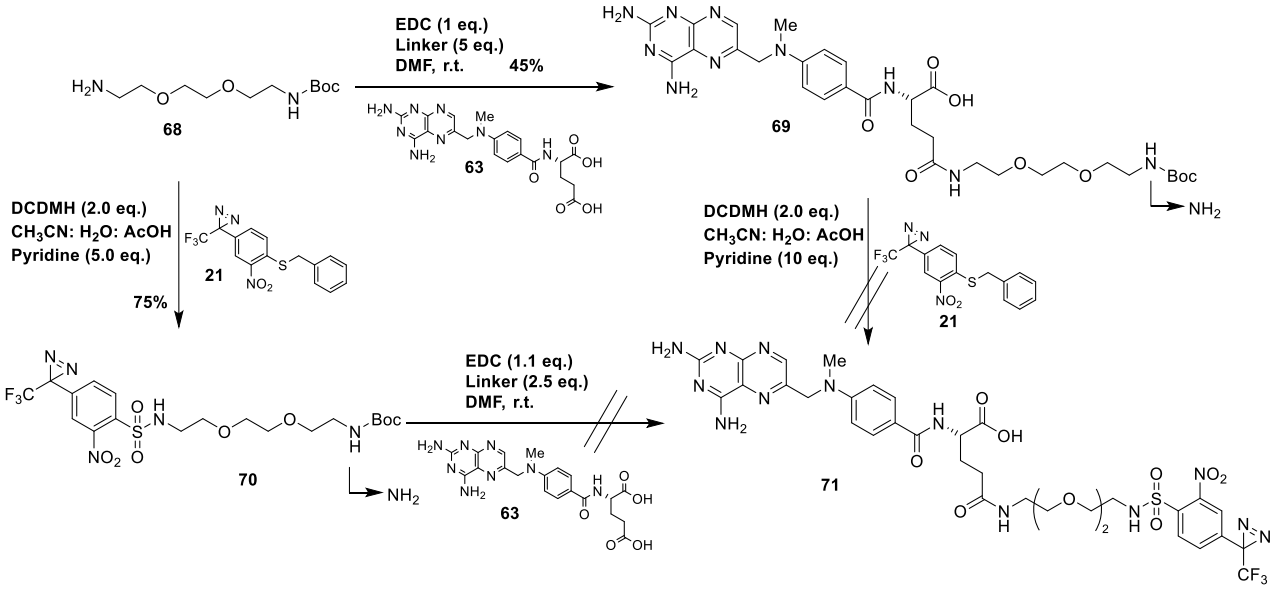

Scheme 4 Towards the synthesis of Ns diazirine bearing MTX

Having to know this, we concluded that Boc is not a suitable choice as a protecting group. Hence, Boc protecting group was replaced by Fmoc (Scheme 5). The diamine ethane ethanediol, **58** were first protected with FmocCl (0.5 eq.). Unfortunately, we failed to

selectively mono-protected the diamine as it favoured the formation of di-Fmoc linker, **72**. Hence, the protecting group was changed to TeocCl and successfully mono-protected the diamine with 42% yield. Next MTX was coupled with the synthesized amine linker using EDC as the coupling agent which afforded us with MTX-γ-diamine ethyl ethanediol, 39% and mixture of MTX α- and -γ- diamine ethyl ethanediol, 39%. Deprotection of teoc was performed in several conditions such as using TBAF[8], PTSA and potassium fluoride. However, we failed to completely deprotect the teoc group. Hence, teoc functionality was deprotected in the presence of TFA[9], which gave us with pegylated methoxtrexate, **75** in quantitative yield. Lastly the deprotected MTX- γ -diamine ethyl ethanediol, **75** was directly coupled with diazirinyl thionyl chloride, **21** via oxidative chlorination using 2,4-dichloro-5,5-dimethyl hydantoin (DCDMH) as the oxidizing agent which finally afforded us with diazirine MTX, **76** with 12% yield [10].

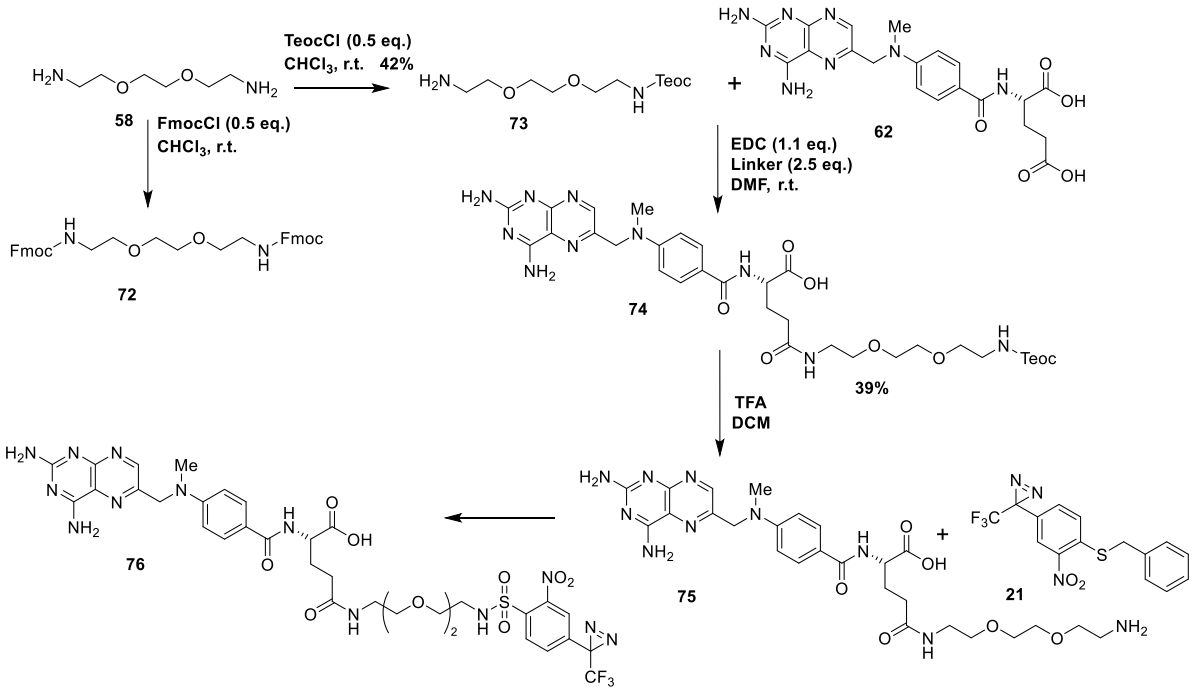

Scheme 5. Synthesis of Ns diazirine bearing MTX

3.3 Photoaffinity labeling

Having the synthesized photolabel in hand, we then proceeded with photolabeling. The synthesized MTX-diazirine probe (5 µM, 10 µl) was subjected to purified DHFR. It was incubated for 1.5h at 37°C before irradiated under UV lamp for 2 min. Upon photoactivation, dilution of SH-BODIPY (100 eq.) and Cs_2CO_3 (100 eq.) in H_2O was added and left reacted for overnight at room temperature. Then, fluorescence detection of the DHFR cross-linked with photoprobe was observed using Fujifilm LAS 4000. Detection of fluorescence band was detected at 21 KDa. Unfortunately, based on the SDS page results, fluorescence band was also detected even without the presence of MTX-probe. This means that there are also possibilities that unspecific labeling had occurred (Fig. 2).

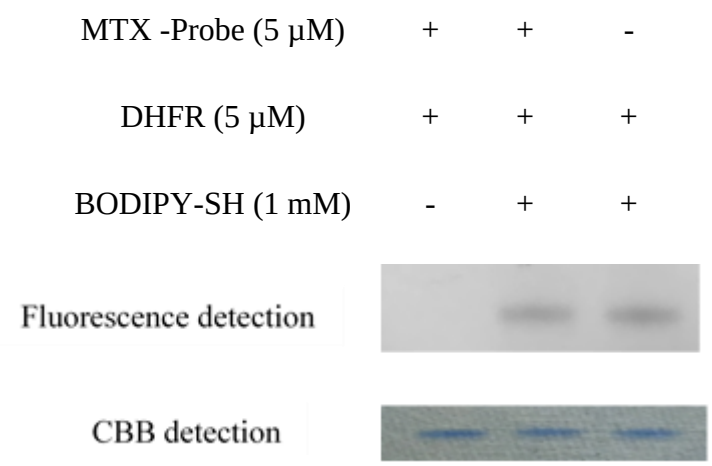

Fig. 2 Fluorescence detection of photocross-linked DHFR at 21 KDa

3.4 Conclusions

Nosyl diazirine photolabel with methotrexate as bioactive ligand was successfully synthesized. After a few attempts, teoc was chosen as the best protecting group used for the synthesis of the amine linker before it was coupled with our MTX. Subsequently, the MTX photolabel probe was incubated with DHFR and MTX-probe before it was irradiated under UV lamp. The mixture was then subjected to BODIPY thiol and followed by analysis using SDS-page and fluorescence detection. The band of the labelled DHFR was detected at 21 KDa with and without the presence of MTX-probe, which indicated that it may have undergo unspecific labeling. Further investigation to increase the photoaffinity labelling efficiency will be done in near future.

3.5 Experimental procedures

Coupling reaction between Boc protected amine linker, 68 and methotrexate, 63

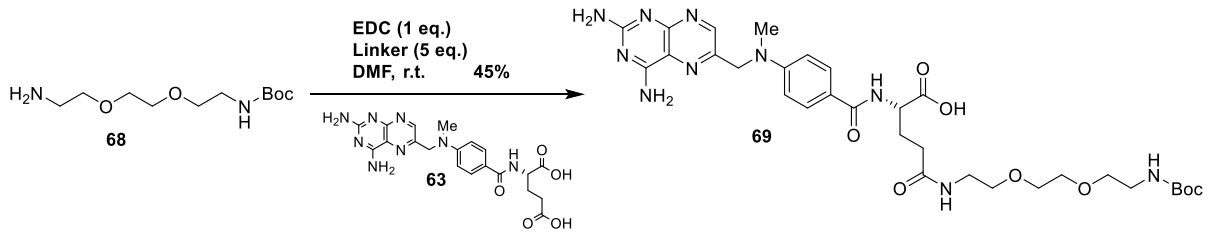

Methotrexate (62.8 mg, 0.14 mmol) was added into a stirred solution of EDC (29.1 mg, 1.1 eq.) in DMF at 0^{o}C. The reaction mixture was left stirring for 1 h before boc protected amine linker, **68** (34.2 mg, 1.0 eq.) was added. Upon the completion of reaction, DMF was evaporated followed by purification using column chromatography (eluent: ethyl acetate: MeOH: H_2O = 5/1/1) which gave us α-amide MTX, **69** (42.0 mg, 45%) and its mixture of γ- and α- amide MTX (38.0 mg, 40%) ^{1}H NMR (CD_3OD, 500 MHz) 8.56 (s, 1H), 7.78 (d, *J*=10 Hz, 2H), 6.86 (d, *J*=10 Hz, 2H), 4.44 (br.s, 1H), 3.67-3.64 (m, 1H), 3.56-3.53 (m, 8H), 3.44-3.40 (m, 5H), 3.24 (br. S, 4H), 3.17-1.16 (t, *J*=5 Hz, 3H), 2.39-2.30 (m, 2H), 1.47 (s, 9H).

Oxidative chlorination of diazirinyl benzyl mercaptan, 21

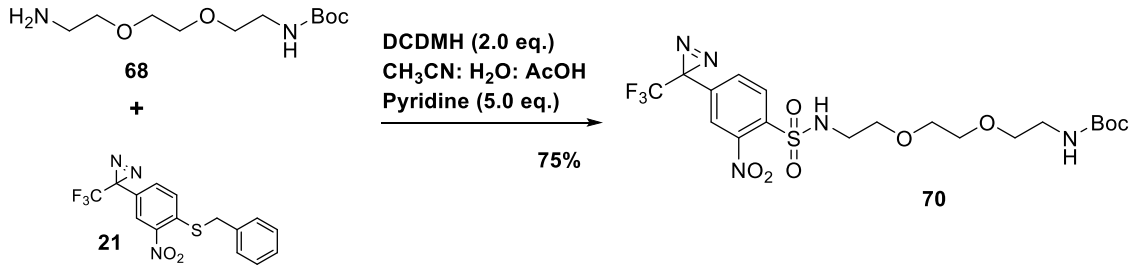

Benzyl mercaptan diazirine (17.5 mg, 0.05 mmol) was added into a solution of 1,3-dichloro-5',5-dimethylhydantoin (DCDMH) (19.5 mg, 2.0 eq.) in a mixture of CH_3CN, AcOH and H_2O (1 ml : 75 µl : 50 µl) at 0oC and left stirring for 2 h. Then pyridine (20 µl, 5.0 eq.) and Boc-amine linker, **68** (24.6 mg, 2eq.) were added and continued stirring overnight. The reaction mixture was then evaporated and further purified using column chromatography (eluent: ethyl acetate: MeOH = 4/1) which gave us with diazirine linker, **70** (20.1 mg, 75%). %). ^{1}H NMR

(CD_3OD, 500 MHz) δ ppm 8.17 (d, *J*=8.5 Hz, 1H), 7.61 (d, *J*=8.5 Hz, 1H), 7.53 (s, 1H), 3.63 (s, 4H), 3.58-3.53 (m, 4H), 3.38 (t, *J*=5.5 Hz, 2H), 3.25 (t, *J*=5.5 Hz, 2H), 1.97 (s, 3H), 1.46 (s, 9H).

Protection of diamine with TeocCl

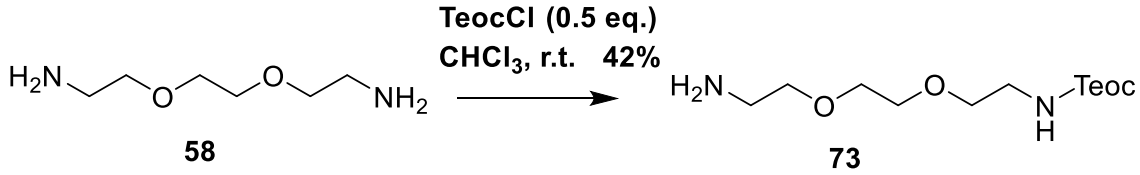

A solution of 2-(Trimethylsilyl) ethyl chloroformate chloride (0.18 g, 0.5 eq.) in chloroform was added into a stirred solution of diamine PEG, **58** (0.2 ml, 1.36 mmol) at 0°C and the temperature was elevated to room temperature. The reaction mixture was left stirring for overnight. Upon completion of the reaction, the mixture was quenched with H_2O and dried over $MgSO_4$. The crude mixture was purified using column chromatography (eluent: ethyl acetate: methanol: H_2O = 5 : 1 : 1) to give Teoc protected compound **73** (0.17 g, 42%). ^1H NMR (500 MHz, $CDCl_3$) δ 4.08 (t, *J*=1.0 Hz, 2H), 3.58 (s, 4H), 3.52 (t, *J*=1.0 Hz, 2H), 3.48 (t, *J* = 1.0 Hz), 3.23 (t, *J* = 1.0 Hz, 2H), 2.82 (t, *J* = 1.0 Hz, 2H), 1.84 (s, 1H), 1.90 (t, *J* = 1.0 Hz, 2H, 0.02 (9H, s)

Coupling reaction between MTX, 73 and Teoc amine linker, 62

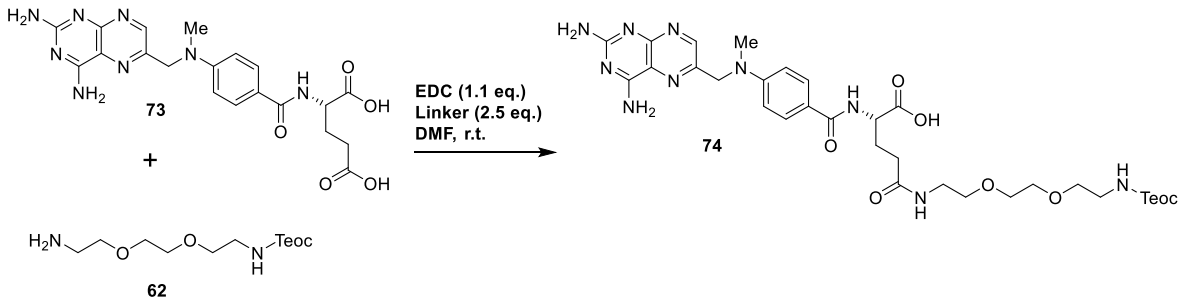

EDC (34 mg, 1.1 eq.) and linker teoc (0.12 g, 4 eq.) were added dropwise into a stirred solution of methotrexate (72.9 mg, 0.16 mmol) in DMF at 0 °C and the temperature was elevated to room temperature. Upon the completion of the reaction, the mixture was evaporated using rotary evaporator followed by purification using column chromatography (eluent: ethyl acetate/methanol/H_2O = 5/1/1) to give a mixture of γ-MTX (49.3 mg, 42%) and α-MTX (51.0

mg, 44%). ^{1}H NMR (500 MHz, $CDCl_3$) 8.50 (br.s, 1H), 7.73 (d, *J*=10.0 Hz, 2H), 6.76 (d, *J*=10.0 Hz, 2H), 4.77 (br.s, 2H), 4.48 (br.s, 2H), 4.08 (t, *J*=5.0 Hz, 2H), 3.56-3.48 (m, 7H), 3.43 (t, *J*=5.0 Hz, 2H), 3.39-3.34 (m, 2H), 3.21 (t, *J*=5.0 Hz, 2H), 3.17 (s, 3H), 2.41-2.34 (m, 2H), 2.17-2.00 (m, 2H), 0.93 (t, *J*=7.0 Hz, 2H), 0.01 (s, 9H)

Deprotection of Teoc

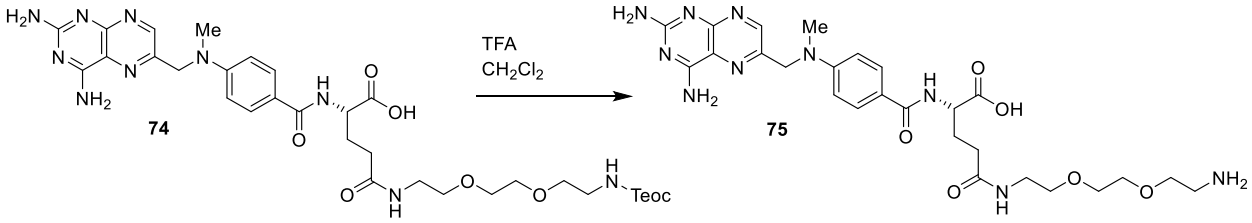

TFA (700 µl) was added dropwise into a stirred solution of protected MTX (28.8 mg, 0.039 mmol) at 0^{O}C for 1 h and was left stirring for another 45 min at room temperature. Upon completion of the reaction, the reaction was evaporated using rotary evaporator and was proceeded with the next step without any purification.

Coupling reaction between diazirine benzyl mercaptan, 21 and MTX amine linker

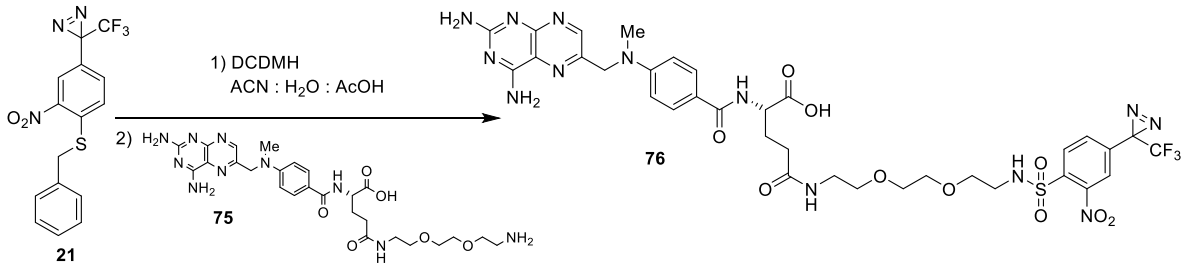

Acetic acid (37.5 µl) and H_2O (25 µl) was added into a stirred solution of 3-(4-(benzylthio)-3-nitrophenyl)-3-(trifluoromethyl)-3H-diazirine (13.6 mg, 0.038 mmol) in acetonitrile (1ml). Then 2,4-Dichloro-5,5-dimethylhydantoin (16.3 mg, 2.2 eq.) was added at 0^{o}C for 3 h before evaporated under vacuum, extracted with dichloromethane, dried over Mg_2SO_4 and evaporated under vacuum. Then the crude mixture was added into a stirred solution of MTX linker (28.6 mg, 2.0 eq.) and TEA (3.0 ml) in H_2O at room temperature for overnight. Upon the completion of the reaction, it was evaporated to dryness and further purified using column chromatography

(eluent: chloroform/methanol/H_2O = 5/1/1) to give compound **76** (7.7 mg, 23%). ^{1}H NMR ($CDCl_3$, 500 MHz) δ 8.57 (s, 1H), 8.17 (d, *J*=10 Hz, 1H), 7.78 (d, *J*=5.0 Hz, 2H), 7.71 (s, 1H), 6.85 (d, *J*=10.0 Hz, 2H), 4.86 (s, 1H), 4.57-4.54 (m, s), 4.14-4.09 (m, 1H), 3.53-3.51 (m, 2H), 3.48-3.46 (m, 2H), 3.44-3.38 (m, 2H), 3.27 (s, 3H), 3.19 (t, *J*=5.0 Hz, 2H), 2.37 (t, *J*=10.0 Hz, 2H)

3.6 NMR Spectra

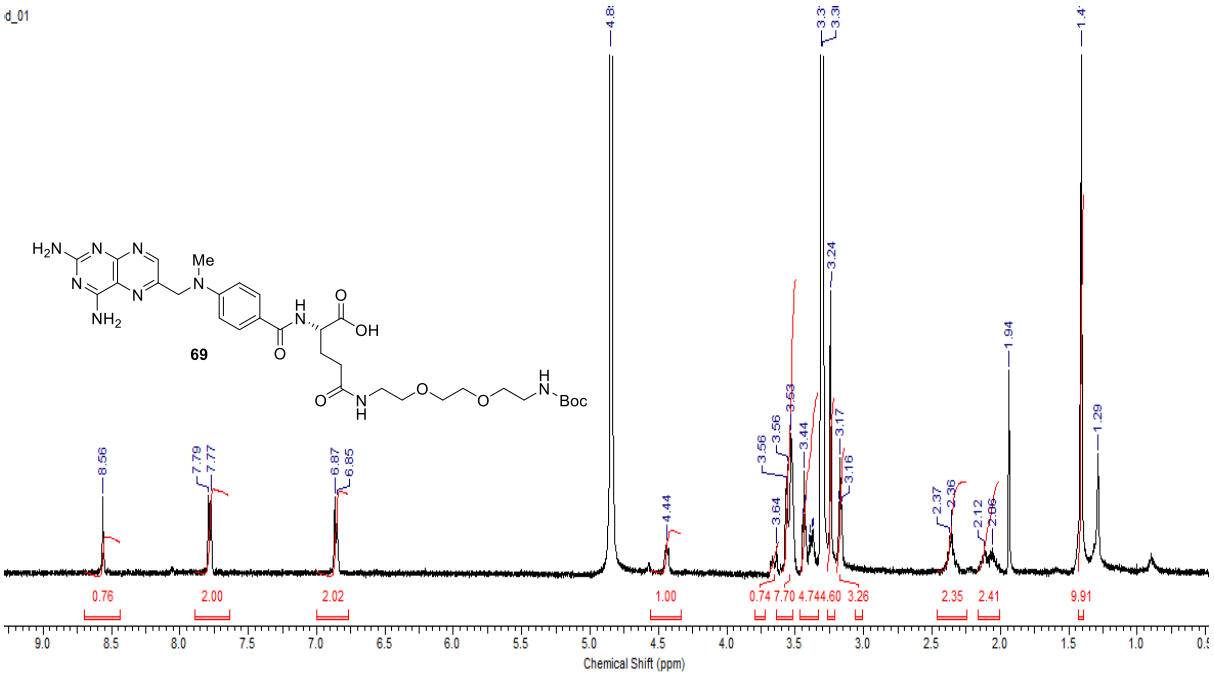

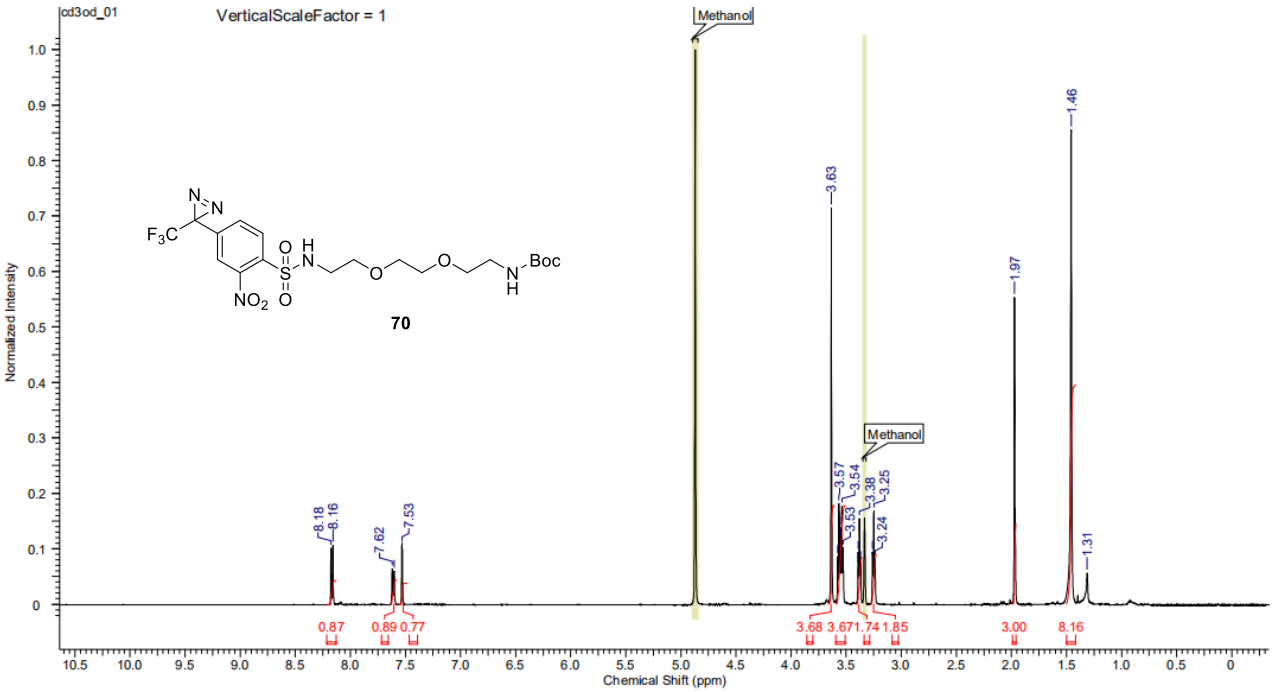

3-54 linker teoc

Acquisition Time (sec)	2.0486	*Date*	Aug 10 2018		*Date Stamp*	Aug 10 2018	
File Name	E:\s_20180810_01 (3_54)\data\cd3od_01.fid\fid		*Frequency (MHz)*	500.51	*Nucleus*	1H	*Number of Transients*	8
Original Points Count	16405	*Points Count*	32768	*Pulse Sequence*	s2pul	*Receiver Gain*	20.00	*Solvent*	METHANOL-d4
Spectrum Offset (Hz)	2967.5671	*Spectrum Type*	STANDARD			*Sweep Width (Hz)*	8008.01	*Temperature (degree C)*	25.000

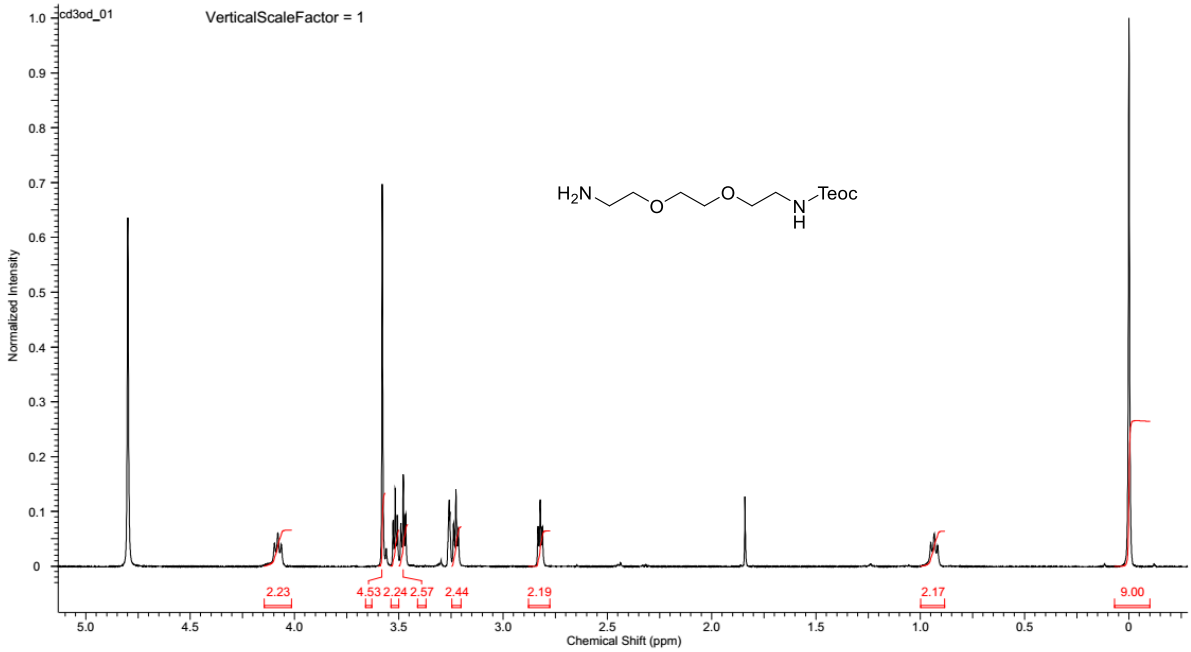

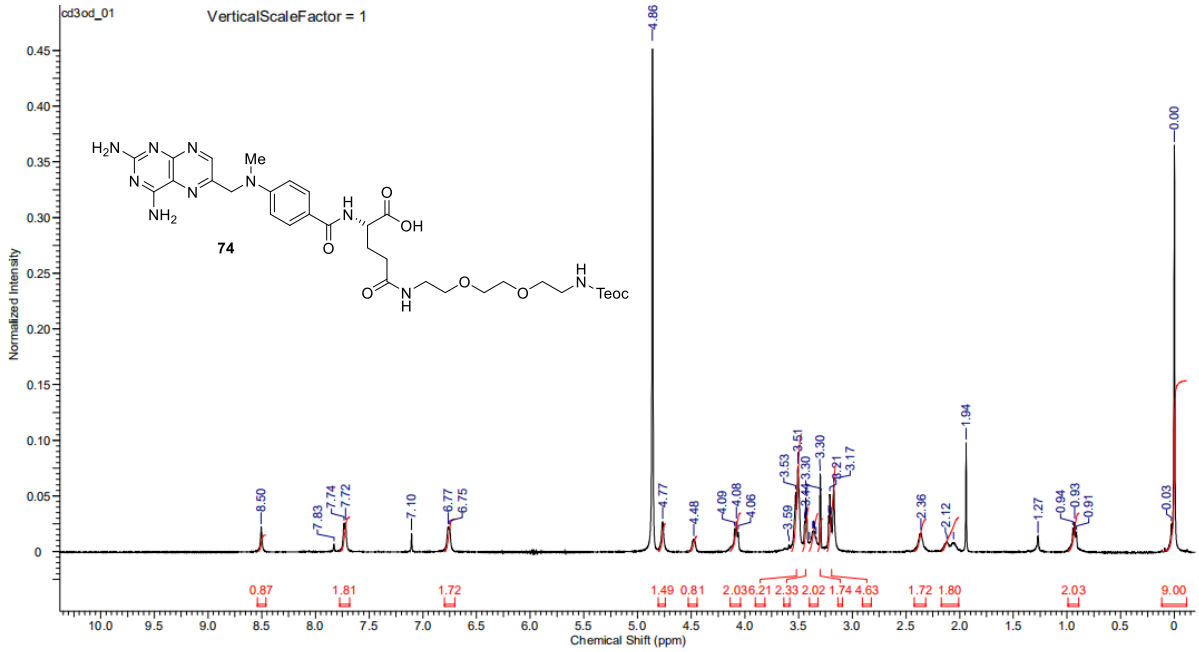

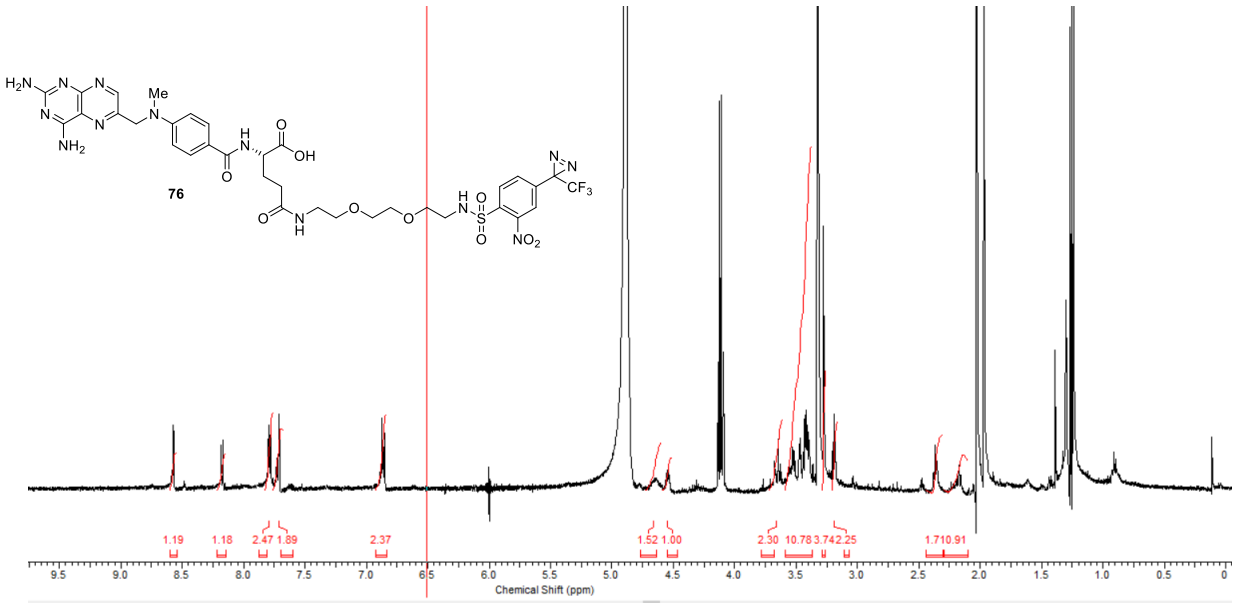

3.7 References

1. Khan, Z. A., Tripathi, R. & Mishra, B. Methotrexate: a detailed review on drug delivery and clinical aspects. *Expert Opin. Drug Deliv.* **9**, 151–169 (2012).

2. Cronstein, B. N. Methotrexate and its Mechanism of Action. *Arthritis Rheum.* **39**, 1951–1960 (1996).

3. Fukushima, H. *et al.* Polymorphisms of MTHFR Associated with Higher Relapse/Death Ratio and Delayed Weekly MTX Administration in Pediatric Lymphoid Malignancies . *Leuk. Res. Treatment* **2013**, 1–9 (2013).

4. Gangjee, A. *et al.* Design, synthesis, and x-ray crystal structure of a potent dual inhibitor of thymidylate synthase and dihydrofolate reductase as an antitumor agent. *J. Med. Chem.* **43**, 3837–3851 (2000).

5. Matthew&, D. A. *et al. Refined Crystal Structures of Escherichia coli and Chicken Liver Dihydrofolate Reductase Containing Bound Trimethoprim" JOURNAL OF BIOLOGICAL CHEMISTRY* **260**, (1985).

6. Freisheim, J. H., Smith, P. L., Klein, T. E. & Price, E. M. Photoaffinity Analogues of Methotrexate as Folate Antagonist Binding Probes. 1. Photoaffinity Labeling of Murine L1210 Dihydrofolate Reductase and Amino Acid Sequence of the Binding Regiont. *Biochemistry* **26**, 4751–4756 (1987).

7. Francis, C. L. *et al.* Total synthesis of methotrexate-γ-TRIS-fatty acid conjugates. *Aust. J. Chem.* **55**, 635–645 (2002).

8. Parlow, J. J., Vazquez, M. L. & Flynn, D. L. A mixed resin bed for the quenching and purification of tetrabutylammonium fluoride mediated desilylating reactions. *Bioorganic Med. Chem. Lett.* **8**, 2391–2394 (1998).

9. Johannes, J. W., Wenglowsky, S. & Kishi, Y. Biomimetic macrocycle-forming Diels-Alder reaction of an iminium dienophile: Synthetic studies directed toward gymnodimine. *Org. Lett.* **7**, 3997–4000 (2005).

10. Pu, Y. M., Christesen, A. & Ku, Y. Y. A simple and highly effective oxidative chlorination protocol for the preparation of arenesulfonyl chlorides. *Tetrahedron Lett.* **51**, 418–421 (2010).

Acknowledgements

First of all, I would like to thank my supervisor, Prof Kenji Monde for the great deal of support and confidence that he has given me through out my Phd journey. I am also immensely grateful for his patience, motivation and enthusiasm which has shaped me to be a better researcher. I would also like to register my heartfelt gratitude to Dr. Yuta Murai and Dr. Yuyama Kohei for their insightful comments and continuous guidance, without which it would not be possible for me to complete my works.

Also, my special thanks to my associate supervisors Prof. Hinou Hiroshi, Prof. Tamaoki Nobuyuki for their valuable suggestions and inputs for progress of my research. I would also like to thank Dr. Tohru Taniguchi, who contributed to my research and involved in valuable discussions.

My deepest heartiest thanks to my husband for his sacrifices and constant continuous support that has always keeps me moving forward despite all the challenges we faced.

I am grateful to the staffs of our laboratory, Ms. Keiko Abe and Ms. Yoshiko Suga for their invaluable assistance and unfailing support especially in the administrative works. I would also like to thank my fellow labmates for their unconditional support during the rough times with all their humour, jokes and parties.

Last but not least, I would like to express my special thanks to my parents for their constant prayers, patience and untiring support in every way during my study. Most of all, I am very grateful to Allah for blessing me with good health and a lot of patience, without which this work will not be complete.

Publications

1. Papers (related to Doctoral Dissertation)

(1) **Aimi Suhaily Saaidin**, Yuta Murai, Takuya Ishikawa, Kenji Monde. “Design and Synthesis of Ligand-tag Exchangeable Photoaffinity Probe Utilizing Nosyl Chemistry via Meisenheimer Complex” *Eur. J. Org. Chem.* 2019, 10.1002/ejoc.201901348